NTNU
Norwegian University of
Science and Technology

Metabolic Engineering of *Bacillus methanolicus* MGA3 for Production of Acetoin

Dennis Tin Chat Chan

Biotechnology (5 year)
Submission date: May 2018
Supervisor: Trygve Brautaset, IBT
Co-supervisor: Marta Irla, IBT

Norwegian University of Science and Technology
Department of Biotechnology and Food Science

Acknowledgement

This past year has been painfully exhausting, but also tremendously eye-opening. I have come to the realization that, in science, mistakes are to be learned from, and success is to be criticised; a lesson I will take with me for life.

I would like to thank everyone in the Cell Factory lab for their approachability and for always reassuring me that there are no dumb questions.

I would like to thank my friends and peers for sharing their own stories of failure and struggles, which was both comforting and motivating. Especially one friend, whom helped me take a break from reality when I needed it the most.

Most of all, I would to thank my supervisor, Marta, whom despite all the frustration I have caused her and my numerous occasions of incompetence, always saw the potential in me. This thesis was immensely enjoyable to perform and write, all thanks to her wit, humour and straightforwardness.

Finally, my parents, for loving me for all that I am.

Trondheim, May 15th, 2018

Dennis Tin Chat Chan

"What are you doing?!"

- My supervisor, on numerous occasions

Abstract

Being a pure, inexpensive, non-food chemical that can be sustainably produced, methanol has attracted great interest as a carbon feedstock for microbial production of commodity/specialty chemicals. In this thesis, methanol-based production of acetoin was achieved by recombinant *Bacillus methanolicus* MGA3 strains. The *alsSD* operons from *Bacillus licheniformis* DSM13 and *Bacillus subtilis* 168 were cloned into expression vector pTH1mp and heterologously expressed in *B. methanolicus* MGA3, creating two acetoin-producing strains with different growth characteristics, MGA3 (pTH1mpLacO-*alsSD*_Bl(GTG)) and MGA3 (pTH1mpLacO-*alsSD*_Bs(GTG)), respectively.

The potential of *B. methanolicus* MGA3 as an acetoin producer was evaluated by assessing acetoin tolerance and by functionally assaying the activity of recombinant enzymes produced. MGA3 (pTH1mpLacO-*alsSD*_Bl(GTG)) achieved the highest acetoin titer of 1.48 ± 0.24 g/L with yield of 0.23 ± 0.04g/L $g_{acetoin}/g_{methanol,}$ growing on methanol as sole carbon source. The relatively narrow engineering effort performed in this thesis highlights the potential of *B. methanolicus* MGA3 as a candidate for industrial production of acetoin. Parameters such as productivity, rate of methanol consumption, etc. are yet to be determined, which leaves room for future engineering strategies to further optimize yield.

In addition, potential production of 2,3-butanediol, of which acetoin is the direct precursor, in *B. methanolicus* MGA3 was investigated.

Sammendrag

Som en ren og relativt billig kjemikalje som kan produseres bærekraftig, har metanol tiltrukket stor interesse som karbonkilde for mikrobiell produksjon av spesialkjemikalier. I denne masteroppgaven ble metanolbasert produksjon av acetoin oppnådd ved rekombinante *Bacillus methanolicus* MGA3 stammer. *alsSD* operonene fra *Bacillus licheniformis* DSM13 og *Bacillus subtilis* 168 ble klonet inn i ekspresjonsvektoren pTH1mp og heterologt uttrykt i *B. methanolicus* MGA3, som førte til to acetoin-produserende stammer med forskjellige vekstegenskaper, henholdsvis, MGA3 (pTH1mpLacO-*alsSD*_Bl(GTG)) og MGA3 (pTH1mpLacO-*alsSD*_Bs(GTG)).

Potensialet for *B. methanolicus* MGA3 som en acetoinprodusent ble evaluert ved å vurdere acetointoleranse og ved å analysere aktiviteten av produserte rekombinante enzymer. MGA3 (pTH1mpLacO-*alsSD*_Bl(GTG)) oppnådde den høyeste titer av acetoin på 1.48 ± 0.24 g/L med utbytte på 0.23 ± 0.04 $g_{acetoin}/g_{metanol}$, ved bruk av metanol som eneste karbonkilde. Den relativt smale tekniske innsatsen utført i denne oppgaven fremhever potensialet til *B. methanolicus* MGA3 som kandidat for industriell produksjon av acetoin. Parametre som produktivitet, rate av metanolforbruk, etc., er ennå ikke bestemt, som gjør plass til fremtidige ingeniørstrategier for å ytterligere optimalisere avkastningen.

I tillegg ble potensiell produksjon av 2,3-butandiol, hvorav acetoin er den direkte forløper, i *B. methanolic*us MGA3 utforsket.

Table of Contents

1 Introduction

The use of fossil fuels and their derivatives as energy source and raw material for production of commercially important chemicals has become increasingly environmentally unsustainable in the past decades. The amount of recoverable oil on the planet is finite, and predicting global peak oil has been a subject of heavy interest ever since global energy demands became centralized on oil (Mabro, 2012). Furthermore, in the face of climate change (Bais *et al.*, 2018) and rising oil-prices, the incentive to develop microbial alternatives for production of commodity and specialty chemicals has become ever so attractive (Liao *et al.*, 2016).

Industrial biotechnology involves the use of microorganisms for the sustainable production of fuels and commodity/specialty chemicals; as a replacement for traditional routes of industrial production, usually reliant on fossil fuels (Sajna, Gottumukkala and Sukumaran, 2015). The metabolism of a cell can be optimized for production of a desired substance, both in terms of product yield and cost-effectiveness. By metabolic engineering, production of high value chemicals from renewable and inexpensive raw materials can be achieved either by manipulation of existing biochemical pathways (homologous engineering) or introduction of foreign pathways (heterologous engineering) to organisms (Woolston, Edgar and Stephanopoulos, 2013).

1.1 Acetoin and 2,3-Butanediol are Specialty Chemicals

Acetoin (3-hydroxy-2-butanone, acetyl methyl carbinol) is a pale to yellow liquid with a sweet, creamy yogurt-like odour (Burdock, 2005) with two stereoisomeric forms, 3S- and 3R-acetoin. Acetoin is volatile, non-ionic, miscible with water and soluble in alcohols (Xiao and Xu, 2007), it is generally recognized as safe (GRAS) by the Joint FAO/WHO Expert Committee on Food Additives (1998), and the US Food and Drug Administration (FDA). The U.S. Department of Energy has classified acetoin as a top priority platform chemical for its development and utilization (Werpy and Petersen, 2004).

2,3-butanediol (2,3-BD) is another highly sought after C4-compund with three stereoisomers: 2S,3S-, meso-2,3- and 2R,3R-BD. Interest in the microbial synthesis of 2,3-BD began as early as 1906 (Harden and Walpole, 1906), but the rising availability of inexpensive fossil fuels at the time halted further development. Today, the decline of fossil fuels has once again instigated the pursuit of sustainable microbial production of this specialty chemical (van Haveren, Scott and Sanders, 2008).

1.1.1 Application of acetoin and 2,3-butanediol

As a flavour and fragrance enhancer, acetoin is extensively utilized as an additive in baked goods, confection, dairy, cosmetic and hygiene products (Burdock, 2005). Acetoin may also act as an insect pheromone, extending its application to agricultural use for pest control and promotion of plant growth (Rudrappa *et al.*, 2010; Chen and Li, 2011), and also as a chelating agent for stabilization of alkoxides (Takahashi *et al.*, 2000; Ohya *et al.*, 2002; Stachiotti *et al.*, 2005). Acetoin is also a precursor for synthesis of various other compounds and is the preferred precursor for synthesis of heterocyclic compounds such as 2,3,5,6-tetramethylpyrazine; a valuable substance used in traditional Chinese medicine (Xiao *et al.*, 2006).

2,3-BD has a heating value of 27.2 kJ/g, comparable to other liquid fuels such as ethanol (29.0 kJ/g) and methanol (22.0 kJ/g). The freezing point of the 2S,3S-BD isomer is −60 °C, making it fit for use as anti-freeze agent (Flickinger, 1980; Soltys, Batta and Koneru, 2001; Ge *et al.*, 2011a). The chemical structure of 2,3-BD makes it a unique precursor for production of other valuable compounds. For instance, 2,3-BD can be dehydrated to produce methyl-ethyl-ketone, an

industrial solvent and liquid fuel additive, or 2,3-butadiene, an important monomer of synthetic rubber (Tran and Chambers, 1987; Bartowsky and Henschke, 2004; van Haveren, Scott and Sanders, 2008). Elsewhere, the derivatives of 2,3-BD are variously applied in the food, pharmaceutical and cosmetic industries, as well as production of printing inks, plasticiser, spandex, etc. (Garg and Jain, 1995).

1.1.2 State-of-the-art production of acetoin and 2,3-butanediol

1.1.2.1 Chemical synthesis of acetoin

Currently, production of acetoin and 2,3-BD occurs mainly by chemical synthesis from fossil-based raw materials. Xiao and Lu (2014) describes three main methods for chemical synthesis of acetoin.

The first method uses diacetyl (DA), a structural analogue of acetoin, and 2,3-BD as starting material. The two specialty chemicals can be reduced and oxidized respectively to produce acetoin in a one-step reaction. The main disadvantage is the high cost of the raw materials, which are also specialty chemicals. In addition, due to possible over-reduction of DA to form 2,3-BD, the process also requires more strict reaction conditions. For these reasons this method has seen no industrial application (Studer and Blaser, 1998).

The second method is a two-step process that begins with butanone or methyl ethyl ketone. Using butanone based method as example, the first step is the halogenation of butanone to make 3-halogenated butanone, which is then hydrolysed to produce acetoin. This method occurs in milder reaction conditions and less sophisticated equipment compared to method one. This method has thus been extensively uses in industrial scale, however, it is also associated with the production of numerous undesired by-products due to the high reactivity of hydrogen on the α-position of butanone. This leads to both reduced acetoin yield and makes downstream processing costly and laborious (Zhu *et al.*, 2011).

In method three, inexpensive acetaldehyde is used as the starting material, and acetoin is produced by condensation reaction catalysed by triazolium ylide or thiazolium ylide. This method also requires less complicated equipment, produces fewer by-products, results in higher yield, and has simpler separation and purification step compared to both previously mentioned

methods. The main disadvantage is the complicated preparation of the triazolium/thiazolium ylide catalysts. Furthermore, while aldehyde is inexpensive, it is volatile, flammable, difficult to store, easily lost during handling and transport, and hazardous for human health and environment. These issues can be resolved by using paraldehyde, which, however, adds one additional step of paraldehyde depolymerization (Ebel *et al.*, 1998)

1.1.2.2 Chemical synthesis of 2,3-butanediol

2,3-BD is chemically synthesized from fossil fuel-based raw materials. Light hydrocarbons from the cracking of longer hydrocarbon chains are purified, obtaining a C4-hydrocarbon rich fraction. This fraction consists of approximately 77 % butenes and 23 % mixture of butane and isobutane. Treatment by chlorohydrination, cyclization and hydrolysis yields a mixture of all three stereoisomeric forms of 2,3-BD which can be purified in downstream processing (Gräfje *et al.*, 2012).

Another method uses starch as raw material for 2,3-BD synthesis. Catalytic hydrolysis of starch yields glucose, which is then converted to sorbitol by hydrogenation. Sorbitol is cracked into a mixture of C2-4 dihydroxy alcohol and polyol. After removal of organic salts, the mixture is distilled and refined, yielding propylene glycol, ethylene glycol and butanediol (Ge *et al.*, 2011b)

Another recently developed method uses ethanol as starting material and involves the use of hydroxide radicals generated from the photolysis of hydrogen peroxide. These hydroxide radicals selectively attack α-hydrogen atom in ethanol to produce hydroxyethyl radicals, which subsequently undergo C–C coupling to form 2,3-BDH. This selective C–H breakage is determined by reaction rate and 2,3-BD purity as high as 91 % can be obtained. Since ethanol can be renewable produced, this method has the advantage of being a sustainable production route (Li *et al.*, 2016)

1.1.3 Biosynthesis and regulation of acetoin and 2,3-butanediol

Production of acetoin and 2,3-BD in microorganisms occur via the 2,3-butanediol pathway (2,3-BD pathway) and begins with glycolysis of saccharides to form pyruvate. In aerobic respiration, pyruvate enters the tricarboxylic acid (TCA) cycle and undergoes a series of metabolic reactions to release stored energy in the form of adenosine triphosphate (ATP). Under

anaerobic conditions, pyruvate may enter the mixed-acid fermentation pathways, which can lead to end-products such as ethanol, acetate, formate, succinate, lactate and 2,3-BD (Magee and Kosaric, 1987).

Pyruvate is the precursor metabolite of 2,3-BD in the 2,3-BD pathway. The 2,3-BD pathway involves three key enzymes: α-acetolactate synthase (ALS), α-acetolactate decarboxylase (ALDC) and 2,3-butanediol dehydrogenase (2,3-BDH, also known as acetoin reductase) which uses NAD^+/NADH as a cofactor. Specific stereoisomers of 2,3-BD are produced by their corresponding 2,3-BDHs (meso-2,3-/2R,3R-/2S,3S-BDH).

The function of the three key enzymes has been characterized in various 2,3-BD producers including *Klebsiella oxytoca* (*K. oxytoca*) (Shin *et al.,* 2012), *Klebsiella terrigena* (*K. terrigena*), *Enterobacter aerogenes* (*E. aerogenes*) (Blomqvist *et al.*, 1993), *Bacillus subtilis* (*B. subtilis*) (Renna *et al.,* 1993; Nicholson, 2008a), *Bacillus licheniformis* (*B. licheniformis*) (Thanh *et al.*, 2010; Huo *et al.*, 2018), *Paenibacillus polymyxa* (*P. polymyxa*) (Tong *et al.*, 2013) and *Enterobacter cloacae* (*E. cloacae*) (Xu *et al.*, 2012).

Beginning with pyruvate as a substrate and thiamine pyrophosphate (TPP) as a co-factor, ALS catalyses condensation of two pyruvate molecules to form α acetolactate; which is then converted to 3R-acetoin in the reaction catalysed by ALDC (**Figure 1.1**) (Magee and Kosaric, 1987; Roncal *et al.*, 2017). α-acetolactate may also undergo non-enzymatic oxidative decarboxylation (NOD) to form DA in the presence of oxygen. DA can be catalytically converted to 3S-acetoin by diacetyl reductase (DAR).

The 2,3-BD stereoisomer produced in the 2,3-BD pathway depends on the enzyme in the microorganism. For example, 3S-acetoin can be reversibly converted to 2S,3S-BD, catalysed by 2S,3S-BDH (Z. Liu *et al.*, 2011), while meso-2,3-BDH from *B. licheniformis* is also able to catalyse the reduction of DA to 3S-acetoin and then further catalyse the conversion of the produced 3S-acetoin to 2S,3S-BDH (Xu *et al.*, 2016). The same meso-2,3-BDH enzyme from *B. licheniformis* can also catalyse the reversible conversion of 3R-acetoin to meso-2,3-BD. In *B. subtilis* and *P. polymyxa*, 3R-acetoin can be reversibly converted to 2R,3R-BD or which is catalysed by 2R,3R-BDH (Renna *et al.*, 1993; Yu *et al.*, 2011).

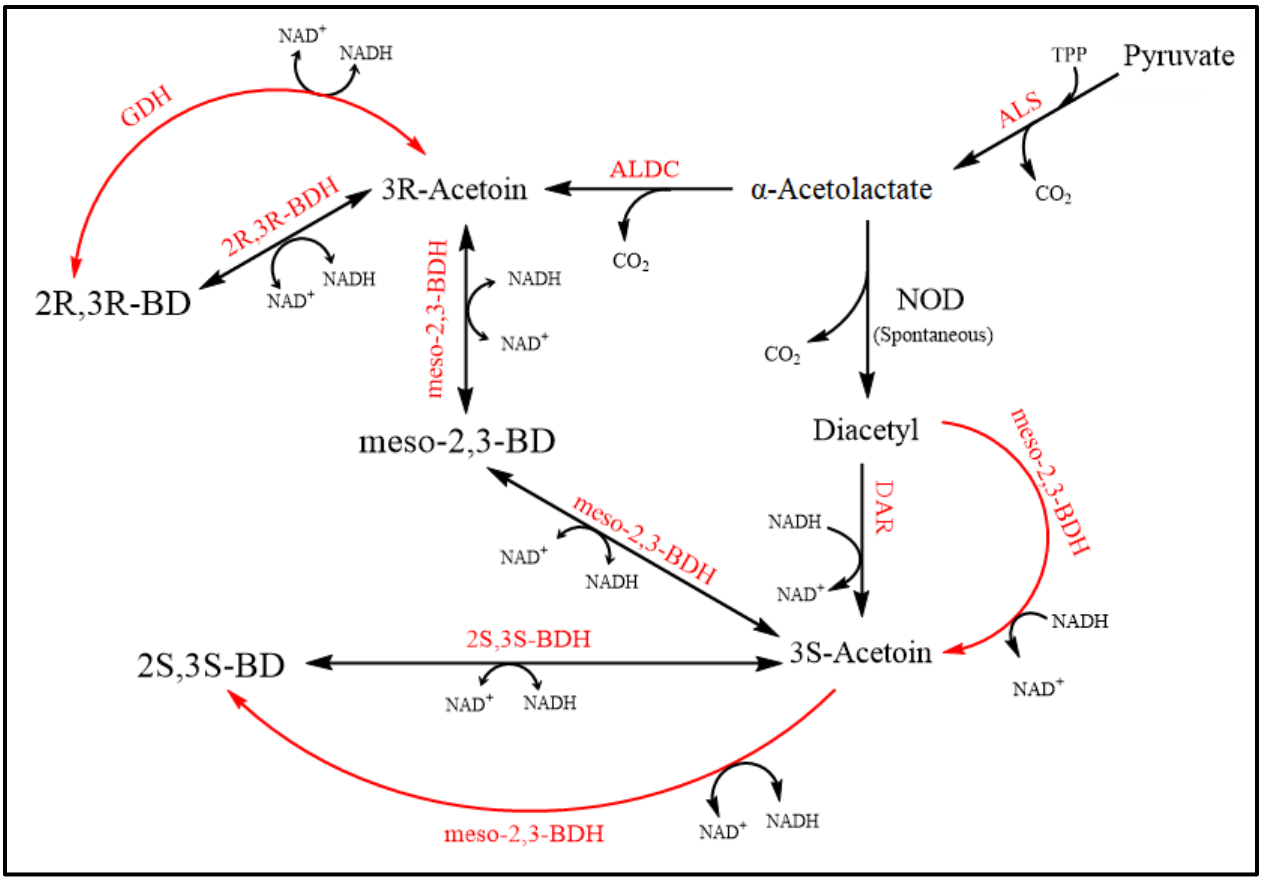

Figure 1.1. Overview of the 2,3-BD pathway, showing the possible biochemical pathways catalysed by different enzymes for the production of all three stereoisomers of 2,3-BD using pyruvate as starting metabolite. Red arrows indicate reactions known to occur in *B. licheniformis* with. Stoichiometry not taken into account. Enzymes in red text. ALDC, α-acetolactate decarboxylase; ALS, α-acetolactate synthase; DAR, diacetyl reductase; -BDH, -butanediol dehydrogenase; GDH, glycerol dehydrogenase; NOD, non-enzymatic oxidative decarboxylation; TPP, thiamine pyrophosphate. Adapted from (Ge, *et al.*, 2016).

Experimental evidence has revealed that glycerol dehydrogenases (GDHs) are also involved in the formation of specific 2,3-BD stereoisomers. In *K. pneumonia*, GDH, encoded by *dhaD*, a catalyses the conversion of 3R-acetoin to 2R,3R-BD, and the conversion of diacetyl to meso-2,3-BD via 3S-acetoin as an intermediate (Chen *et al.*, 2014). The GDH enzyme in *B. licheniformis* 10-1-A was functionally assayed and demonstrated the ability to catalyse conversion of 3R-acetoin to 2R,3R-BD (Li *et al.*, 2013a).

As reviewed by Yang *et al.*(2017), 2,3-BDHs originating from *B. subtilis*, *B. licheniformis*, *K. oxytoca*, *E. cloacae* are in general NADH dependent (Wang *et al.*, 2012; Raedts *et al.*, 2014;

Fu *et al.*, 2016a; Yang *et al.*, 2017). The isomer identity of the 2,3-BD produced differ among species, although in general, a mix of two isomers is formed (Ji *et al.*, 2011).

Along with ALS, there are four other TPP-dependent dependent enzymes capable of catalysing production of α-acetolactate. The four other enzymes are acetohydroxy acid synthase (AHAS), pyruvate decarboxylase (PDC), pyruvate oxidase (POX) and pyruvate dehydrogenase (PDH) (Forlani, Mantelli and Nielsen, 1999; Xiao and Lu, 2014a). As reviewed by Xiao and Lu (2014), POX, PDC, and PDH catalyse different main reactions in different organisms. α-acetolactate and acetoin are by-products resulting from the side reactions these enzymes can also catalyse, which has been demonstrated and studied in plant cells, yeast and bacteria.

AHAS has been described as the anabolic α-acetolactate synthase, while ALS as the catabolic counterpart. AHAS plays a key role in the biosynthesis of the branched-chain amino acids L-valine, L-leucine and L-isoleucine. The enzyme catalyses the condensation reaction of two pyruvate molecules, to produce α-acetolactate, or of 2-ketobutyrate, to produce 2-aceto-2-hydroxybutyrate. The latter enzyme product may undergo a series of reaction to eventually form L-isoleucine, whileα-acetolactate may also undergo several reactions to eventually be converted to L-valine or L-leucine (Chiarla *et al.*, 1997). Interestingly, *in vitro* studies with purified ALDC from *Lactococcus lactis* (*L. lactis*) have showed that ALDC is allosterically activated by binding of the three branched amino acids (Phalip *et al.*, 1994), suggesting that the enzyme plays a role in preventing excessive accumulation of the amino acids. This highlights the possible intricate relationship of the 2,3-BD pathway with other biochemical pathways.

The regulation and location of the genes encoding the three key enzymes differ among bacterial species. For example, *K. terrigena* and *E. aerogenes* have all three genes co-located on their genome as the *budABC* operon. While in *B. subtilis*, *alsS* (encoding ALS) and *alsD* (encoding ALDC) are found within the *alsSD* operon, while the gene encoding 2,3-BDH is located separately (Frädrich *et al.*, 2012). One common feature between the *budABC* and *alsSD* operons described for the species above, is that they are regulated at the transcriptional level by a LysR-type regulator protein. In *B. subtilis*, the regulator protein is encoded by *alsR* which is transcribed in the opposite direction to the *alsSD* operon, regulated by its own promoter. Disruption of *alsR* gene leads to near zero expression of the *alsSD* operon (Renna *et al.*, 1993).

In *K. terrigena,* the *budABC* operon is regulated by BudR, encoded by the *budR* gene, also transcribed in the opposite direction and is separated by a non-translated 106 bp region from the *budABC* operon (Mayer, Schlensog and Bock, 1995).

1.1.4 Physiological role of acetoin and 2,3-butanediol

The 2,3-BD pathway is part of the mixed-acid fermentation pathway in which acidic end-products such as acetate, succinate, lactate and formate may accumulate, causing undesired increase in intracellular acidity. Shifting the metabolic flux towards the synthesis of neutral acetoin and 2,3-BD allows the cell to regulate intracellular pH levels (Yu and Saddler, 1982; Vivijs *et al.,* 2014). In addition, the conversion of acetoin to 2,3-BD is reversible and so the pathway likely plays a role in the regulation of reducing power within the cell (Johansen, Bryn and Stormer, 1975).

Acetoin and 2,3-BD may also be catabolized when nutrient availability is scarce (Oppermann, Schmidt and Steinbuchel, 1991). In *B. subtilis* 168, the *acoABCL* operon encodes four genes (*acoA, acoB, acoC* and *acoL*) that form the acetoin dehydrogenase complex involved in the degradation of acetoin for energy when other preferred energy sources, such as glucose, are depleted. The operon is regulated by the protein product of the *acoR* gene, which acts as a transcriptional regulator. Expression of this operon has been shown to be induced by the presence of acetoin and repressed by glucose in the growth medium (Huang, Oppermann-Sanio and Steinbüchel, 1999; Ali *et al.,* 2001). In *B. licheniformis DSM13,* the two operons *acoABCL* and *acuABC* were identified to be involved in acetoin catabolism (Thanh *et al.,* 2010).

Interestingly, it was recently proposed that the *alsSD* operon to be involved in anti-cell lysis mechanism in *Staphylococcus aureus* by preventing accumulation of acetate in acetate-mediated cell death and lysis (Chaudhari *et al.,* 2016).

1.1.5 Engineering strategies for acetoin and 2,3-butanediol microbial production

Table 1.1 shows an overview of strategies employed by earlier studies to optimize acetoin yield by microbial production. As extensively reviewed by Xiao *et al.* (2014) and Yang *et al.* (2017), there are numerous reports of enhanced acetoin and 2,3-BD production achieved by metabolic

engineering, optimizing fermentation conditions, or combination of both, in various microorganism, a few examples will be described here.

The first step in metabolic engineering is often to identify a suitable specie for production. In the case of acetoin and 2,3-BD, naturally high 2,3-BD producers such as *K. pneumonia*, *K. oxytoca* and *E. aerogenes* are attractive candidates (Mayer, Schlensog and Bock, 1995; Ji, Huang, Du, Zhu, Ren, Li, *et al.*, 2009; Ma *et al.*, 2009; Ji *et al.*, 2010; Jung *et al.*, 2012). Ma *et al.* (2009) evaluated *K. pneumonia* DSM strain as a potential 2,3-BD producer, and reported a maximum titer of 150 g/l after 38 hours in fed-batch fermentation (working volume 3 L) with a productivity of 4.21 g/(L h) by optimizing fermentation conditions only.

Table 1.1. Summary of strategies and results of acetoin producing microorganisms from selected previous studies.

Strain	**Substrate**	**Strategy**	**Titer (g/L)**	**Yield (g/g)**	**Reference**
B. amyloliquefaciens E-11	Glucose	Increased acetoin tolerance by adaptive evolution. Optimized culture conditions.	71.5	0.41	Luo *et al.* (2014)
B. licheniformis WX-02Δ*budC*ΔacoR	Glucose	Inactivation of *budC*, *acoR* and *gdh* genes. Optimized culture conditions.	78.8	0.31	Lu *et al.* (2017)
B. licheniformis MEL09	Glucose	Wild type; optimized culture conditions, thermophilic production.	41.3	0.42	Liu *et al.*, (2011)
B. subtilis UW06	Glucose	*bdhA* and *acoA* double-knockout and overexpression of *alsSD* operon.	20.0	0.38	Wang *et al.* (2012)
B. subtilis DL01	Glucose	Wild type; stage-enhanced agitation.	76.0	0.42	Dai *et al.*, (2015)
P. polymyxa CS107	Glucose	Wild type; optimization of medium components and oxygen supply.	55.3	0.76	Zhang *et al.* (2012)

Overexpression of the three key enzymes in the 2,3-BD pathway is a common strategy to increase production of acetoin and 2,3-BD. *K. oxytoca* M1 strain grown on glucose achieved a titer of 118.5 g/L after 97 hours of fed-batch fermentation with a working volume of 1-L. Upon introducing the pUC18MC-*budC* plasmid harbouring the *budC* gene to the bacterium, the resulting recombinant strain, *K. oxytoca* M1(pUC18CM-*budC*) achieved an even higher titer of 142.5 g/L 2,3-BD under same conditions compared to its parents strain (Cho *et al.*, 2015).

Heterologous expression of the 2,3-BD pathway gene cluster has been demonstrated in the model organism *Escherichia coli* (*E. coli*), which does not naturally produce acetoin or 2,3-BD (Sadaharu *et al.*, 1997; Nakashima, Akita and Hoshino, 2014; J. E. N. Müller *et al.*, 2015). For instance, the recombinant *E. coli* MQ1 harbouring the co-expressing plasmid pTrc99a-*budB-budA-ydjL* reached a relatively high 2R,3R-BD titer of 115 g/L by fed-batch cultivation with yield and productivity up to 0.42 g/g and 1.44 g/(L h), respectively (Ji *et al.*, 2015)

The reversible conversion of acetoin to 2,3-BD is NAD^+/NADH dependent, and so co-factor engineering has been widely applied to optimized yield of both acetoin and 2,3-BD (Bao *et al.*, 2015; Yang *et al.*, 2015; Liang and Shen, 2017). A common strategy to accumulate 2,3-BD is by heterologously expression NADH oxidase to lower NADH/NAD^+ ratio, as was done in *K. pneumonia* (Ji *et al.*, 2013). Other engineering strategies applicable to both acetoin and 2,3-BD production include shutting off competing pathways to increase flux towards the 2,3-BD pathway (Ji *et al.*, 2008) and increasing pyruvate concentrations by overexpressing the rate-limiting steps in glycolysis (Yang *et al.*, 2013).

1.2 The “Methanol Economy”

The “Methanol Economy” is a suggested future economy in which methanol has replaced fossil fuels as a means of energy storage and raw material for commodity and specialty compounds (Olah, 2003; Olah, Goeppert and Prakash, 2009).

1.2.1 Methanol is an already established platform chemical

Methanol (methyl alcohol, MeOH) is a clear liquid at room temperature that is miscible with water. The simple alcohol has an energy density of 22.7 MJ/kg, making it well suited as an energy storage compound (Bertau *et al.*, 2014). Compared to hydrogen and biogas, it is easy to store and transport, and existing oil refineries can be easily accommodated to process methanol (Tibdewal, Saxena and Gurumoorthy, 2014). Methanol can also be produced as a pure chemical, allowing complete utilization compared to biomass-waste residues such as sugarcane molasses (Nærdal *et al.*, 2014).

Methanol is an established carbon feedstock in the chemical industry, being converted to various other important commodity chemicals (formaldehyde, methyl *tert*-butyl ether, acetic acid, dimethyl ether, etc.). For these reasons its production, storage and transport regulations are well established (Ott *et al.*, 2012).

1.2.2 Methanol can be produced from renewable biomass

Today, methanol is mostly commercially produced from synthesis gas (syngas), which is a mixture of hydrogen gas and carbon monoxide/carbon dioxide. It is a valuable intermediate used for the heterogenous catalytic production of both ammonia and methanol (Ott *et al.*, 2012). A wide range of carbon-containing raw materials can be used for production of syngas, including coal, natural gas and oil (Yin *et al.*, 2005; Aasberg-Petersen *et al.*, 2008). However, given the societal and environmental drawbacks of fossil fuels (Barbir, Veziroğlu and Plass, 1990), production of bio-methanol from renewable sources such as biogas (Kralj and Kralj, 2010) and industrial biomass-waste has been an area of active research. Hamelinck and Faaj (2002) reviews the bioconversion of biomass to methanol via syngas, in which main steps include a gasification of the biomass, steam reforming to purify the syngas, and finally methanol synthesis.

Furthermore, Kamarudin *et al.* (2013) investigated the production of methanol from different types of industrial biomass-wastes (livestock waste, wood residue, rice husks, sugarcane bagasse, etc.) by pyrolysis. Although the yields were too low to be economical, it highlights the potential of a closed-loop production model were waste material can be recycled (Kamarudin *et al.*, 2013). Lastly, Feng *et al.* (2011) investigated the key parameters that can be optimized to increase efficiency and yield of the biomass-syngas-methanol production line by simulations with a kinetic model (Feng *et al.*, 2011)

Moreover, there are several active refineries commercially producing bio-methanol at an industrial scale. Located in the Netherlands, BioMCN (http://www.biomcn.eu/) is one of Europe's largest methanol producers and is the first company in the world to produce and sell industrial quantities of high quality bio-methanol.

In Canada, Enerkem (https://enerkem.com/) specializes in utilizing municipal waste resources to produce renewable chemicals, including methanol.

Lastly, a bio-methanol plantation with an expected capacity of 375 000 L of bio-methanol per day is to be constructed in the Hagfors area, Sweden. It takes an advantage of the locations abundance of forest biomass (Gillberg, 2009; Bertau *et al.*, 2014).

In conclusion, a larger share of methanol production is expected to become more sustainable in the future, which supports its potential as a future mainstay energy source.

1.2.3 Methanol as feedstock for microbial production of valuable chemicals

Methylotrophy is the utilization of organic compounds containing one or more carbon atoms, but free of carbon-carbon bonds (C1 compounds), by microorganisms. Obligate methylotrophs can only use C1 compounds as sole carbon and energy sources, while facultative methylotrophs are capable of growing on other compounds in addition to C1 compounds (Dalton, 1983). As reviewed by Zhang *et al.* (2017), more and more research is being dedicated to developing methods for utilizing methylotrophs to convert methanol to valued chemicals.

In the proposed "Methanol Economy", valuable chemicals such as essential amino acids, acetoin and 2,3-BD are sustainably produced from methanol (Olah, Goeppert and Prakash, 2009), and methylotrophic bacteria capable of growing on methanol could be the tool for the bioconversion

of methanol to industrially relevant chemicals. Due to the lack of genetic tools for many methylotrophic species, introduction of synthetic methylotrophy in model organisms such as *E. coli* has been explored and demonstrated (J. E. N. Müller *et al.*, 2015; Whitaker *et al.*, 2017).

1.3 *Bacillus methanolicus* is a Potential Candidate for Microbial Production

During the initial attempts at isolating thermophilic methylotrophs dating back to 1988 (Dijkhuizen *et al.*, 1988), several strains of thermotolerant methanol utilizing spore-forming bacteria were obtained. Phylogenetic analysis of 16S and 5S rRNA of those strains revealed a new species belonging to the *Bacillus* genus. The new species was named *Bacillus methanolicus* (*B. methanolicus*).

1.3.1 *Bacillus methanolicus* displays plasmid dependent methylotrophy

B. methanolicus is a Gram-positive facultatively methylotrophic thermophile capable of utilizing methanol as its sole carbon and energy source. It is capable of growing at temperatures between 35°C and 60°C (Arfman *et al.*, 1992), with an optimal growth temperature at 50–53°C (Bozdag, Komives and Flickinger, 2015). The genome of the model strain, *B. methanolicus* MAG3 has been sequenced, revealing a 19 kbp plasmid designated pBM19, a 69 kbp plasmid designated pBM69 and a single circular 3,3 Mbp chromosome (Tonje M.B. Heggeset *et al.*, 2012). Methylotrophy in *B. methanolicus* MGA3 is pBM19-dependent. Brautaset *et al.* (2004) demonstrated that pBM19-cured *B. methanolicus* MGA3 was incapable of utilizing methanol as carbon source (Brautaset *et al.*, 2004).

The pBM19 plasmids contains the *mdh* gene encoding a NAD^+-dependent methanol dehydrogenase (MDH) which catalyses the oxidation of methanol to formaldehyde, using NAD^+ as co-factor. MDHs are classified into 3 distinct groups based on their electron acceptor: pyrroloquinoline quinone (PQQ) dependent, NAD^+-dependent, or oxygen dependent (Dalton, 1983; Krog *et al.*, 2013).

Electron microscopy has provided insight into the molecular structure of MDH found in *B. methanolicus*, revealing a decamer where each subunit contains one Zn^{2+} atom, one or two Mg^{2+} atoms and a non-covalently bound NAD^+ (Vonck *et al.*, 1991). *In vitro* studies with purified enzymes have shown that the relatively low NAD^+-dependent MDH activity is strongly stimulated by addition of soluble activator (ACT) protein encoded by *act* gene found on the chromosome.

Interestingly, the genome sequence of *B. methanolicus* reveals two additional *mdh* genes found on the chromosome, *mdh2* and *mdh3*, encoding MDH2 and MDH3. The deduced MDH2 and MDH3 proteins are 96 % identical to each other, sharing 61 % and 62 % overall sequence identity to the pBM19-encoded *MDH* protein (Tonje M.B. Heggeset *et al.*, 2012).

In addition to *mdh*, pBM19 contains five other genes coding for enzymes involved in ribulose monophosphate (RuMP) pathway: *pfk*, encoding phosphofructokinase (PFK); *rpe*, encoding ribulose-5-phosphate-3-epimerase (RPE); *tkt*, encoding transketolase (TKT); *glpX*, encoding fructose-1,6-bisphosphatase (GlpX) and finally *fba*, encoding fructose-1,6-bisphosphate aldolase (FBA). The RuMP pathway is an assimilatory pathway allowing the fixation of formaldehyde produced from methanol in reaction catalysed by MDH (Jakobsen *et al.*, 2006).

1.3.2 Formaldehyde assimilation via ribulose monophosphate pathway

There are three major groups of bacteria that fix formaldehyde via the RuMP pathway, Gram-negative obligate methylotrophs, Gram-positive facultative methylotrophs, and thermotolerant *Bacillus* species; *B. methanolicus* belonging to the latter (de Vries, Kües and Stahl, 1990). The RuMP pathway can be divided into 3 phases: fixation, cleavage and regeneration (Zhang *et al.*, 2017).

The fixation phase involves 2 unique enzymes, 3-hexulose-6-phosphate synthase (HPS) and 6-phospho-3-hexuloisomerase (PHI) encoded by *hps* and *phi* respectively. HPS catalyses the fixation of formaldehyde with ribulose-5-phosphate (Ru-5-P) to produce the intermediate hexulose-6-phosphate (H-6-P). PHI subsequently catalyses conversion of H-6-P to fructose-6-phosphate (F-6-P), which enters the cleavage phase involving the lower glycolytic pathway. PFK catalyses phosphorylation of F-6-P to fructose-1,6-biphosphate (FBP), while FBA catalyses cleavage of FBP to produce glyceraldehyde-3-phosphate (GAP) and dihydroxyacetone phosphate (DHAP), the latter can be converted to GAP in a rearrangement reaction catalysed by triose phosphate isomerase (TPI) (Kato, Yurimoto and Thauer, 2006). GAP can be converted to acetyl-CoA with pyruvate as an important intermediate metabolite. Acetyl-CoA can then enter the TCA cycle to release stored energy (Fernie, Carrari and Sweetlove, 2004).

Ru-5-P needs to be regenerated in order to for the cycle to be repeated. There are two variants of the regeneration phase: the transaldolase (TA) variant and the sedoheptulose-1,7-bisphosphatase (SPBase) variant. Both of them involve three enzymes: TKT, RPE, and ribose 5-phosphate isomerase (RPI) and both involve the production of sedoheptulose 7-phosphate (S-7-P) (Stolzenberger *et al.*, 2013).

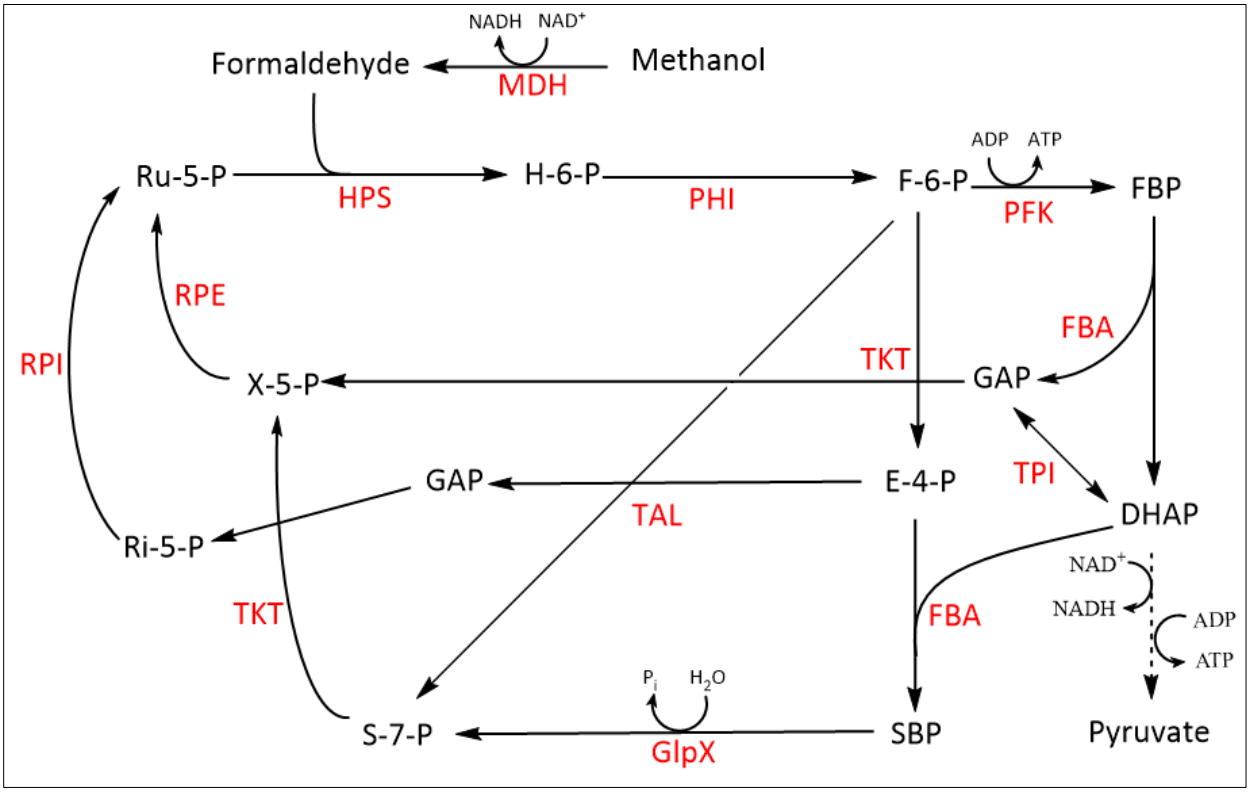

Figure 1.2. Overview of biochemical reactions involved in methanol oxidation and assimilation via the RuMP cycle in *B. methanolicus*. Enzymes are labelled red. Stoichiometry not taken into account. Dashed arrow indicates multiple reactions. Enzymes: FBA, fructose-1,6-bisphosphate aldolase; GlpX, fructose-1,6-bisphosphatase; HPS, 3-hexulose-6-phosphate synthase; MDH, methanol dehydrogenase; PFK, phosphofructokinase; PHI, 6-phospho-3-hexuloisomerase; RPE, ribulose-5-phosphate-3-epimerase; RPI, ribose-5-phoshate isomerase; TAL, transaldolase; TKT, transketolase; TPI, triose phosphate isomerase. Metabolites: DHAP, dihydroxyacetone phosphate; E-4-P, erythrose-4-phosphate; FBP, fructose-1,6-biphosphate; F-6-P, fructose-6-phosphate; GAP, glyceraldehyde-3-phosphate; H-6-P, hexulose-6-phosphate; Ri-5-P, ribose-5-phosphate; Ru-5-P, ribulose-5-phosphate; SBP, sedoheputlose-1,7-biphosphate; S-7-P, sedoheptulose-7-phosphate; X-5-P, xylose-5-phosphate. Adapted from (Heggeset *et al.*, 2012)

In the TA variant, erythrose-4-phosphate (E-4-P) and F-6-P are directly converted to S-7-P and GAP in a reaction catalysed by transaldolase (TAL). TKT acts upon these respective C7 and C3 compounds to produce ribose-5-phosphate (Ri-5-P) and xylose-5-phosphate (X-5-P). Ri-5-P and X-5-P are converted to Ru-5-P in the reactions catalysed by RPI and RPE, respectively. In the SBPase variant, DHAP and E-4-P are the starting molecules. They are condensed to form sedoheputlose-1,7-biphosphate (SBP), in a reaction catalysed by FBA. SBP is subsequently dephosphorylated in reaction catalysed by GlpX to form S-7-P. S-7-P and GAP are converted to Ri-5-P and X-5-P in reaction catalysed by TKT. Both Ri-5-P and X-5-P are subsequently converted to Ru-5-P (Brautaset *et al.*, 2004; Stolzenberger *et al.*, 2013).

Inspection of the *B. methanolicus* MGA3 genome revealed a chromosomally located *tal* gene encoding TAL and that all five genes encoding RuMP pathway enzymes found in pBM19 has a chromosomally located homolog. MGA3 thus contains all the enzymes for both variants of the RuMP pathway (Tonje M.B. Heggeset *et al.*, 2012).

Recent work has elucidated different biochemical properties between the chromosomal and plasmid variants of some of the RuMP enzymes in *B. methanolicus*. *In vitro* analysis of the plasmid-encoded FBA (FBA^P) shows that it has a higher affinity for GAP and DHAP than the chromosome-encoded homolog FBA (FBA^C), indicating that FBA^P plays a role in gluconeogenesis. On other hand, FBA^C is likely to be responsible for catalysing the cleavage of FBP (Stolzenberger *et al.*, 2013). Enzyme assay of purified chromosomally encoded GlpX ($GlpX^C$) revealed higher catalytic efficiency for the dephosphorylation of FBP, while the plasmid encoded GlpX ($GlpX^P$) demonstrated both of SBPase and fructose-1,6-biphosphatase activity. Based on *in vitro* experimental results, $GlpX^P$ appears to be a promiscuous phosphatase and the major SBPase acting in the SBPase variant of the RuMP cycle (Stolzenberger *et al.*, 2013).

Real-time PCR studies with *B. methanolicus* cells grown on methanol reveal upregulation of the expression of all genes found in pBM19 (from 4- to 60-fold), as well as the chromosomal *hps* and *phi* genes. These seven enzymes (excluding MDH) are all involved in the SBPase variant of the RuMP pathway. Hence, the SBPase variant appears to be preferred RuMP pathway in *B. methanolicus* (Brautaset *et al.*, 2004; Jakobsen *et al.*, 2006; Stolzenberger *et al.*, 2013).

In addition to the assimilatory RuMP cycle, formaldehyde has been experimentally shown to enter a linear tri- and tetraglutamylated tetrahydrofolate (THF) dissimilatory pathway (Pluschkell

and Flickinger, 2002; J. Müller *et al.*, 2015). Formaldehyde is highly toxic due to its high reactivity with thiol and amide groups found in proteins and DNA respectively (Chen *et al.*, 2016). The intracellular formaldehyde concentration can be efficiently regulated by the three pathways mentioned above and prevent undesired accumulation. Understanding the carbon flux from methanol is important in optimizing yields of desired products in engineered *B. methanolicus* strains (Brautaset *et al.*, 2007).

1.3.3 Genetic tools available for *Bacillus methanolicus*

For a bacterium to be a potential candidate as a microbial producer of valuable chemicals, it needs to have a well-established genetic toolbox that allows efficient manipulation of its cellular metabolism. This is one of the primary reasons model organisms such as *E. coli* are popular as potential microbial producers and the reasoning behind efforts in engineering synthetic methylotrophy in *E. coli* (Yan, Lee and Liao, 2009; Xu *et al.*, 2014; Ji *et al.*, 2015).

Recent transcriptome analysis has enabled insight to the transcriptional landscape of *B. methanolicus* and allowed determination of consensus sequences of several regulatory elements including ribosome binding sites (RBS), -10 and -35 consensus sequences in the promoter region, transcription start sties (TSS) and translation start sites (TLS). The average distance between some of these regulatory elements has also been analysed, as previous studies with synthetic promoter libraries (SPL) have revealed that the sequence and length of the spacer regions surrounding the -10 and -35 regions can have a profound effect on the expression level of reporter genes (Jensen and Hammer, 1998; Li and Zhang, 2014).

The RBS consensus sequence in *B. methanolicus* MGA3 was determined to be “aGGaGg”, identical to the bacterial consensus sequence AGGAGG (Shine and Dalgarno, 1974). Nucleotides in capital letters were present in approximately 90 % of the analysed sequences, while small letters equal present in 40 % or lower. The distance between the RBSs and the TLSs varies between 5 to 10 nt with an average spacing of 7.4 bases. The −10 promoter sequence “TAtaaT”, which is identical to the *E. coli* -10 consensus sequence TATAAT, was also identified. The average distance between the -10 consensus sequence to its neighbouring TSS was 6.7 nt. A weakly conserved −35 motif “ttgana” was also determined, which shares similarity to the -35 consensus sequence TTGACA (Irla *et al.*, 2015).

The genetic toolbox for *B. methanolicus* has been intensely developed since its first isolation and characterization. Identification of a *Bme*TI restriction-modification (RM) system, which serves as a protective system against viral infection, within *B. methanolicus* laid the foundation for the first established transformation protocol (Cue, Lam and Hanson, 1996; Cue *et al.*, 1997). Two *E. coli*/*B. subtilis* shuttle vectors, pEN1 and pHP13, were initially evaluated for use in engineering *B. methanolicus* (Cue *et al.*, 1997). The pHP13 plasmid has since been widely used as an expression vector in *B. methanolicus* and has been modified with the addition of the *mdh* promoter from pBM19, yielding pHP13mp. The *mdh* promoter is constitutively active in both *E. coli* DH5α and *B. methanolicus* MGA3 (Nilasari *et al.*, 2012; Nærdal *et al.*, 2014). Furthermore, addition of a *Pci*I restriction site downstream of the *mdh* promoter, allowing a one-step cloning procedure, lead to the creation of the pTH1mp expression vector (**Figure 1.3**) (Jakobsen *et al.*, 2009; Brautaset *et al.*, 2010; Krog, Heggeset, *et al.*, 2013; Nærdal *et al.*, 2015).

pNW33N, an established shuttle *E. coli*/*Bacilli* vector, and the optimized green fluorescent protein (GFPuv) was tested for applicability in *B. methanolicus*, resulting in the pNW33N-*mdh*-GFPuv plasmid, by sub-cloning of the *mdh* promoter from pBM19. The authors demonstrate the use of a shorter transformation protocol for *B. methanolicus* and demonstrates the use of GFPuv as a viable reporting system (Nilasari *et al.*, 2012).

As mentioned above, much of the previous metabolic engineering studies performed in *B. methanolicus* uses pHP13/pTH1mp as expression vectors. In an effort to expand the genetic toolbox of *B. methanolicus*, Irla *et al.* (2016) compared three plasmids with different copy numbers: pUB110Smp, pNW33Nmp and pBV2mp, to pTH1mp as new candidates for gene expression in *B. methanolicus* MGA3. The pUB110Smp plasmid displayed high segregational stability over 60 generations, determined by following GFPuv fluorescence levels. On the other hand, pTH1mp-*gfpuv* showed lower stability over the same course. Combined with its high copy number and compatibility with pTH1mp, pUB110Smp is a very feasible expression vector for *B. methanolicus* MGA3 (Irla *et al.*, 2016).

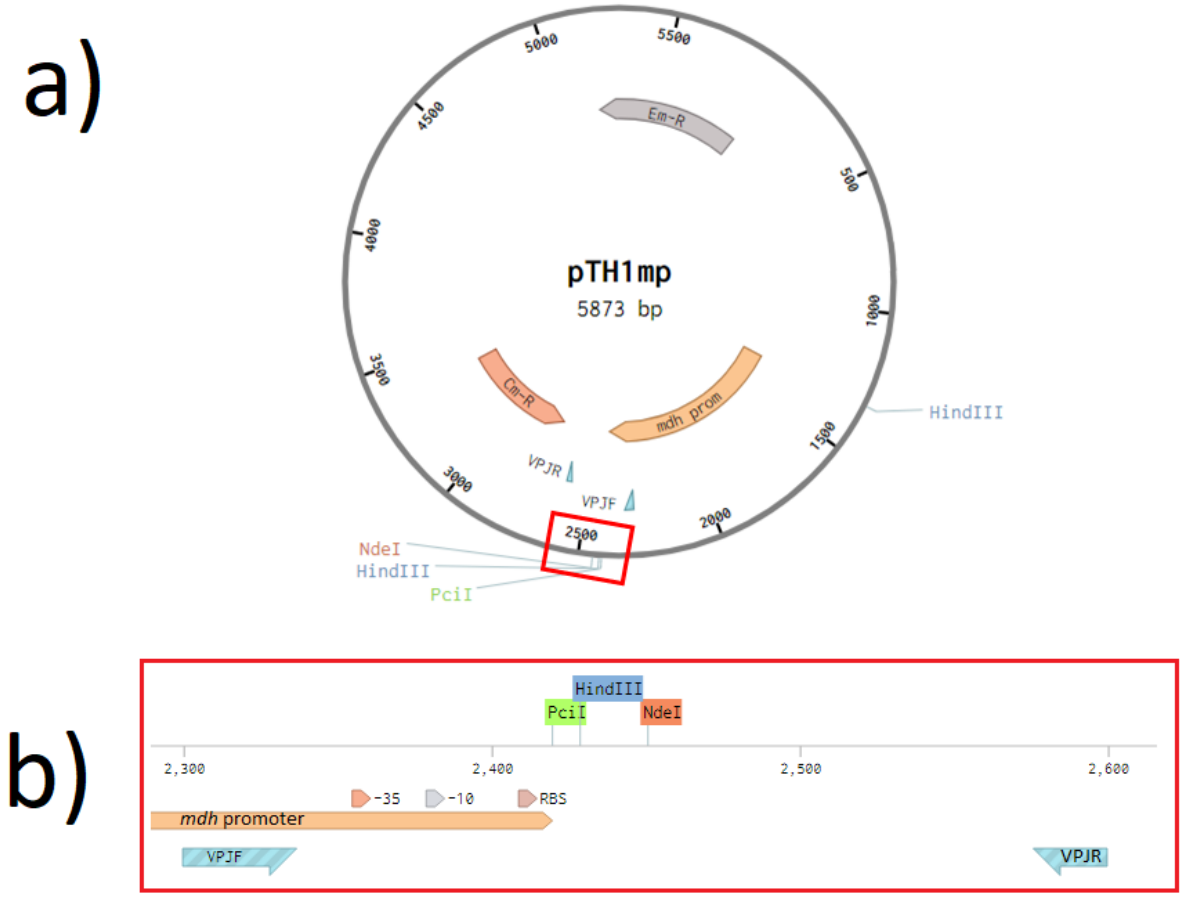

Figure 1.3. pTH1mp plasmid. Scale bar shows arbitrary position of base pairs. Only few selected annotations shown. a), binding sites of VPJF/VPJR primer pair (blue triangles) used for colony PCR (**Chapter 2.11.1**) are indicated. mdh prom, *mdh* promoter of pBM19; Cm-R, coding region of selection marker *cmr* gene conferring resistance to chloramphenicol; Em-R, coding sequence of selection *emr* gene conferring erythromycin resistance. Restriction sites of *Hind*III, *Nde*I and *Pci*I are indicated. Red rectangle highlights cloning site. b), enlarged view of the cloning site on the pTH1mp plasmid. Binding sites of VPJF/VPJR primer pair (striped blue arrows) used for colony PCR (**Chapter 2.11.1**) are indicated. Positions of -10 (grey arrow), -35 (orange arrow) consensus sequences and RBS (brown arrow) are shown. Cut sites of *Hind*III, *Nde*I and *Pci*I are indicated.

1.3.4 *Bacillus methanolicus* is an already established microbial producer

Initial interest in *B. methanolicus* MGA3 as a microbial producer stems from the high amount of L-glutamate by the wild type strain MGA3 during methanol-controlled high cell density fed-batch fermentations (Brautaset *et al.*, 2007). *B. methanolicus* MGA3 growing on methanol as carbon and energy source produced up to 59 g/L L-glutamate, on par with the current industrial

L-glutamate producer *Corynebacterium glutamicum* (*C. glutamicum*) (Ikeda and Takeno, 2013). Wild type *B. methanolicus* MGA3 produces however, only up to 0.2g/L of L-lysine in fed-batch fermentation (Brautaset *et al.*, 2003). Given the high value of L-lysine, which is an important amino acid in high demand, mainly used as animal feed for livestock, much research was dedicated to establishing *B. methanolicus* as a potential L-lysine producer. Efforts lead to the creation of multiple L-lysine overproducing by classical mutagenesis, including the auxotrophic L-lysine overproducing *hom-1* (encoding homoserine dehydrogenase) mutant NOA2#13A52-8A66 (Schendel *et al.*, 1990; Hanson *et al.*, 1996), which has reported to be able to produce 65 g/L of L-lysine during fed-batch methanol-controlled fermentations, albeit with significant titers of accumulating L-glutamate (Brautaset *et al.*, 2003). Furthermore, another *B. methanolicus hom-1* mutant strain, designated M168-20, was isolated by classical mutagenesis which achieved significantly higher L-lysine and L-glutamate titers (11 g/L and 69 g/L respectively) than wild-type MGA3 (Brautaset *et al.*, 2010).

There are several studies characterizing enzymes involved in the biosynthetic pathway of L-glutamate and L-lysine in *B. methanolicus*, paving the way for a more systematic approach in engineering amino acid producing strains. For example, Jakobsen *et al.* (2009) demonstrated that overexpression of enzymes involved in the aspartate pathway in MGA3 increased L-lysine production significantly, without affecting specific growth rate (Jakobsen *et al.*, 2009). The genomes of the aforementioned L-lysine overproducing strains NOA2#13A52-8A66 (Hanson *et al.*, 1996) and M168-20 (Brautaset *et al.*, 2010) were recently sequenced (Nærdal *et al.*, 2017); and the genes involved in the biosynthetic pathway of L-lysine, other amino acids and primary cell metabolism were mapped. Recent work has also demonstrated the possible heterologous expression of *cadA* (encoding lysine decarboxylase) gene from *E. coli* and glutamate decarboxylase gene from *Sulfobacillus thermosulfidooxidans* (gad^{St}) in *B. methanolicus* MGA3, which enabled production of cadaverine and γ-aminobutyric acid (GABA), respectively (Nærdal *et al.*, 2014; Irla *et al.*, 2017).

1.4 The Systematic Metabolic Engineering of *Bacillus methanolicus* MGA3 for Methanol-Based Production of Acetoin

The most prominent advantage of *B. methanolicus* is the ability to grow on inexpensive methanol as carbon and energy source, which can be exploited to convert methanol to acetoin (**Figure 1.1**). A systematic approach was undertaken in establishing acetoin producing *B. methanolicus* MGA3 strains.

First, acetoin tolerance in MGA3 was explored, and then *alsSD* operons from *B. licheniformis* DSM13, *B. subtilis* 168, *E. cloacae* SDM and *P. polymyxa* ATCC 12321 were cloned to the expression vector pTH1mp and heterologously expressed in MGA3. Enzyme activity and acetoin yield was then evaluated in successfully constructed strains. Furthermore, as acetoin is the precursor of 2,3-BD in the 2,3-BD the genes encoding 2,3-BDHs from the donor organisms were also cloned into pTH1mp and separately assayed in *B. methanolicus* MGA3, for potential acetoin reducing activity. The four donor organisms in this thesis are briefly described below.

1.4.1 *Bacillus licheniformis*

B. licheniformis is a Gram-positive rod-shaped endospore forming bacterium (Waschkau *et al.*, 2008). Growth and production of acetoin and 2,3-BD at 50°C and above is well described for this bacterium. (Wang *et al.*, 2012; Jurchescu *et al.*, 2013; Li *et al.*, 2013a). *B. licheniformis* is capable of producing and catabolizing acetoin and 2,3-BD, and the *alsS* and *alsD* genes are located within an operon designated *alsSD* (Qin, Gao and Wang, 2000; Huo *et al.*, 2018). The *budC* gene encoding meso-2,3-BDH has been characterized, and the enzyme encoded by *gdh* gene has demonstrated acetoin reducing activity (Ge, Li, Gao, *et al.*, 2016). Both genes are located separately from the *alsSD* operon. Interest in *B. licheniformis* as a potential 2,3-BD producer began as early as 1992 (Nilegaonkar *et al.*, 1992); various metabolic engineering strategies have been employed since to further this bacterium's potential as a microbial producer

Li *et al.* (2013a) determined the optimal fermentation conditions for 2,3-BD production in *B. licheniformis* 10-1-A, and demonstrated that the strain is capable of thermophilically producing 2,3-BD (highest titer and yield was achieved at 50 °C). Gene inactivation or overexpression of a specific 2,3-BDH has also enabled production of optically pure desired

2,3-BD isomer (Wang *et al.*, 2012; Fu *et al.*, 2016b). For example, (Qi *et al.*, 2014) demonstrated the production of high purity 2R,3R-BD with their genetically modified *B. licheniformis* WX-02 *ΔbudC* strain.

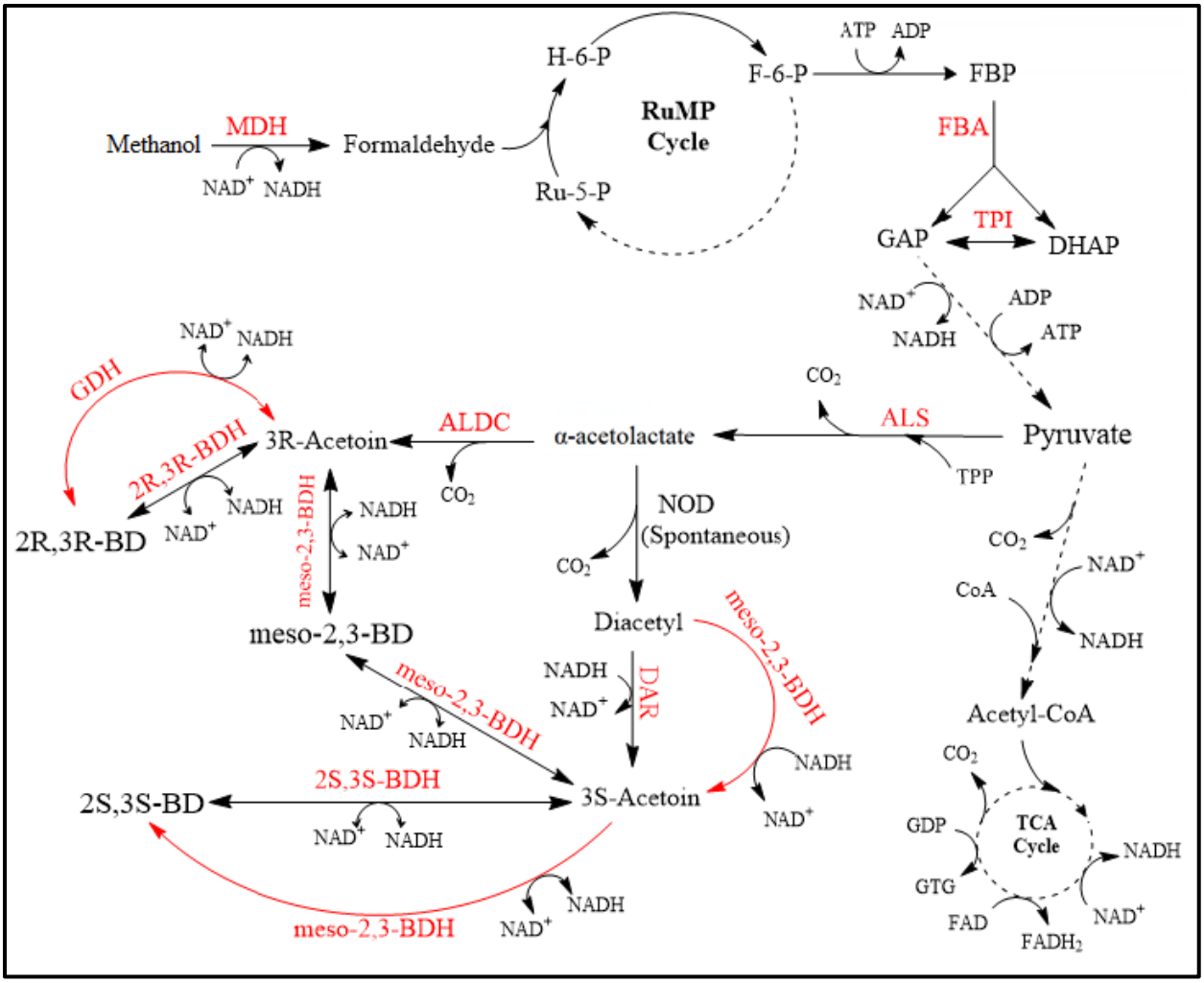

Figure 1.4. Overview of the biochemical conversion of methanol to acetoin and the three stereoisomeric forms of 2,3 BD in *B. methanolicus* MGA3. Enzymes in red text. Dashed lines indicate multiple reactions. Red arrows indicate reactions known to occur in *B. licheniformis* with. Stoichiometry not taken into account. NOD, non-enzymatic oxidative decarboxylation Enzymes: ALDC, α-acetolactate decarboxylase; ALS, α-acetolactate synthase; -BDH, -butanediol dehydrogenase; DAR, diacetyl reductase; FBA, fructose-1,6-biphosphate aldolase GDH, glycerol dehydrogenase; MDH, methanol dehydrogenase; TPI, triose phosphate isomerase. Metabolites: DHAP, dihydroxyacetone phosphate; H-6-P, hexulose-6-phosphate; F-6-P, fructose-1,6-biphosphate; GAP, glyceraldhyde-3-phosphate; Ru-5-P, ribulose-5-phosphate; TPP, thiamine pyrophosphate.

1.4.2 *Bacillus subtilis*

B. subtilis is also a Gram-positive rod-shaped bacterium. It is commonly found in soil and undergrowth, as well as human gastrointestinal tract (Pandey and Palni, 1997; Tam *et al.*, 2006). Several reports indicate *B. subtilis* to be a mesophile, growing optimally at 37 °C (Cook, 1996; el-Helow and Khattab, 1996; Vojcic *et al.*, 2012) . In this native 2,3-BD producer, the *alsS* and *alsD* genes are located in a *alsSD* operon positively regulated by the ALR protein, encoded by the *alsR* gene (Renna *et al.*, 1993). The previously erroneously named gene *bdhA* encoding a functional 2,3-BDH is found in a separate location (Nicholson, 2008b). The production of acetoin and 2,3-BD has been extensively explored in *B. subtilis*. (Biswas *et al.*, 2012; M. Wang *et al.*, 2012; Yang *et al.*, 2015). Knockout of the *bdhA* gene and *acoABCL* operon in *B. subtilis* was demonstrated to be an effective strategy to accumulate acetoin in growth medium (Wang *et al.*, 2012).

1.4.3 *Enterobacter cloacae*

E. cloacae is a Gram-negative mesophilic bacterium commonly found in the human gut flora (Gill and Suisted, 1978; Keller *et al.*, 1998). The genome of *E. cloacae* subsp. *dissolvens* SDM (*E. cloacae* SDM) strain was recently sequenced, revealing the presence of the *budABCR* operon coding for the three key enzymes involved in the 2,3-BD pathway (Xu *et al.*, 2012). The potential of this bacterium as a 2,3-BD producer is well documented (Gill and Suisted, 1978; A. Wang *et al.*, 2012; Zhang *et al.*, 2014; Li *et al.*, 2015), and it has been demonstrate to be capable of converting inexpensive industrial biomass-waste to 2,3-BD (Xu *et al.*, 2012; Zhang *et al.*, 2014; Li *et al.*, 2015). Acetoin production by *E. cloacae* SDM has also been explored. For instance, a systematically engineered *E. cloacae* SDM 53 strain was able to utilize lignocellulosic hydrolysate for production of acetoin, achieving a titer of 45.6 g/L acetoin, with productivity 1.52 g/(L h)

Furthermore, in a systematic approach to metabolically engineer *E. coli* for 2,3-BD production, various 2,3-BD gene clusters from different microorganisms were heterologously expressed in *E. coli* BL21. *E. cloacae* SDM *budABCR* operon was cloned into the expression vector pET28a, yielding pET-RABC. The *E. coli* BL21/pET-RABC strain produced the highest amount of

2,3-BD among the strains tested (73.8 g/L after 64 hours, productivity of 1.19 g/L h^{-1}) in optimized conditions (Xu *et al.*, 2014).

1.4.4 *Paenibacillus polymyxa*

P. polymyxa is a Gram-positive aerobic, rod-shaped, endospore-forming bacterium that can be found in soil and symbiotically associated with plant roots (Jeon *et al.*, 2010). Its property as a plant growth-promoting rhizobacterium capable of nitrogen fixation is well described (Timmusk *et al.*, 2005). The effect of *P. polymyxa* GBR-1 strain colonizing ginseng roots have been studied at different temperatures (4°C to 30°C) indicating that *P. polymyxa* is a mesophile (Timmusk *et al.*, 2005; Jeon *et al.*, 2010; Kim *et al.*, 2016). The genome of *P. polymyxa* ATCC 12321 and *P. polymyxa* DSM365 was recently sequenced (Tong *et al.*, 2013; Xie *et al.*, 2015) and a novel 2R,3R-BDH functionally characterized (Yu *et al.*, 2011). The bacterium is able almost exclusively produce 2R,3R-BD (>98 %) when grown under anaerobic conditions (Mingchao *et al.*, 2011). Previous studies have demonstrated the capability of *P. polymyxa* as a 2,3-butanediol producer (De Mas, Jansen and Tsao, 1988; Akhtar, 2007; Häßler *et al.*, 2012; Gao *et al.*, 2013). Zhang *et al.* (2012) isolated a high acetoin producing strain designated CS107, which was later identified as *P. polymyxa*. *P. polymyxa* CS107 strain, grown on glucose, achieved a maximum acetoin concentration of 55.3 g/L with productivity of 1.32 g/(L h) and yield of 75.62 % in fed-batch fermentation in a 5-L jar.

2 Materials and Methods

2.1 Strains, Plasmids and Primers

Overview of the strains used in this thesis are shown in **Table 2.1**. Plasmids used in this study are shown in **Table 2.2**. Synthetic primers and other oligonucleotides used in this study were designed in Benchling and ordered from Sigma®, Life Sciences (**Table 2.3**).

Table 2.1. Overview of bacterial strains used in this thesis.

Name	Description	Reference or Source
B. licheniformis DSM13	Wild type strain.	(Waschkau *et al.*, (2008)
B. methanolicus MGA3	Wild type strain.	(Schendel *et al.*, 1990)
B. subtilis 168	Wild type strain.	(Burkholder and Giles, 1947)
E. coli DH5α	General cloning strain. Engineered for high-efficiency transformations.	(Bethesda, 1986)
P. polymyxa ATCC 12321	Wild type strain.	Bielefeld University

Table 2.2. Overview of plasmids used in this study

Name	Description	Reference
pET-RABC	Contains 2,3-BD pathway gene cluster from *E. cloacae* SDM.	Xu *et al.*, (2014)
pTH1mp	pH13mp expression vector with *mdh* promoter from pBM19. *Pci*I restriction site downstream of *mdh* promoter. Clm^r.	(Irla *et al.*, 2016)
pTH1mpLacO	pTH1mp with the 21 bp *lac* repressor recognition sequence cloned between *mdh* promoter and RBS.	This thesis
pTH1mp-*alsSD*_Bl	pTH1mp assembled with *alsSD* operon from *B. licheniformis* DSM13.	This thesis.
pTH1mpLacO-*alsSD*_Bl	pTH1mp assembled with *lacO* fragment and *alsSD* operon from *B. licheniformis* DSM13.	This thesis.
pTH1mpLacO-*alsSD*_Bl(GTG)	pTH1mp-*alsSD*_Bl with GTG as start codon.	This thesis.
pTH1mp-*alsSD*_Bs	pTH1mp assembled with *alsSD* operon from *B. subtilis* 168.	This thesis.
pTH1mpLacO-*alsSD*_Bs	pTH1mp assembled with *lacO* fragment and *alsSD* operon from *B. subtilis* 168	This thesis.
pTH1mpLacO-*alsSD*_Bs(GTG)	pTH1mp-*alsSD*_Bs with GTG as start codon	This thesis.
pTH1mp-*alsSD*_Ec	pTH1mp assembled with *alsSD* operon from *E. cloacae* SDM	This thesis.
pTH1mpLacO-*alsSD*_Ec	pTH1mp assembled with *lacO* fragment and *alsSD* operon from *E. cloacae* SDM	This thesis.
pTH1mpLacO-*alsSD*_Ec(GTG)	pTH1mpLacO-*alsSD*_Ec with GTG as start codon	This thesis.

Table. 2.2. Continued.

Name	Description	Reference
pTH1mp-*alsSD*_Pp	pTH1mp assembled with *alsSD* operon from *P. polymyxa* ATCC 12321	This thesis.
pTH1mpLacO-*alsSD*_Pp	pTH1mp assembled with *lacO* fragment and *alsSD* operon from *P. polymyxa* ATCC 12321	This thesis.
pTH1mp-*budC*_Bl	pTH1mp assembled with *budC* gene cloned from *B. licheniformis* DSM13.	This thesis.
pTH1mp-*gdh*_Bl	pTH1mp assembled with *gdh* gene cloned from *B. licheniformis* DSM13.	This thesis.
pTH1mpLacO-*gdh*_Bl	pTH1mp assembled with *lacO* fragment and *gdh* gene cloned from *B. licheniformis* DSM13.	This thesis.
pTH1mp-*bdhA*_Bs	pTH1mp assembled with *bdhA* gene cloned from *B. subtilis* 168.	This thesis.
pTH1mp-*budC*_Ec	pTH1mp assembled with *bdhA* gene cloned from *E. cloacae* SDM	This thesis.
pTH1mpLacO-*budC*_Ec	pTH1mp assembled with *lacO* fragment and *bdhA* gene cloned from *E. cloacae* SDM	This thesis.
pTH1mp-*bdhA*_Pp	pTH1mp assembled with *bdhA* gene cloned from *P. polymyxa* ATCC 12321.	This thesis.

Table 2.3. Overview of synthetic primers used in this thesis. 3'-overhang region overlapping with 5'-terminal of *Nde*I and *Pci*I double digested pTH1mp is underlined. 5'-overhang overlapping with 3'-end terminal of *Nde*I and *Pci*I double digested pTH1mp is underlined with bold line. Overlapping terminal regions allow cloning by Gibson Assembly (Gibson *et al.*, 2009) (**Chapter 2.9**).

Name	**Description**	**Sequence 5' → 3'**
D022	For amplification of *alsSD* operon from *B. licheniformis* DSM13, FWD.	ATAAATAGGAGGTAGTACATATGAAT AATGTAGCCGCTAA
D023	For amplification of *alsSD* operon from *B. licheniformis* DSM13, REV.	GACCTATGGCGGGTACCATATTACTCG GGATTGCCTCC
D003	For amplification of *alsSD* operon from *B. subtilis* 168, FWD.	ATAAATAGGAGGTAGTACATATGACA AAAGCAACAAAAGAAC
D026	For amplification of *alsSD* operon from *B. subtilis* 168, REV.	GACCTATGGCGGGTACCATATTATTCA GGGCTTCCTTCAGTT
D005	For amplification of *alsSD* operon from *E. cloacae* SDM, FWD.	ATAAATAGGAGGTAGTACATATGATG CACTCATCTGCCTG
D027	For amplification of *alsSD* operon from *E. cloacae* SDM, REV.	GACCTATGGCGGGTACCATATCACAA AATCTGGCTGAGATGGAGCTGGCCCAT
D024	For amplification of *alsSD* operon from *P. polymyxa* ATCC 12321, FWD.	ATAAATAGGAGGTAGTACATATGAGT ACCAAAGTTCAAGCTGTTC
D025	For amplification of *alsSD* operon from *P. polymyxa* ATCC 12321, REV.	GACCTATGGCGGGTACCATATTACTGC GCACCTTCAGTAAC
D028	For amplification of *alsSD* operon from *B. licheniformis* DSM13, substituting GTG as start codon, FWD.	ATAAATAGGAGGTAGTACATGTGAAT AATGTAGCCGCTAA
D029	For amplification of *alsSD* operon from *B. subtilis* 168, substituting GTG as start codon, FWD.	ATAAATAGGAGGTAGTACATGTGACA AAAGCAACAAAAGAAC
D030	For amplification of *alsSD* operon from *E. cloacae* SDM, substituting GTG as start codon, FWD.	ATAAATAGGAGGTAGTACATGTGATG CACTCATCTGCCTG

Table 2.3. Continued.

Name	Description	Sequence 5' → 3'
D015	For amplification of *budC* from *B. licheniformis* DSM13, FWD.	ATAAATAGGAGGTAGTACATATG AGTAAAGTATCTGGAAAAATTGC
D016	For amplification of *budC* from *B. licheniformis* DSM13, REV.	GACCTATGGCGGGTACCATATTA ATTAAATACCATTCCGCCAT
D017	For amplification of *gdh* from *B. licheniformis* DSM13, FWD.	ATAAATAGGAGGTAGTACATATG TCAAAATCAGTAAAATCAGTCA
D018	For amplification of *gdh* from *B. licheniformis* DSM13, REV.	GACCTATGGCGGGTACCATATTA ATCGTGATAAGATTCTGCAA
D011	For amplification of *bdhA* from *B. subtilis* 168, FWD.	ATAAATAGGAGGTAGTACATATG AAGGCAGCAAGATGGCA
D012	For amplification of *bdhA* from *B. subtilis* 168, REV.	GACCTATGGCGGGTACCATATTA GTTAGGTCTAACAAGGATTTTGA
D013	For amplification of *bdhA* from *E. cloacae* SDM, FWD.	ATAAATAGGAGGTAGTACATATG CAAAAAGTTGCTCTCGT
D014	For amplification of *bdhA* from *E. cloacae* SDM, REV.	GACCTATGGCGGGTACCATATTA GTTGAACACCATCCCAC
D009	For amplification of *bdhA* from *P. polymyxa* ATCC 12321, FWD.	ATAAATAGGAGGTAGTACATATG CAAGCATTGAGATGGCA
D010	For amplification of *bdhA* from *P. polymyxa* ATCC 12321, REV.	GACCTATGGCGGGTACCATATTA AGCTTGCGG AGATACCA
VPJF	Binds 120 bp upstream of *Pci*I restriction site on pTH1mp. For colony PCR to determine presence of gene insert in plasmid construct, FWD.	TCTAATCCTTCTAAAAAATATAAT TTAGAAAACTAAG
VPJR	Binds 149 bp downstream of *Nde*I restriction site on pTH1mp. Used to determine presence of gene insert in plasmid construct, REV.	GGTGCGGGCCTCTTCGCTATTAC G
TDBF	For amplification of pTH1mp backbone, FWD.	TATGGTACCCGCCATAGGTCTAG AGCTTGAA
THBR	For amplification of pTH1mp backbone. Region complementary to *lacO* fragment is underlined and bolded. REV.	**AAAACTAGTTTAAATGCTA**ATCT GGATGTTTGTC

2.2 Recipes of Media, Buffers and Other Solutions Used in This Thesis

Table 2.4. Lysogeny broth (LB) medium recipe. Sterilized by autoclaving at 121 ˚C for 20 min.

Components	**Weight (g/L)**
Tryptone (Oxoid)	10.0
Sodium Chloride (VWR, BDH Chemicals)	10.0
Yeast Extract (Oxoid)	5.0
Bacterial Agar (Oxoid) (for solid medium only)	15.0
Distilled H_2O	Add up to 1L

Table 2.5. Super optimal broth with Sucrose (SOBSuc) medium recipe. Sterilized by autoclaving at 121 ˚C for 20 min.

Components	**Weight (g/L)**
SOB medium (Difco™)	28.00
Sucrose (VWR, BDH Chemicals)	85.58
Bacterial Agar (Oxoid) (for solid medium only)	15.00
Distilled H_2O	Add up to 1L

Table 2.6. Minimal vitamin mineral (MVcM) high salt buffer recipe (10x). Sterilized by autoclaving at 121 ˚C for 20 min.

Components	**Weight (g/L)**
K_2HPO_4 (EMSURE®)	40.93
$NaH_2PO_4*H_2O$ (VWR, BDH Chemicals)	14.90
$(NH_4)_2SO_4$ (Sigma-Aldrich®)	21.14
Distilled H_2O	Add up to 1L

Table 2.7. MVcM media recipe. pH adjusted to 7.2 with HCl and NaOH. Sterilized by autoclaving at 121 ˚C for 20 min.

Components	**Volume (mL/L)**
MVcM High Salt Buffer (10x)	100
Distilled H_2O	Add up to 1L

Table 2.8. Minimal vitamin mineral with yeast extract (MVcMY) media recipe. pH adjusted to 7.2 with HCl and NaOH. Sterilized by autoclaving at 121 ˚C for 20 min.

Components	**Amount**
MVcM High Salt Buffer (10x)	100 mL
Yeast Extract (Oxoid)	0.25 g
Distilled H_2O	Add up to 1L

Table 2.9. Volume of additives added to per 0.1 L MVcM or MVcMY media before inoculation of MGA3 strains.

Components	**Volume (mL/0.1L)**
Methanol (VWR, BDH Chemicals)	0.811
$MgSO_4$ (1M) (VWR, BDH Chemicals)	0.100
MVcM Complete Vitamins 1000X (Schendel *et al.*, 1990)	0.100
MVcM BPTI Trace Metals 1000X (Schendel *et al.*, 1990)	0.100

Table 2.10. Electroporation buffer (EPB) recipe. Sterilized by filtration.

Component	**Weight (g/L)**
HEPES (Sigma® Life Sciences)	0.06
PEG_{8000} (Aldrich® Chemistry)	62.50
Distilled H_2O	Add up to 1L

Table 2.11. Psi medium recipe, pH adjusted to 7.6 with KOH. Sterilized by autoclaving at 121 ˚C for 20 min.

Component	**Weight (g/0.5L)**
Yeast extract	2.5
Tryptone	10.0
$MgSO_4 \cdot 7H_2O$	5.12
Distilled H_2O	Add up to 500 mL

Table 2.12. Transformation Buffer 1 (TFB1) recipe, pH adjusted to 5.8 with diluted acetic acid. Sterilized by filtration.

Component	**Amount**
K-Ac (Potassium Acetate)	0.588 g
RbCl	2.42 g
$CaCl_2*2H_2O$	0.389 g
$MnCl_2*4H_2O$	3.146 g
Glycerol	30 mL
Distilled H_2O	Add up to 200 mL

Table 2.13. Transformation Buffer 2 (TFB2) recipe, pH adjusted to 6.5 with diluted NaOH. Sterilized by filtration

Component	Amount
3-(N-morpholino)propanesulfonic acid (MOPS)	0.21 g
$CaCl_2$ *$2H_2O$	1.1 g
RbCl	0.121 g
Glycerol	15 mL
Distilled H_2O	Add up to 100 mL

Table 2.14. Phosphate buffer A (0.1M, pH = 7.0, 10 mM $MgCl_2$) recipe for enzyme assay of *alsSD* operon-encoded protein products.

Component	Volume (mL/L)
K_2HPO_4 (1M) (EMSURE®)	61.5
KH_2PO_4 (1M) (EMSURE®)	38.5
$MgCl_2$ (1M) (VWR, BDH Chemicals)	10.0
Distilled H_2O	Add up to 1L

Table 2.15. Phosphate buffer B (1mM, pH = 7.4) recipe for 2,3-BDH and GDH enzyme assay.

Component	Volume (mL/L)
K_2HPO_4 (1M) (EMSURE®)	80.2
KH2PO4 (1M) (EMSURE®)	19.8
Distilled H_2O	Add up to 1L

Table 2.16. 5 % α-naphthol solution recipe scheme.

Volume 2.5 M NaOH (mL)	α-Naphthol (Sigma-Aldrich®) (g)
50	2.50

Table 2.17. 0.5 % creatinine solution recipe scheme.

Volume Phosphate Buffer A	Creatinine (Sigma-Aldrich®) (g)
50	0.250

2.3 General Cultivation Conditions

General cultivation conditions for *E. coli* DH5α and *B. methanolicus* MGA3 strains are described below. Specific cultivation conditions are described for each experimental procedure.

For *E. coli* DH5α strains, cells were cultivated in either liquid or solid LB medium (**Table 2.4**) supplemented with 15 µL/mL chloramphenicol as selection marker at 37 °C, 225 rpm unless stated otherwise.

Depending on experimental procedure, *B. methanolicus* MGA3 and MGA3 strains were cultivated in either SOBsuc (**Table 2.5**), MVcM (**Table 2.7**) or MVcMY (**Table 2.8**) at 50 °C, 200 rpm. MVcM and MVcMY media were supplemented with additives supporting growth of *B. methanolicus* MGA3 (**Table 2.9**) and 5 µL/mL chloramphenicol (if needed) before inoculation. All media were pre-warmed at 50 °C for 30 min before inoculation with MGA3 strains.

All bacterial cultivations were carried out in shake flasks (baffled for MGA3 strains) sterilized by autoclaving at 121 °C for 20 min beforehand. Medium/culture occupied at most 20 % of flask volume during cultivation.

2.4 Genomic DNA Isolation and Purification

The following protocol for isolation of gDNA from donor organisms *B. licheniformis* DSM13, *B. subtilis* 168 and *P. polymyxa* ATCC 12321 was adapted from Eikmanns *et al.* (1994).

A single colony was used to inoculate 5 mL of LB medium and incubated at 37 °C, 225 rpm overnight. Overnight culture was centrifuged (7830 rpm for 5 min) and supernatant was discarded. Cells were washed with 5 mL Tris-EDTA-buffer (TE-buffer) (pH = 7.6) and centrifuged as above. Supernatant was discarded and cells were resuspended in 1 mL freshly made 15 mg/mL lysozyme (dissolved in TE, pH = 7.6) solution supplemented with 5 µL RNAse-solution (10 mg/mL ion-free water) and incubated at 37 °C for 3 hours.

3 mL of lysis-buffer (10 mM Tris-HCL, 400 mM NaCl, 2 mM Na_2EDTA, pH = 8.2) was added, followed by 220 µL of 10 % sodium dodecyl sulfate (SDS) solution, and lastly, 150 µL of serine proteinase K solution (20 mg/mL ion-free water). Components were mixed with caution and incubated at 60 °C for 2 hours.

1 mL of 6 M NaCl solution was then added, solution was mixed vigorously (not vortexed) until white precipitate was visible and then centrifuged (25 °C, 7830 rpm for 30 min). 1-2 mL of supernatant was transferred to a sterile Falcon tube (50 mL) and 2.5 volumes of ice-cold absolute ethanol was added and mixed with caution.

Precipitated gDNA was extracted by a pipette tip and washed in 70 % ethanol. DNA was allowed to dry shortly on pipette tip before being dissolved in 200 µL TE in a microtube. gDNA was stored in 4 °C.

2.5 DNA Amplification by Polymerase Chain Reaction

Polymerase chain reaction (PCR) is the *in vitro* amplification of a target DNA sequence by use of short oligonucleotides, called primers, that bind specifically to either end of the target region through complementary base-pairing, allowing a heat-stable DNA polymerase to elongate the bound primer, synthesising a copy the target sequence. The reaction is temperature sensitive and cycling of temperature allows the process to be repeated multiple times, producing up to millions of copies of the target sequence (Green and Sambrook, 2012).

Genomic DNA (gDNA) of *B. licheniformis* DSM13, *B. subtilis* 168 and *P. polymyxa* ATCC 12321 were isolated and used as template for the amplification of the operons and genes encoding enzymes involves in the 2,3-BD pathway. The 2,3-BD pathway gene cluster of *E. cloacae* SDM was available in the previously constructed pET-RABC plasmid, which was used as template (Xu *et al.*, 2014). The 2,3-BD pathway genes were amplified using either the CloneAmp™ HiFi PCR Premixes (TAKARA) or the Q5® High-Fidelity DNA Polymerase (New England Biolabs (NEB)) protocol. An overview of primers used for amplification of a specific operon or gene is shown in **Table 2.3**.

For amplification with the CloneAmp™ HiFi PCR premixes, components described in **Table 2.18** were mixed in a PCR tube (0.2 mL) and temperature cycling was performed in a Mastercycler® Gradient (Eppendorf) under the thermocycling conditions listed in **Table 2.19**.

For amplification with Q5® High-Fidelity DNA Polymerase, reaction mixes were prepared according to **Table 2.20**, using the thermocycling condition shown in **Table 2.21**.

Table 2.18. PCR mix recipe (25 µL) for gene amplification with CloneAmp™ HiFi PCR premixes

Components	**Volume µL**
CloneAmp™ HiFi PCR Premix	12.5
Forward Primer	2.0
Reverse Primer	2.0
Template	< 100 ng
Distilled water	Add up to 25 µL

Table 2.19. Thermocycling conditions for PCR with the CloneAmp™ HiFi PCR Premix

Step	Temperature (°C)	Time (s)	
Denaturation	98	10	
Annealing	55	5 or 15	30-35 Cycles
Extension	72	5/kb	
Hold	4	Indefinite	

Table 2.20. PCR mix recipe (50 µL) for gene amplification with Q5® High-Fidelity DNA Polymerase protocol. DSMO and betaine are optional additives that help separate DNA strands (Frackman *et al.*, 1998).

Component	Volume (µL)
Q5 Reaction Buffer (5x)	10.0
dNTPS (10 mM)	1.0
Forward Primer (10 µM)	2.5
Reverse Primer (10 µM)	2.5
Template DNA	Variable
Q5 High-Fidelity DNA Polymerase	0.5
DMSO (or Betaine (5M))	1.5 (or 10.0)
Distilled water	Add up to 50 µL

Table 2.21. Thermocycling conditions for PCR with Q5® High-Fidelity DNA Polymerase protocol.

Step	Temperature (°C)	Time (s)	
Initial Denaturation	98	60	
Denaturation	98	10	
Annealing	55	30	30-35 Cycles
Extension	72	30/kb	
Final Extension	72	120	
Hold	4	Indefinite	

2.5.1 Gradient PCR

The optimal annealing temperature (T_m) of a primer can be empirically determined by gradient PCR (gPCR) (Green and Sambrook, 2012). Using the Mastercycler® Gradient, a T_m-gradient was set and multiple PCR runs were performed in parallel, with all other conditions remaining the same. Subsequent analysis after separation of amplified DNA sequences by agarose gel electrophoresis allows determination of optimal T_m for amplification of desired sequence with the specific primer pair.

2.5.2 PCR purification

PCR purification was done using the QIAquick PCR Purification Kit (QIAGEN) according to manufacturer protocol with the following changes: 30 µL of MilliQ water pre-warmed to 50 °C was used to elute the DNA from column instead of provided elution buffer in kit.

DNA concentration in eluded sample was determined using a NanoDrop™ One Microvolume UV-Vis spectrophotometer (Thermo Fischer Scientific™).

2.6 Agarose Gel Electrophoresis and Gel Imaging

Agarose gel electrophoresis (AGE) is performed to separate DNA fragments based on their length by forced migration through a porous matrix of agarose polymers. In order to visualize the DNA in the gel, stains such as ethidium bromide, hat bind to DNA and fluoresce under ultraviolet (UV) light is applied. A DNA standard (DNA ladder) containing DNA fragments of known size can be run along with the samples. Comparison with the standard allows determination of the size of DNA fragments present in the sample. (Green and Sambrook, 2012).

The general procedure for AGE was as follows. One-part Purple Gel Loading Dye (6x) (NEB) was mixed with five parts DNA sample. 0.8% agarose gel with 20 µL with GelRed® (Biotium) was cast to a suitable size with desired number of wells equal to number of DNA samples and submerged in a Tris-acetate-EDTA-buffer (TAE-buffer) (Sanderson *et al.*, 2014). 6 µL of DNA-Loading dye mixture was loaded onto the gel. One or two wells were reserved for 6 µL DNA ladder (TrackIt™ 1 Kb Plus, Invitrogen™) solution. Electrophoresis was performed at 80-100 Volt for 45-60 minutes and all images were captured and edited with the ChemiDoc™ XRS+ Imaging System (Bio-Rad).

2.7 Plasmid Purification and DNA Gel Extraction

Plasmid purification is performed to extract plasmid DNA from cells, which can be used for downstream analysis and application. The most common method of plasmid isolation is by alkaline-extraction (Green and Sambrook, 2012).

Plasmid purification was done using the QIAprep Spin miniprep Kit (QIAGEN), performed according to manufacturer protocol with the following changes: Instead of provided elution buffer, 30 µL of MilliQ water pre-warmed to 50 °C was used to elute the DNA from column in the final step. DNA concentration in eluded sample was determined using a NanoDrop™ One Microvolume UV-Vis spectrophotometer (Thermo Fischer Scientific™).

All DNA gel extraction procedures were done with 0.8 % agarose gel with 20 µL GelGreen® (Biotium). After separation by AGE, DNA fragments were illuminated under UV light and desired DNA fragment was excised using a scalpel. Extraction of DNA from agarose gel was done using the QIAquick Gel Extraction Kit (Qiagen), performed according to manufacturer protocol with the following changes: sample was washed twice with washing-buffer before elution with 30 µL of MilliQ water pre-warmed to 50 °C. DNA concentration in eluded sample was determined using a NanoDrop™ One Microvolume UV-Vis spectrophotometer (Thermo Fischer Scientific™).

2.8 Double Restriction Enzyme Digestion

Restriction enzymes (RE) are endonucleases that cuts double-stranded DNA at a specific sequence of bases at a recognized restriction site. The restriction site and cleavage pattern depends on the RE employed (Green and Sambrook, 2012).

Double restriction enzyme digestion of pTH1mp was performed with REs *Nde*I (NEB) and *Pci*I (NEB) in NEBuffer 3.1 for optimal activity of both REs. Reaction mixture was prepared accordingly to **Table 2.22** and incubated at 37 °C for 2-3 hours.

Table 2.22. Double restriction enzyme digestion reaction mix, using REs *Nde*I and *Pci*I.

Components	**Volume**
NdeI	0.5 µL / 1 µg DNA
PciI	0.5 µL / 1 µg DNA
DNA	0.5-10 µg
NEBuffer 3.1 (10x)	5 µL
Distilled water	Add up to 50 µL

2.9 Gibson Assembly

Gibson Assembly (GA) is the one-step isothermal *in vitro* recombination of multiple DNA fragments. The technique requires all fragments to share terminal sequence overlaps, which can be created by designing primers with complementary overhangs that can be used to amplify the to-be-assembled fragments.

In a GA reaction mix, T5 exonuclease cleaves nucleotides at the 5'-end at both terminal regions of double-stranded DNA fragments. The created single stranded segments in the 3' terminals of digested fragments anneal, allowing Phusion DNA polymerase to bind to the complementary region and elongate the strand. Finally, *Taq* DNA ligase seals the remaining nicks. This approach allows easy and rapid cloning of multiple DNA fragments into a vector, without relying on the presence of restriction sites (Gibson *et al.*, 2009).

In this thesis, GA was performed to assemble amplified gene insert, double digested pTH1mp and the *lacO* fragment (when relevant) into a single plasmid construct to be transformed into *E. coli* DH5α. Primers containing complementary overhangs for gene amplification (**Table 2.3**) were designed using the Benchling Gibson Assembly Wizard. 15 µL of GA master-mix (Gibson *et al.*, 2009) were aliquoted to PCR tubes and stored in -20°C prior to use. DNA fragments and double digested vector were added in equimolar amounts to reaction mix, distilled water was added to a final reaction volume of 20 µL. Reaction mix was incubated at 50 °C for 1 hour and stored at -4 °C prior to transformation. Weight of fragments and vector were calculated using equation (1).

$$Fragment\ Quantity\ (ng) = Vector\ Quantitity\ (ng) * \frac{Fragment\ Size\ (bp)}{Vector\ Size\ (bp)} \qquad (1)$$

2.10 Preparation and Transformation of Chemically Competent *Escherichia coli* DH5α Cells

2.10.1 Preparation of chemically competent *Escherichia coli* DH5α cells

Pre-culture was prepared by inoculating 25 mL of LB medium with a single colony and incubated at 37 °C, 225 rpm overnight. Main culture was prepared by inoculating 100 mL of Psi medium (**Table 2.11**) with pre-culture and incubated at 37°C, 225 rpm until OD_{600} reached 0.4. The culture was then incubated on ice for 15 min before harvesting by centrifugation (4 °C, 3000 rpm, 5 min). Supernatant was discarded and cells were resuspended in 40 mL cold TFB1 (**Table 2.12**) and incubated on ice for 10 min. Cells were harvested as above and resuspended in 3 mL cold TFB2 (**Table 2.13**). 100 µL aliquots were stored in -80 °C.

2.10.2 Transformation of chemically competent *Escherichia coli* DH5α cells

The following protocol for heat-shock transformation of chemically competent *E. coli* DH5α cells was adapted from Dagert and Ehrlich (1979).

100 µL of competent *E. coli* DH5α cells were mixed with 10 µL of Gibson Assembly reaction mix in a microtube and incubated on ice for 30 min. Cells were heat-shocked at 42 °C for 45 seconds and subsequently incubated on ice for 90 seconds. 900 µL of LB medium was added, followed by incubation at 37 °C for 45 min. Cells were harvested by centrifugation (8000 rpm, 5 min). Supernatant was discarded and cells were resuspended in remaining LB medium before plating out in solid LB medium supplemented with chloramphenicol (15 µL/mL). Plates were incubated at 37 °C overnight. Colonies with plasmid containing gene insert were screened by colony PCR or RDA, and sent for sequencing. Colonies with verified plasmid constructs were used to inoculate 5 mL of LB medium supplemented with chloramphenicol. Culture was incubated at 37 °C, 180 rpm overnight. 650 µL of overnight culture was mixed with 350 µL 87 % glycerol in a cry-tube and stored at -80 °C.

2.11 Colony Screening Methods

2.11.1 Colony Polymerase Chain Reaction

Colony PCR (cPCR) using the VPJF/VPJR primer pair with the Expand™ High Fidelity PCR System (Roche) was performed to screen for colonies with plasmids containing cloned gene insert. After AGE of an amplified sample, a band of ca. 300 bp indicates empty pTH1mp vector (ca. 350 bp for pTH1mpLacO), while a band size corresponding to the cloned gene insert, in addition to 269 bp (ca. 320 bp for pTH1mpLacO), indicates the presence of the cloned gene within the plasmid. In this way, multiple colonies can be screened simultaneously by running cPCRs in parallel.

Table 2.23 shows the recipe for preparation of 50 µL reaction mix. The volume of each cPCR reaction was 10 µL, aliquoted to PCR tubes from a master-mix. For a high number of reactions, the volume of each component was adjusted accordingly to make a larger master-mix. Colonies to be screened were picked using a sterile pipette-tip and streaked on fresh solid LB medium before being added to the reaction mix. Reaction was carried out in a Mastercycler® Gradient thermocycler. Thermocycling condition used are shown in **Table. 2.24.**

Table 2.23. Reaction Mix recipe for Expand™ High Fidelity PCR System. Master-mix was made by adjusting volume of reagents accordingly. DSMO and betaine are optional additives that help separate DNA strands (Frackman *et al.*, 1998)

Component	Volume (µL)
Expand High Fidelity Buffer (10x) with 15 mM $MgCl_2$	10.0
dNTPS (10 mM)	1.0
Forward Primer (10 µM)	2.0
Reverse Primer (10 µM)	2.0
Cell Material from Colony	---
Expand High Fidelity Enzyme Mix	0.5
DMSO (or Betaine (5M))	1.5 (or 10.0)
Distilled water	Add up to 50 µL

Table 2.24. Overview of thermocycling condition used for cPCR with the Expand™ High Fidelity PCR System.

Step	Temperature (°C)	Time (s)	
Initial Denaturation	98	120	
Denaturation	98	15	
Annealing	54	30	30 – 35 Cycles
Extension	72	50 – 150	
Final Extension	72	420	
Hold	4	Indefinite	

2.11.2 Restriction digestion analysis

Restriction digestion analysis (RDA) is based on the presence of restriction sites found within the gene insert. Digestion of purified plasmids from a single colony using specific REs and subsequently separating the resulting fragments by AGE creates a specific pattern of bands on the gel, indicating either presence or absence an insert.

A single DH5α colony was used to inoculate 5 mL of LB medium supplemented with chloramphenicol and incubated at 37 °C and 225 rpm overnight and streaked out on a separate LB agar plate. Plasmid DNA was purified from overnight culture. 10 µL aliquots of RDA reaction mix were prepared according to **Table 2.25** and incubated at 37 °C for 2-3 hour. Resulting DNA fragments were separated by AGE. Overview of expected fragment sizes for a plasmid positive for a specific gene insert is shown in **Table 2.26**, fragment sizes of empty vectors with all three possible enzyme combinations are also included.

Table 2.25. Restriction enzyme digestion reaction mix scheme using REs *Nde*I and *Hind*III. For plasmids requiring only one restriction enzyme, the excluded enzyme amount was replaced with distilled water, with all other reagent volumes remaining the same.

Reagent	Amount
*Hind*III	1.0 µL
NdeI	0.5 µL
Plasmid DNA	200 ng
NEBuffer 2.1 or CutSmart (See **Table 2.26**)	1 µL
Distilled water	Add up to 10 µL

Table 2.26. Overview of enzyme(s) and buffer to be used for RDA of plasmid constructs. Expected fragment sizes after separation by AGE for each plasmid is shown. CS, CutSmart.

Plasmid	Enzyme(s)	NEB Buffer	Fragment Sizes for Digested Plasmid
pTH1mp	*Hind*III	2.1	4773 + 1100
pTH1mp	*Nde*I	CS	5873
pTH1mp	*Nde*I + *Hind*III	2.1	4751 + 1100 + 22
pTH1mp-*alsSD*_Ec	*Nde*I	CS	7772 + 564
pTH1mp-*budC*_Ec	*Nde*I + *Hind*III	2.1	5523 + 1093
pTH1mp-*alsSD*_Bs	*Nde*I	CS	6951 + 1438
pTH1mp-*bdhA*_Bs	*Nde*I	CS	6453 + 433
pTH1mp-*alsSD*_Bl	*Hind*III	2.1	5773 + 2621
pTH1mp-*budC*_Bl	*Hind*III	2.1	5380 + 1248
pTH1mp-*gdh*_Bl	*Nde*I + *Hind*III	2.1	5856 + 1093
pTH1mp-*alsSD*_Pp	*Nde*I	CS	182 + 5842
pTH1mp-*bdhA*_Pp	*Hind*III	2.1	4758 + 1672 + 468

2.12 Sample Preparation for Sanger Sequencing

Table 2.27 shows the recipe scheme used for preparation of plasmid sample to be sent for sequencing. Sanger sequencing was done by GATC Biotech. All components were assembled in a microtube, primer pair used was either gene-specific or primer pair VPJF/VPJR (**Table 2.3**).

Table 2.27. Sample preparation recipe for Sanger sequencing.

Components	Amount
Primer (Forward) (10 mM)	2.5 µL
Primer (Reverse) (10 mM)	2.5 µL
Plasmid	50-80 µg
Distilled water	Add up to 10 µL

2.13 Preparation and Transformation of Electrocompetent *Bacillus methanolicus* MGA3 Cells

The following protocols for preparation and transformation of electrocompetent *B. methanolicus* MGA3 cells were adapted from Jakobsen *et al.* (2006).

2.13.1 Preparation of electrocompetent *Bacillus methanolicus* MGA3 cells

B. methanolicus MGA3 pre-culture was prepared by inoculating cells from glycerol stock (stored in -80 °C) in 25 mL of pre-warmed SOBsuc medium and grown for 16-18 hours at 50 °C, 200 rpm.

Next, 25mL pre-warmed SOBsuc medium was inoculated with the pre-culture to an OD_{600} of 0.1-0.2 and incubated at 50 °C, 200 rpm for ca. 3-4 hours. All OD_{600} measurements were performed using a Helios Epsilon spectrophotometer (Thermo Fischer Scientific™). Main culture was prepared by inoculating four separate baffled flasks each containing 100 m pre-warmed SOBsuc medium to an OD_{600} of 0.05. Culture was incubated at 50 °C, 200 rpm until OD_{600} between 0.18-0.30 was reached.

All main cultures were transferred to Falcon tubes (50 mL) for a total of eight tubes and centrifuged (25 °C, 7830 rpm for 10 min). Supernatants were discarded; cells were then washed twice with 4.5 mL EPC (**Table 2.10**) in each tube. After final centrifugation, supernatants were discarded and all cells were resuspended in remaining EPB and collected in one tube. 100 µL of cell suspension was aliquoted into sterile microtubes and stored at -80 °C.

2.13.2 Transformation of electrocompetent *Bacillus methanolicus* MGA3 cells

100 µL of electrocompetent cells were mixed with 0.5-1.0 µg of plasmid DNA in a microtube and transferred to an ice-cold electroporation cuvette (0.2 or 0.1 cm electrode-gap, BioRad). After incubating on ice for 30 min, cells were electroporated by exposure to a single electrical pulse (200 Ω, 25 µF/cm, 2.5 kV) using a Gene-Pulser Xcell (Bio-Rad). 1 mL of pre-warmed SOBsuc was added immediately after electroporation, cell suspension was then transferred to 12.5 mL of pre-warmed SOBsuc media and incubated for 5-6 hours at 50 °C, 200 rpm.

After incubation cell culture was harvested and centrifuged (25 °C, 7830 rpm for 5 min). Supernatant was discarded and cells were resuspended in remaining SOBsuc medium and plated out in solid SOBsuc medium supplemented with chloramphenicol (5 µL/mL). Plates were incubated in a sealed plastic bag at 50 °C until visible colonies formed.

Five colonies were picked to inoculate five 125 mL unbaffled flasks containing pre-warmed 12.5 mL MVcMY medium with additives supporting growth and chloramphenicol. Cultures were incubated at 50 °C, 200 rpm overnight and harvested when OD_{600} reached 2.0-2.5. Glycerol stocks were prepared by mixing 9 mL of overnight culture with 3 mL of 87 % glycerol in a Falcon tube (50 mL). 1 mL of the bacterial glycerol stock was aliquoted to cryo-tubes and stored directly at -80 °C.

2.14 Acetoin Toxicity Experiment for MGA3 (pTH1mp)

Acetoin exists in a liquid monomeric form, but may form a solid dimer by dimerization with itself. The monomer and dimer state has melting temperatures of 15 °C and 90 °C, respectively. acetoin monomers can be easily recovered by dissolving or melting the solid dimers (O'Neil, 2013).

Solid acetoin (monomer + dimer mix, Alfa Aesar) was melted by incubating at 90 °C for 10 min with occasional agitation. Liquid acetoin was sterilized by passing through a sterile filter prior to addition to cultivation medium. MGA3 (pTH1mp) pre-culture was prepared by inoculating cells from glycerol stock (stored in -80 °C) in 25 mL of pre-warmed MVcMY media with additives supporting growth and chloramphenicol (5 µL/mL).

Pre-culture was incubated at 50 °C, 200 rpm for 16-18 hours. Prior to inoculation of main culture, 25 mL MVcM medium was supplemented with additives, chloramphenicol and acetoin before pre-warming. Growth medium was inoculated to a start OD_{600} of 0.2 in 25 mL incubated at 50 °C, 200 rpm. Triplicate cultures with acetoin concentrations of 0.0, 0.5, 1.0, 5.0, 7.5, 10.0, 15.0, 25.0 and 50.0 g/L were tested. The OD_{600} of all cultures were recorded every 2 hours after inoculation for 10 hours. Final OD_{600} measurement was made 24 hours after inoculation.

2.15 Preparation of Crude Extract for Enzyme Assay

2.15.1 Harvesting cell material from DH5α strains

Pre-cultures of DH5α strains were prepared by inoculating cells from glycerol stock (stored in -80 °C) in 25-50 mL of pre-warmed LB media supplemented chloramphenicol (15 µL/mL) and incubated at 37 °C, 225 rpm for 16-18 hours. 50 mL of LB media were inoculated to a start OD_{600} of 0.2 and incubated at 37°C, 225 rpm for 4 hours.

OD_{600} was measured before harvesting 20 mL of cell culture twice in two separate Falcon tubes (50 mL), and subsequently centrifuged (4 °C, 4000 rpm for 10 min). Supernatant was discarded and cells were washed twice with one of two phosphate buffers, depending on which enzyme is overproduced in the strain (**Table 2.14** and **Table 2.15**). Triplicate samples were harvested and stored at -80 °C prior to assay for enzymatic activity.

2.15.2 Harvesting cell material from MGA3 strains

Pre-cultures of MGA3 strain were prepared by inoculating from glycerol stock (stored in -80 °C) in 25-50 mL of pre-warmed MVcMY media with additives necessary for growth and chloramphenicol (5 µL/mL). Culture was incubated at 50 °C, 200 rpm for 16-18 hours. 50 mL of pre-warmed MVcM media were inoculated with 1 mL of five-times concentrated pre-culture to a start OD_{600} of 0.2. Additives necessary for growth and chloramphenicol were added before pre-warming media. Main culture was incubated at 50 °C, 200 rpm for 6 hours.

OD_{600} was measured before harvesting 20 mL of cell culture twice in two separate falcon tubes (50 mL), and subsequently centrifuged (4 °C, 4000 rpm for 10 min). Supernatant was discarded and cells were washed twice with one of two phosphate buffers (**Table 2.14** and **Table 2.15**)., depending on which enzyme is overproduced in the strain. Triplicate samples were harvested and stored at -80 °C prior to assay for enzymatic activity.

2.15.3 Cell disruption by sonication

Frozen cells were thawed on ice and resuspended in 1 mL of appropriate phosphate buffer. Cell lysis was done by sonication (5 min, output control 4) using a Branson Sonifier® 250 (Emerson). Falcon tube was kept in ice-bath during sonication. Disrupted cell suspension was centrifuged (4 °C, 14,000 rpm for 1 hour) and supernatant was collected as crude extract to be assayed for enzyme activity. Protein concentration in crude extract was determined by Bradford assay (**Chapter 2.17**).

2.16 Enzyme Assays and Establishing Acetoin Standard Curve

2.16.1 Acetoin standard curve

Acetoin quantification method was based on the Voges-Proskauer (VP) reaction. In presence of OH^- ions, acetoin is oxidized to diacetyl, a chemical reaction catalysed by α-naphthol. Diacetyl reacts with the guanidine group from creatinine, to form a pink-red coloured product (Sylvia, 2009).

A 1000 mg/L Acetoin (Fluka™) stock solution was prepared and diluted to 0, 10, 20, 40, 60, and 80 mg/L concentrations. 333 µL of standard solutions was mixed with 333 µL of 5 % α-naphthol solution (**Table 2.16**) and 333 µL 0.5 % creatine solution (**Table 2.17**) in a microtube. Two standard curves at two different temperatures were made by incubating the reaction mixes at 37 °C and 50 °C for 15-20 min at with occasional agitation to allow colour development. Absorbance was measured at 530 nm with SpectraMax Plus 384 Microplate Reader spectrophotometer (Molecular Devices, LLC).

2.16.2 α-acetolactate synthase and α-acetolactate decarboxylase enzyme assay

The protocol for the simultaneous enzymatic assay of ALS and ALDC described below was partially adapted from Wiegeshoff and Marahiel (2007). ALS catalyses the conversion of pyruvate to α-acetolactate, while ALDC catalyse the conversion of α-acetolactate to acetoin. The latter reaction also occurs in a highly acidic environment.

2.16.2.1 Assay of crude extracts from DH5α strains

Crude extracts were first appropriately diluted in order to observe linear range of enzymatic activity. Assay was performed by addition of 10 µL cell crude extract to 323 µL assay reaction mix consisting of phosphate buffer A (100mM, pH = 7.0, 10mM $MgCl_2$) (**Table 2.14**) supplemented with 0.2 mM TPP (Sigma®, Life Sciences) and 10 mM Na-pyruvate (Sigma®, Life Sciences). Assay was performed in triplicate at 37 °C and 50 °C. Reaction was terminated by addition of 333 µL 5 % α-naphthol solution to the reaction mix after 30, 60 and 120 seconds. 333 µL 0.5 % creatine solution was then added to the assay mix and incubated at the respective temperature of the reaction for 15-20 min, allowing colour development. Absorbance was

measured at 530 nm with SpectraMax Plus 384 Microplate Reader spectrophotometer (Molecular Devices, LLC).

One unit of enzyme activity (U) was defined as amount of acetoin (mM) produced per minute, per 1 mL of crude extract under described conditions. The specific activity (U/mg) was defined as amount of acetoin produced per minute, per mg of protein in crude extract. Protein concentration in crude extract was determined by Bradford Assay. Blank was made by replacing crude extract with phosphate buffer in the assay mix. Background activity was determined by replacing Na-pyruvate with phosphate buffer at respective temperatures.

2.16.2.2 Assay of crude extracts from MGA3 strains

For MGA3 strains, assay was performed as described for DH5α with the following changes: 50 µL of diluted crude extract was added to assay reaction mix and reaction was terminated after 5, 10 and 20 min. Assay was performed in triplicate at 50 °C only.

One unit of enzyme activity (U) was defined as amount of acetoin (mM) produced per minute, per 1 mL of crude extract under described conditions. The specific activity (U/mg) was defined as amount of acetoin produced per minute, per mg of protein in crude extract. Protein concentration in crude extract was determined by Bradford Assay. Blank was made by replacing crude extract with phosphate buffer in the assay mix. Background activity was determined by replacing Na-pyruvate with phosphate buffer at respective temperature.

2.16.3 2,3-butanediol dehydrogenases assay

Activity of 2,3-BDH and GDH was determined as previously described by Ge *et al.* (2016). Reduction of acetoin to 2,3-BD, catalysed by 2,3-BDH and GDH (in *B. licheniformis*) involves the oxidation of NADH to NAD^+. Hence, activity can be determined by measuring the decrease in absorbance at 340 nm over time, corresponding to the gradual oxidation of NADH consumed during the reaction. The molar extinction coefficient of NADH at 340 nm is 6.22 $M^{-1}cm^{-1}$ (Bernt and Hess, 1965).

2.16.3.1 Assay of crude extracts from DH5α strains

Crude extracts were first appropriately diluted in order to observe linear range of enzymatic activity. Assay was performed by addition of 980 µL of assay reaction mix consisting of

phosphate buffer B (67 mM, pH = 7.4) (**Table 2.15**) supplemented with 5 mM acetoin (Fluka™) and 0.2 mM NADH (Sigma®, Life Sciences) to 20 µL crude extract in a quartz crystal cuvette (PerkinElmer™) for a total reaction volume of 1 mL. Enzyme assay was performed in triplicate at 37 °C and 45 °C. Absorbance was measured at 340 nm every 5 seconds for 3 min using a SpectraMax Plus 384 Microplate Reader spectrophotometer (Molecular Devices, LLC) at respective temperatures.

One unit of activity (U) was defined as the amount NADH (mM) consumed per minute, per mL crude extract. The specific activity was defined as the amount of NADH (mM) consumed per minute, per mg of protein in crude extract. Protein concentration in crude extract was determined by Bradford Assay. Blank was made by replacing crude extract and NADH with phosphate buffer in the assay mix. Background activity was determined by replacing acetoin with phosphate buffer in the assay mix. Protein concentration in crude extract was determined by Bradford assay.

2.16.3.2 Assay of crude extracts from MGA3 strains

For MGA3 strains, assay was performed as described for DH5α except at 45 °C only, in triplicate. All procedures remained the same.

One unit of activity (U) was defined as the amount NADH (mM) consumed per minute, per mL crude extract. The specific activity was defined as the amount of NADH consumed per minute, per mg of protein in crude extract. Protein concentration in crude extract was determined by Bradford Assay. Blank was made by replacing crude extract and NADH with phosphate buffer in the assay mix. Background activity was determined by replacing acetoin with phosphate buffer in the assay mix.

2.17 Quantification of Protein Concentration

Protein concentration was determined by the Bradford dye-binding method, a colorimetric method involving the binding of Coomassie brilliant blue G-250 dye to primarily basic (especially arginine) and aromatic amino acid residues in proteins. The binding of the dye to protein residues causes it to shift its absorbance maximum from 465 nm to 595 nm (Bradford, 1976). Hence, the higher the absorbance measured at 595nm, the higher the concentration of protein in sample. The Standard curve with bovine serum-albumin (BSA) (Sigma®, Life Sciences) was established.

BSA standard curve was reconstituted by preparing a 5 mg/mL BAS stock solution, which was subsequently diluted to concentrations 0.0, 0.2, 0.4, 0.6 and 0.9 mg/mL. Protein Quantification Dye Reagent (Bio-Rad) was diluted by adding one volume of dye-reagent to four volumes distilled water. The reaction mix consisted of 20 µL of standard solution and 1 mL of diluted dye-reagent in a microtube. Reaction mix was vortexed and allowed to develop colour at incubate at room temperature for 5-10 min, before absorbance was measured at 595 nm.

For protein quantification of cell crude extract, the crude extract was first appropriately diluted within the linear range of the BSA standard curve. 20 µL of crude extract was added to 1 mL dye-reagent, with all remaining procedures performed as described above.

2.18 Growth Experiment of Acetoin Synthesizing MGA3 Strains and Acetoin Quantification

2.18.1 Growth experiment procedure

Pre-culture of MGA3 (pTH1mp-*alsSD*_Bl(GTG)) and MGA3 (pTH1mp-*alsSD*_Bs(GTG)) were prepared by inoculating cells from glycerol stock (stored in -80 °C) in 25 mL of pre-warmed MVcMY media, supplemented with additives and chloramphenicol (5 µL/mL), at 50 °C, 200 rpm for 16-18 hours.

25 mL of pre-warmed MVcM media with additives and chloramphenicol was inoculated to a start OD_{600} of 0.1-0.2 and incubated at 50 °C, 200 rpm. OD_{600} was measured every 2 hours for 10 hours. Supernatant was collected 24 hours after inoculation by centrifugation (25 °C, 7830 rpm for 15 min) and quantified for acetoin concentration. Performed in triplicates.

2.18.2 Determination of acetoin concentration in culture supernatant

Supernatant was first appropriately diluted within the linear range of the acetoin standard. 333 µL of diluted supernatant was mixed with 333 µL of 5 % α-naphthol solution and 333 µL 0.5 % creatine solution in a microtube. Colour was allowed to develop for 15-20 min at 50 °C with occasional agitation before measuring absorbance at 530 nm with SpectraMax Plus 384 Microplate Reader spectrophotometer (Molecular Devices, LLC).

3 Results

3.1 PCR Amplification of the 2,3-BD Pathway Operons and Genes from Donor Organisms and Construction of Expression Vectors

Sequences of the operons and genes encoding the enzymes involved in the 2,3-BD pathway from in *B. licheniformis* DSM13, *B. subtilis* 168, *E. cloacae* SDM and *P. polymyxa* ATCC 12321 are listed in **Table 3.1**. All genes and operons of interest were successfully PCR amplified (**Figure 3.1**) using designed primer pairs (**Table 2.3**). Plasmid constructs were transformed into *E. coli* DH5α, and screened for colonies positive for gene insert using colony PCR (**Figure 3.2**), in which cell material from colonies was used as template, and RDA (**Figure 3.3**). Sequences of cloned plasmids were verified by Sanger sequencing (data not shown). Five constructs with verified sequences were successfully transformed into MGA3 (**Table 3.2**).

Table 3.1. Operons and genes cloned from the four donor organisms and their respective lengths in base pairs. Sequences retrieved from NCBI GenBank sequence databank,

Donor Organism	Gene or Operon	Length (bp)	Encodes
B. licheniformis DSM13	*alsSD*	2591	ALS and ALDC
B. licheniformis DSM13	*budC*	823	Meso-2,3-BDH
B. licheniformis DSM13	*gdh*	1144	GDH
B. subtilis 168	*alsSD*	2589	ALS and ALDC
B. subtilis 168	*bdhA*	1081	2R,3R-BDH
E. cloacae SDM	*alsSD*	2533	ALS and ALDC
E. cloacae SDM	*budC*	811	2,3-BDH
P. polymyxa ATCC 12321	*alsSD*	2669	ALS and ALDC
P. polymyxa ATCC 12321	*bdhA*	1093	2R,3R-BDH

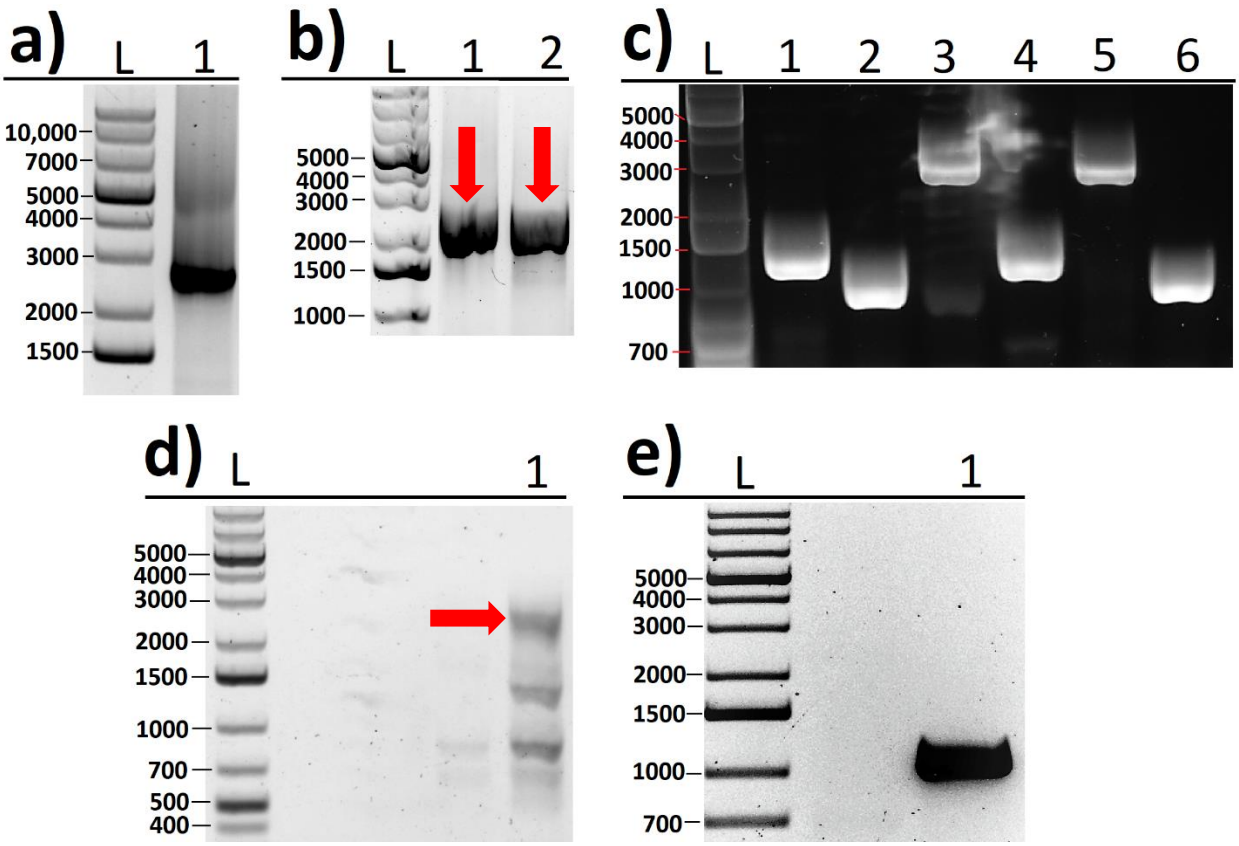

Figure 3.1. PCR amplified DNA fragments suspended in agarose and separated by gel electrophoresis. Length of DNA fragments were estimated by comparison to DNA ladder (band sizes indicated in bp). L = GeneRuler^{TM} 1 kb plus DNA Ladder; a)-1, *alsSD* operon from *E. cloacae* SDM (GTG as start codon); b)-1, *alsSD* operon (red arrow) from *B. subtilis* 168 (GTG as start codon); b)-2, *alsSD* operon (red arrow) from *E. cloacae* SDM (GTG as start codon); c)-1, *gdh* from *B. licheniformis* DSM13; c)-2, *budC* from *B. licheniformis* DSM13; c)-3, *alsSD* operon from *B. licheniformis* DSM13 (ATG as start codon); c)-4, *bdhA* gene from *B. subtilis* 168; c)-5, *alsSD* operon from *B. subtilis* 168 (ATG as start codon); c)-6, *bdhA* gene from *E. cloacae* SDM; d-1), *alsSD* operon (red arrow) from *P. polymyxa* ATC12321 (excised and purified by DNA gel extraction); e)-1, *bdhA* gene from *P. polymyxa* ATCC 12321

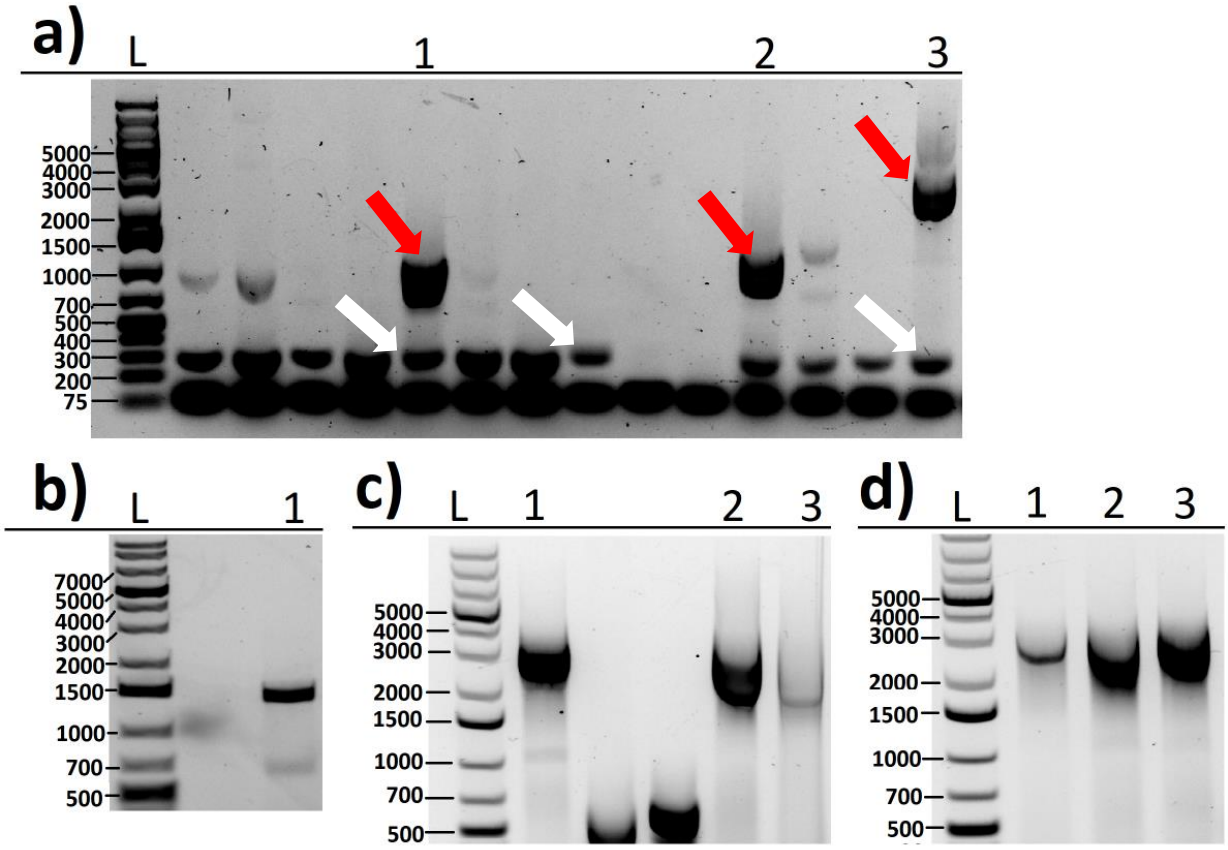

Figure 3.2. Representative images of colony screening by colony PCR using VPJF/VPJR primer pair. White arrows point at ca. 300 bp bands, indicating empty vector. Length of DNA fragments were estimated by comparison to DNA ladder (band sizes indicated in bp). L = GeneRuler^{TM} 1 kb plus DNA Ladder; a)-1, amplified *bdhA* gene (red arrow) from *E. cloacae* SDM; a)-2, amplified *gdh* gene (red arrow) from *B. licheniformis* DSM13; a)-3, amplified *alsSD* operon (red arrow) from *P. polymyxa* ATCC 12321; b)-1, amplified *gdh* gene from *B. licheniformis DSM13*, c)-1/2/3, amplified *alsSD* operon from *B. subtilis* 168 (GTG as start codon); d)-1/2/3, amplified *alsSD* operon from *B. licheniformis* DSM13. Presence of negative band (white arrow) in a)-1/2/3 indicate presence of both empty vector and plasmids positive for insert within cell or colony. Negative bands were not present in b), c) or d).

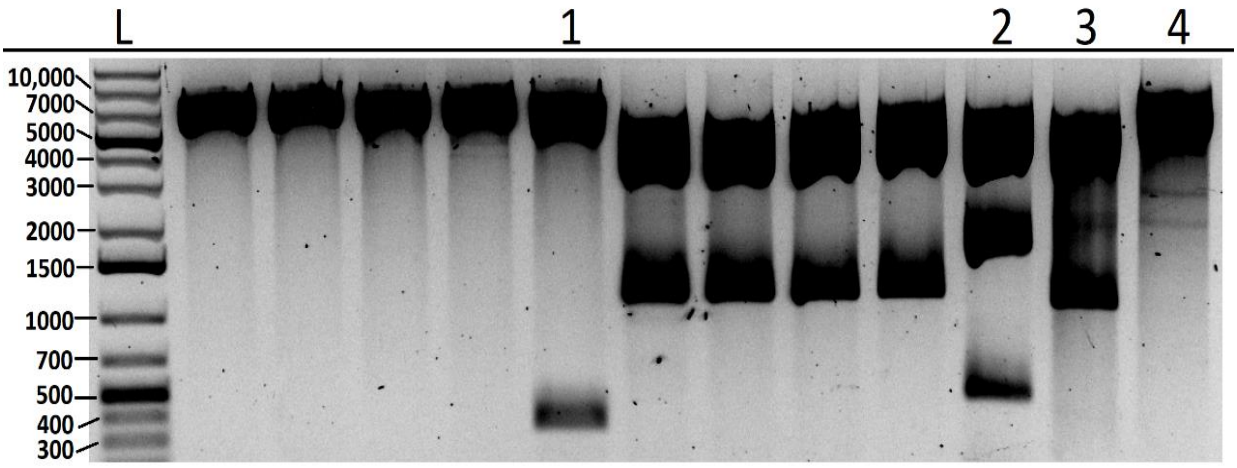

Figure 3.3. Representative image of colony screening by RDA using *Hind*III and *Nde*I (see **Table 2.26** for overview of band patterns). Band patterns of digested plasmids (pTH1mp-*alsSD*_Pp) and (pTH1mp-*bdhA*_Pp) purified from overnight culture with DH5α as cloning host. Length of DNA fragments were estimated by comparison to DNA ladder (band sizes indicated in bp). L = GeneRuler^{TM} 1 kb plus DNA Ladder; 1, band pattern indicating presence of *alsSD* operon from *P. polymyxa* ATCC 12321 in plasmid; 2, band pattern indicating presence of *bdhA* gene from *P. polymyxa* ATCC 12321; 3, empty pTH1mp vector digested with *Hind*III only; 4, empty pTH1mp vector digested with *Nde*I only.

Table 3.2. Overview of constructed expression vectors. pTH1mpLacO is a derivative of pTH1mp with the *lac* operator (binding site of LacI) from *E. coli* inserted downstream of the *mdh* promoter and upstream of the *B. methanolicus* RBS. (GTG) indicate start codon of gene insert was changed from ATG to GTG. +, successfully transformed; -, not transformed.

Plasmid Construct	**Constructed vector (Confirmed by Sanger Sequencing**	**Transformed into MGA3**
pTH1mp-*alsSD*_Bl	-	-
pTH1mpLacO-*alsSD*_Bl	-	-
pTH1mpLacO-*alsSD*_Bl(GTG)	+	+
pTH1mp-*alsSD*_Bs	-	-
pTH1mpLacO-*alsSD*_Bs	-	-
pTH1mpLacO-*alsSD*_Bs(GTG)	+	+
pTH1mp-*alsSD*_Ec	-	-
pTH1mpLacO-*alsSD*_Ec	-	-
pTH1mpLacO-*alsSD*_Ec(GTG)	-	-
pTH1mp-*alsSD*_Pp	-	-
pTH1mpLacO-*alsSD*_Pp	+	-
pTH1mp-*budC*_Bl	+	+
pTH1mp-*gdh*_Bl	-	-
pTH1mpLacO-*gdh*_Bl	+	+
pTH1mp-*bdhA*_Bs	+	+
pTH1mp-*budC*_Ec	-	-
pTH1mpLacO-*budC*_Ec	+	-
pTH1mp-*bdhA*_Pp	+	-

.

3.2 Acetoin Toxicity in *Bacillus methanolicus* MGA3 (pTH1mp)

To determine the feasibility of *B. methanolicus* MGA3 as an acetoin producer, the bacterium's tolerance towards acetoin was explored. IC_{50} of acetoin for *B. methanolicus* MGA3 (pTH1mp) was determined by measuring OD_{600} of batch-cultures grown in 25 mL MVcM media with varying acetoin concentrations (**Figure 3.4**). At 50 g/L acetoin, no growth was observed in the 10-hour observation period. Significant decrease in growth rate was first observed at an acetoin concentration of 7.5 g/L, which showed 10.5 % lower growth rate compared to control grown in absence of acetoin. A separately conducted acetoin toxicity experiment with comparable conditions showed no significant inhibitory effect on growth rate at acetoin concentrations up to 5 g/L (**Figure A.0.2** and **Table A.0.1**). Using linear regression analysis of the relationship between specific growth rates and acetoin concentration, IC_{50} of acetoin for *B. methanolicus* MGA3 (pTH1mp) was determined to be 25.8 g/L (293 mM).

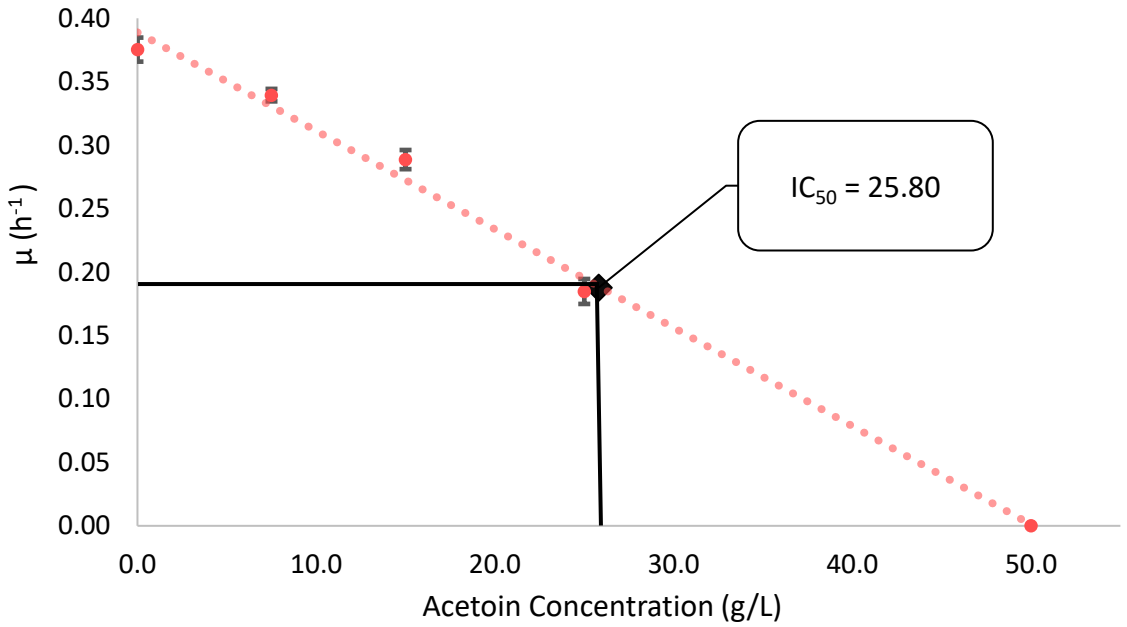

Figure 3.4. Specific growth rate of MGA3 (pTH1mp) cultivated in various acetoin concentrations. Cells grown in MVcM media supplemented with 0.2 M methanol and other additives at 50°C, 200 rpm. IC_{50} of acetoin indicated (black diamond). Specific growth rates determined by exponential regression analysis of semi-log OD_{600} vs. time plot. No growth observed at 50 g/L acetoin. Data are mean values of biological triplicates, error bars represent standard deviations of the mean.

3.3 Enzyme Assay Results of *Escherichia coli* DH5α and *Bacillus methanolicus* MGA3 Recombinant Strains

To assay for functional activity of ALSs, ALDCs and 2,3-BDHs in the transformed recombinant *E. coli* DH5α and *B. methanolicus* MGA3 strains, crude extracts of each strain were prepared. In both types of assays DH5α (pTH1mp) and MGA3 (pTH1mp) were used as control for their respective strains.

3.3.1 Activity of *alsSD*-encoded enzymes in *Escherichia coli* DH5α

Specific activity (U/mg) was defined as amount of acetoin (mM) produced per min, per mg of protein in crude extract. Significant specific activity in crude extract was observed at both 37 °C and 50 °C for all recombinant DH5α strains compared to control (**Figure 3.5**). In addition, all enzymes show higher specific activity at 50 °C compared to 37 °C.

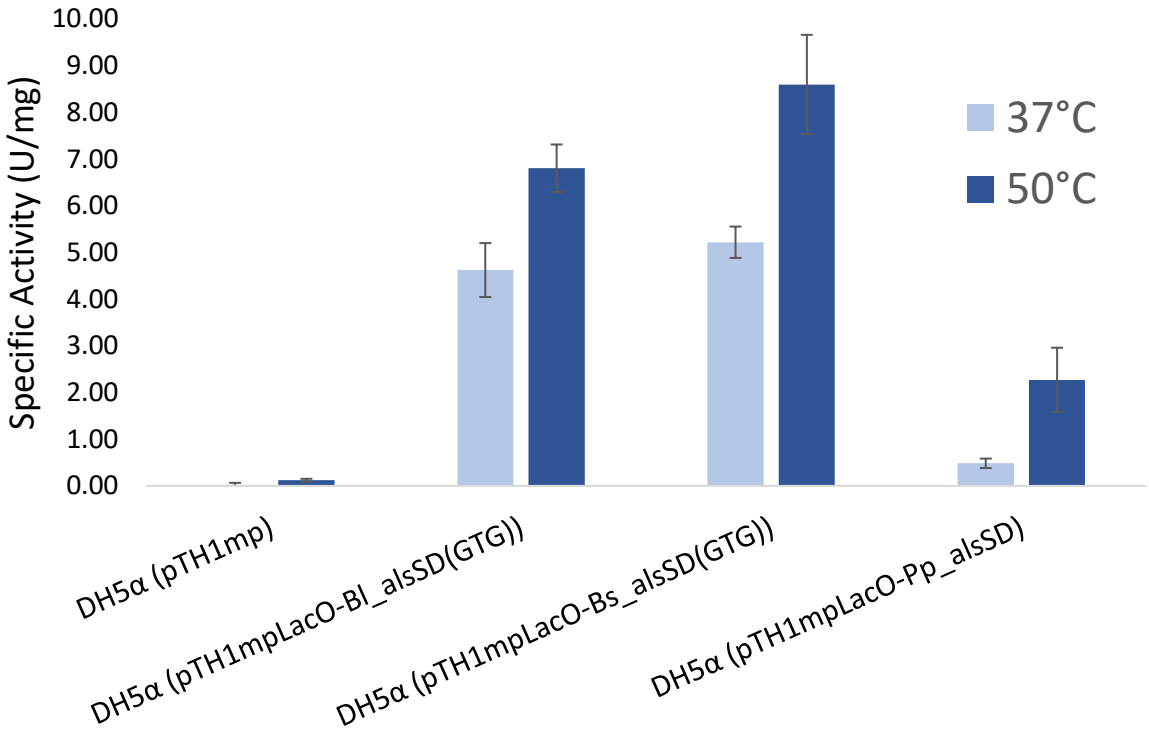

Figure 3.5. Specific activities of enzymes encoded by the *alsSD* operon in recombinant *E. coli* DH5α at 37°C (light blue) and 50°C (dark blue). Data are mean values of biological duplicates. Error bars indicate standard deviation of the mean.

Enzymatic activity in crude extract of DH5α (pTH1mpLacO-*alsSD*_Bs(GTG)) was highest, 5.22 ± 0.34 and 8.60 ± 1.06 U/mg at 37 °C and 50 °C, respectively. DH5α (pTH1mpLacO-*alsSD*_Bl(GTG)) and DH5α (pTH1mpLacO-*alsSD*_Bs(GTG)) strains displayed similar levels of activity of activity at both temperatures assayed. Enzymatic activity in crude extract from DH5α (pTH1mpLacO-*alsSD*_Pp) was lowest in comparison to the two other strains at both temperatures assayed; 0.48 ± 0.1 and 2.27 ± 0.6 U/mg at 37 °C and 50 °C, respectively.

3.3.2 Activity of *alsSD*-encoded enzymes in *Bacillus methanolicus* MGA3

Both MGA3 (pTH1mp-*alsSD*_Bl(GTG)) and MGA3 (pTH1mp-*alsSD*_Bs(GTG)) showed significant levels of activity compared to the control strain MGA3 (pTH1mp). Activity of control strain was relatively high, 2.7 ± 0.3 U/mg at 50 °C, which indicates background production of acetoin in MGA3 (pTH1mp). Crude extract from MGA3 (pTH1mpLacO-*alsSD*_Bl(GTG)) displayed the highest activity of 17.8 ± 0.1 U/mg, while MGA3 (pTH1mpLacO-*alsSD*_Bs(GTG)) showed a lower activity of 12.0 ± 0.7 U/mg.

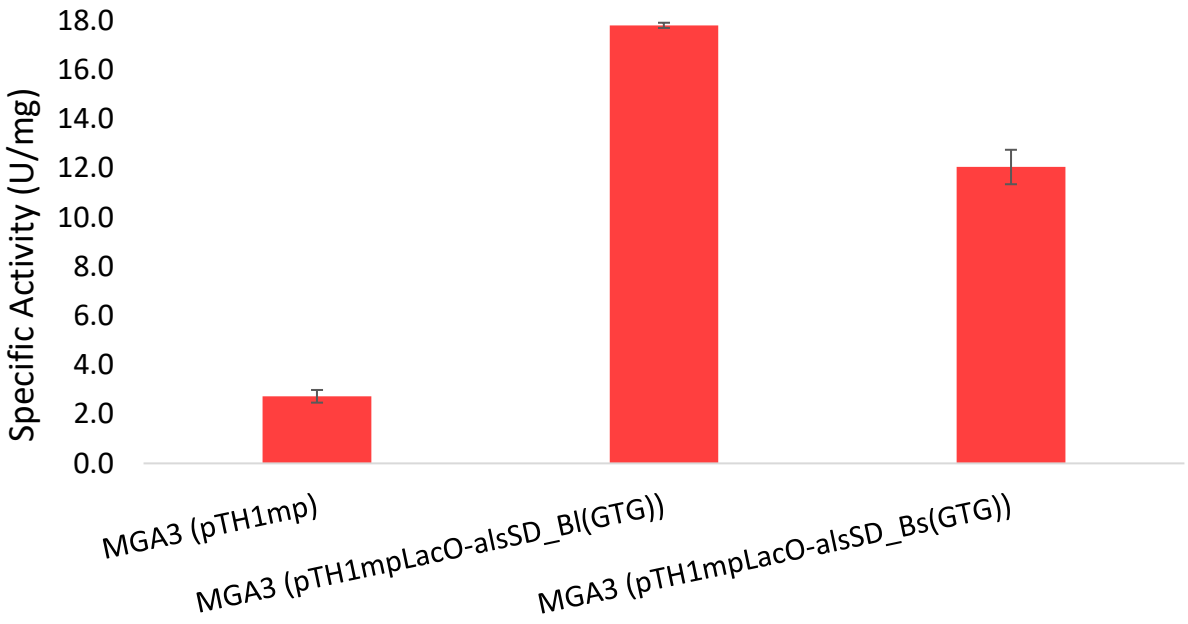

Figure 3.6. Specific activities at 50°C of enzymes encoded by the *alsSD* operon in recombinant *B. methanolicus* MGA3. Data are mean values of biological triplicates, error bars indicate standard deviation of the mean.

3.3.3 Activity of 2,3-butandediol dehydrogenase in *Escherichia coli* DH5α

Crude extract of DH5α (pTH1mp) displayed a near-zero enzymatic activity of 0.002 ± 0.002 and 0.018 ± 0.003 U/mg at 37 °C and 45 °C respectively (**Figure 3.7**). 2,3-BDH from DH5α (pTH1mpLacO-*budC*_Ec) showed lower activity at higher temperatures, from 49.7 ± 5.8 U/mg at 37°C to 31.0 ± 2.5 U/mg at 45°C. Nonetheless, it displayed the highest activity at both temperatures in comparison to the four other strains. At both 37 °C and 45 °C, relatively high activities of 2,3-BDH from DH5α (pTH1mp-*bdhA*_Pp) (17.0 and 15.5 U/mg, respectively) and meso-2,3-BDH from DH5α (pTH1mp-*budC*_Bl) (14.9 ± 1.4 and 13.4 ± 0.8 U/mg, respectively) are observed. Both are slightly less than half the activity of 2,3-BDH from DH5α (pTH1mpLacO-*budC*_Ec) at both temperatures. The two remaining strains, DH5α (pTH1mp-*bdhA*_Bs) and DH5α (pTH1mpLacO-*gdh*_Bl), displayed higher acetoin reducing activity compared to control, but much lower compared to the three previously mentioned enzymes at both temperatures.

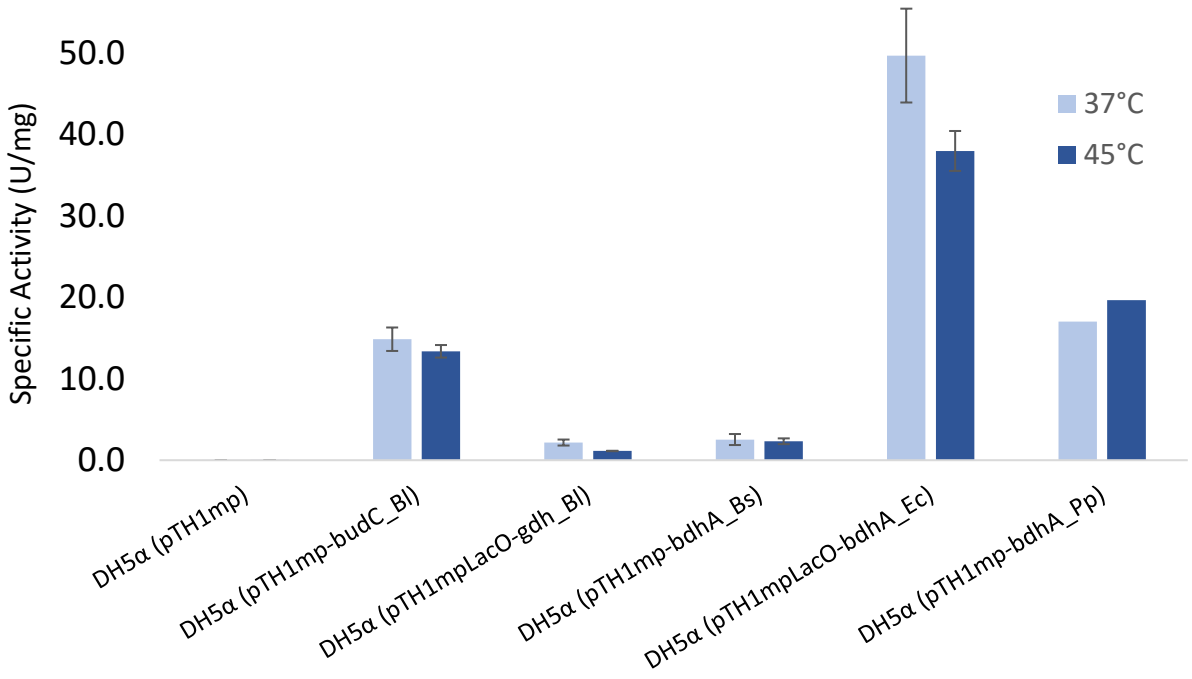

Figure 3.7. Specific activities of acetoin reducing enzymes overproduced in recombinant *E. coli* DH5α strains at 37 °C (light blue) and 45 °C (dark blue). All data are mean values of biological duplicates; except for DH5α (pTH1mpLacO-*bdhA*_Pp) which is a single measurement. Error bars indicate standard deviation of the mean.

At 37 °C, activity in crude extract of DH5α (pTH1mp-*bdhA*_Bs) was 2.6 ± 0.7 U/mg and remains similar at 45°C, 2.3 ± 0.4 U/mg. Activity of GDH in DH5α (pTH1mp-*gdh*_Bl) decreases at 45°C, going from 2.2 ± 0.37 at 37°C, to 1.1 ± 0.00 at 45°C. In general, increasing the temperature leads to similar or lower activity in all enzymes.

3.3.4 Activity of 2,3-butanediol dehydrogenase in *Bacillus methanolicus* MGA3

Crude extract from MGA3 (pTH1mp) has an expected near-zero activity of 0.05 ± 0.04 U/mg (**Figure 3.8**). Enzymatic activity in the crude extract from MGA3 (pTH1mp-*bdhA*_Bs) was the highest by 1.47 ± 0.02 U/mg, 4.2-fold and 6.4-fold higher than activity in crude extract from MGA3 (pTH1mp-*budC*_Bl) (0.35 ± 0.02 U/mg) and MGA3 (pTH1mpLacO-*gdh*_Bl) (0.23 ± 0.02 U/mg), respectively. Recombinant MGA3 strains overexpressing *bdhA* from *E. cloacae* SDM and *P. polymyxa* ATCC 12321 are missing.

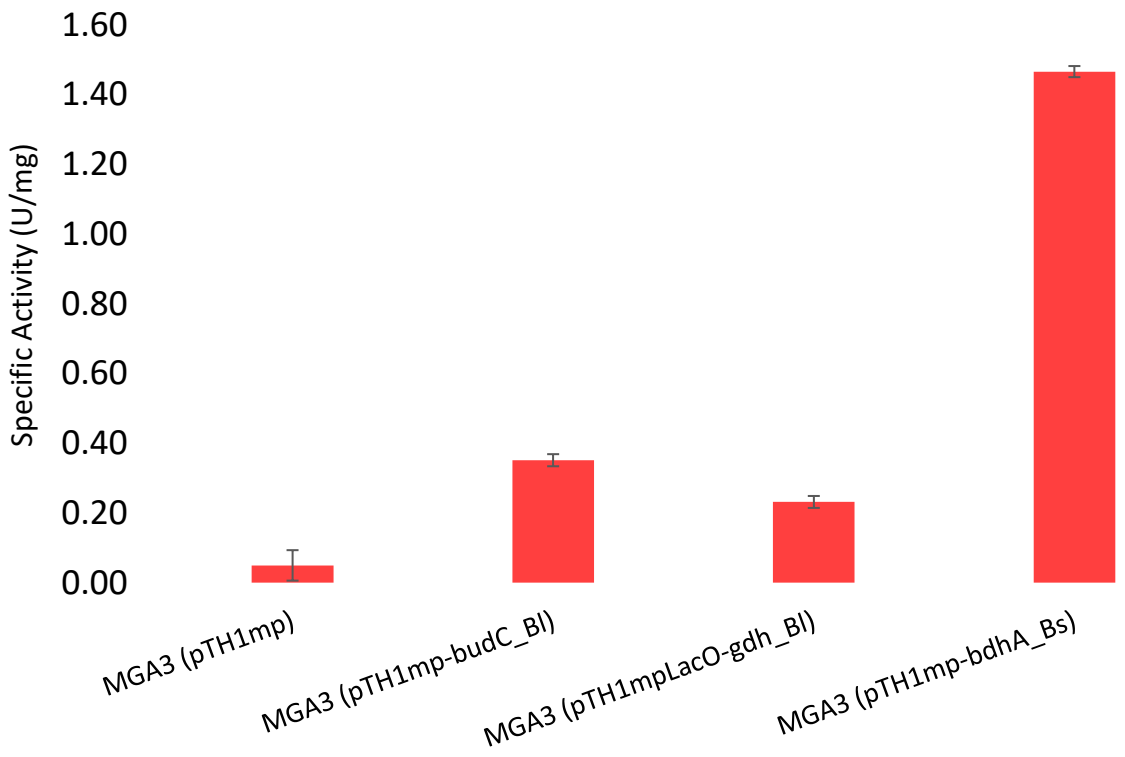

Figure 3.8. Specific activities at 45 °C of acetoin reducing enzymes overproduced in recombinant *B. methanolicus* MGA3 strains. Data are mean values of biological triplicates, error bars indicate standard deviation of the mean.

3.4 Batch Cultivation of Acetoin Producing *Bacillus methanolicus* MGA3 Recombinant Strains

MGA3 (pTHmpLacO-*alsSD*_Bl(GTG)) and MGA3 (pTH1mpLacO-*alsSD*_Bs(GTG) were cultivated for 24-hours growing on 25 mL MVcM media supplemented with 0.2 M methanol. Acetoin titer in supernatant was quantified at the end of experiment (**Table 3.3**). Acetoin titer and yield in supernatant of MGA3 (pTH1mp) was near zero, and strain had a growth rate of 0.36 ± 0.00 h^{-1}.

Supernatant of MGA3 (pTH1mpLacO-*alsSD*_Bl(GTG)) had the highest acetoin titer of 1.48 ± 0.24 g/L with yield of 0.23 ± 0.04 g/g. However, specific growth rate (μ) was 75 % lower compared to control strain. MGA3 (pTH1mpLacO-*alsSD*_Bl(GTG)) did not enter stationary phase in the 10-hour observation period (**Figure A.0.3**).

Acetoin titer in the supernatant of MGA3 (pTH1mpLacO-*alsSD*_Bs(GTG)) was 0.62 ± 0.00 g/L 24 hours after inoculation. 2.4-fold lower than titer in MGA3 (pTH1mpLacO-*alsSD*_Bs(GTG), but had a growth rate (0.35 ± 0.00 h^{-1}) comparable to growth rate of control strain.

Yield of MGA3 (pTH1mpLacO-*alsSD*_Bs(GTG)) after 24-hour batch cultivation was 0.10 ± 0.00 g/g, 2.3-times lower than yield of MGA3 (pTH1mpLacO-*alsSD*_Bl(GTG)).

Table 3.3. Specific growth rate and acetoin concentration in supernatant 24 hours after batch-cultivation of acetoin producing MGA3 strains. Cells were grown in MVcM media supplemented with 0.2 M methanol and additives supporting growth, 50 °C, 200 rpm. Data are mean values of biological triplicates. Standard deviation of the mean is included.

Strain	**Acetoin Titer (g/L)**	**μ (h^{-1})**	**Yield (g/g)**
MGA3 (pTH1mpLacO-*alsSD*_Bl(GTG))	1.48 ± 0.24	0.09 ± 0.01	0.10 ± 0.00
MGA3 (pTH1mpLacO-*alsSD*_Bs(GTG))	0.62 ± 0.00	0.35 ± 0.00	0.23 ± 0.04
MGA3 (pTH1mp) [a]	0.02 ± 0.01	0.36 ± 0.00	0.004 ± 0.001

a = Performed in separate experiment, but in comparable conditions.

4 Discussion

All previous metabolic engineering efforts performed with *B. methanolicus* MGA3 have been dedicated to production of L-glutamate, L-lysine, cadaverine or γ-aminobutyric acid using methanol as substrate (Schendel *et al.*, 1990; Jakobsen *et al.*, 2009; Brautaset *et al.*, 2010; Nærdal *et al.*, 2014, 2017; Irla *et al.*, 2017). To date, this thesis is the first demonstration of engineering *B. methanolicus* MGA3 for the methanol-based production of a non-amino acid specialty chemical.

4.1 Strategy for Cloning 2,3-Butanediol Pathway Expression Vectors

The aim of this thesis was to create and analyse the *B. methanolicus* acetoin producing strains, four microbial species were used as gene donors for this approach. *B. licheniformis* DSM13, *B. subtilis* 168, *E. cloacae* SDM and *P. polymyxa* ATCC 12321 are all native 2,3-BD producers. The sequences of their operons and genes encoding the enzymes involved in the 2,3-BD pathway was retrieved from National Centre for Biotechnology Information (NCBI) GenBank sequence databank. Primers used for operon and gene amplification were designed in Benchling using the Gibson Assembly Wizard and ordered from Sigma®, Life Sciences. The pTH1mp expression vector has already been extensively used for heterologous expression in *B. methanolicus* MGA3 (Brautaset *et al.*, 2010; Krog, Tonje Marita Bjerkan Heggeset, *et al.*, 2013; Nærdal *et al.*, 2014, 2017; Irla *et al.*, 2017) and was therefore chosen for gene expression in this thesis. pTH1mp was purified from DH5α (pTH1mp) by plasmid DNA purification and linearized by double digestion with *Pci*I and *Nde*I. All primers used in this study contain an overhang segment complementary to the terminal regions of digested pTH1mp allowing cloning of gene insert into vector backbone by Gibson Assembly (Gibson *et al.*, 2009). Furthermore, the spacer length between *B. methanolicus* MGA3 RBS and start codon was adjusted to 8 bps, which has previously been suggested to be the optimal interval (Irla *et al.*, 2015).

Genomic DNA (gDNA) of *B. licheniformis* DSM13, *B. subtilis* 168 and *P. polymyxa* ATCC 12321 were isolated and used as template for PCR amplification. Primer pairs D022/D023, D003/D026 and D024/D025 (**Table 2.3**) were used for PCR amplification of the *alsSD* operons from *B. licheniformis* DSM13, *B. subtilis* 168 and *P. polymyxa* ATCC 12321 respectively with the start codon optimized to ATG (Donnell and Janssen, 2001). *E. cloacae* SDM and was cloned

with primer pair D005/D027 using the previously constructed pET-RABC as template (Xu *et al.*, 2014). In addition, the *budC* and *gdh* gene from *B. licheniformis* DSM13 and *bdhA* genes from *B. subtilis* 168, *E. cloacae* SDM and *P. polymyxa* ATCC 12321 were cloned in the same manner to evaluate the potential production of 2,3-BD in *B. methanolicus* MGA3 (See **Table 2.3** for primers used). As shown in **Figure 3.1**, the operons and genes were successfully amplified and subsequently cloned into pTH1mp by Gibson Assembly before transformation into DH5α. Chloramphenicol was used as selection marker and colonies of transformants were screened by colony PCR (cPCR) or restriction digestion analysis (RDA) for presence of gene insert. The plasmids of colonies positive of insert was purified from overnight culture and sent for sequencing.

4.1.1 Introduction of genes in the 2,3-butanediol pathway may impose lethal levels of metabolic burden on *Escherichia coli* DH5α cells

For all strains except DH5α (pTH1mp-*budC*_Bl), DH5α (pTH1mp-*bdhA*_Bs) and DH5α (pTH1mp-*bdhA*_Pp), sequencing results of purified plasmids from overnight culture revealed presence of mutations deleterious for gene expression and protein function, despite the use of a high-fidelity polymerase (**Chapter 2.5**). Sequencing results were analysed with the Benchling sequence alignment tool by comparison of the sequencing results with designed construct. Example of deleterious mutations included single base deletions resulting in loss of open reading frame (ORF), deletion of large fragments (ca. 100 bp) in coding region and base substitutions in the hexameric -10 or -30 promoter sequences (data not shown). Overproduction of plasmid-encoded proteins in recombinant *E. coli* strains has previously been demonstrated to cause promoter deletions within the expression construct (Kawe, Horn and Plückthun, 2009).

The are several reasons causing detrimental mutation in expression constructs introduced into cells. For instance, introduction of plasmids has been shown to impose several forms of metabolic burden on *E. coli* cells (Silva, Queiroz and Domingues, 2012). (Bentley *et al.*, 1990; Glick, 1995). Metabolic burden is defined as the portion of a host cell's metabolic resources, such as ATP and carbon building blocks, that are dedicated to operating a non-native pathway (Wu *et al.*, 2016). Simply maintaining and replicating introduced plasmid DNA takes a toll on

cellular resources. Higher plasmid size and copy number has been suggested to increase the magnitude of this "basal" plasmid-induced burden (Seo and Bailey, 1985).

Moreover, expression vectors designed for protein overproduction impose an even more pronounced level of metabolic burden due to the additional consumption of cellular resources associated with protein production (Wittmann *et al.*, 2007). Rozkov *et al.* (2004) reported significantly lower growth rates and biomass yields of plasmid transformed *E. coli* cells and attributed the negative effects to the expression of the *Kan*^{r} marker gene in plasmid pGSK001 (pUC9-based vector with an empty mammalian expression cassette). Various other studies have reported similar negative effects in other bacteria as well, such as *Azotobacter vinelandii* (Glick, Brooks and Pasternak, 1986) and *Pseudomonas putida* (Hong, Pasternak and Glick, 1991). Heterologous expression of certain genes can be highly toxic in *E. coli,* leading to cell death and lysis (Brosius, 1984; Hashemzadeh-Bonehi *et al.*, 1998; Saida *et al.*, 2006), but even the overproduction of "benign"/low-active proteins drains the pool of metabolic resources, especially when genes are under control of extremely strong promoters and Shine-Dalgarno sequences (von Gabain and Bujard, 1979; Kawe, Horn and Plückthun, 2009).

Expression of the *alsSD* operon leads to production of ALS and ALDC which work in tandem to catalyse conversion of pyruvate to acetoin. In other words, the transformation plasmids pTH1mp-*alsSD*_Bl, pTH1mp-*alsSD*_Bs, pTH1mp-*alsSD*_Ec and pTH1mp-*alsSD*_Pp containing *alsSD* operons under the control of the constitutively active *mdh* promoter (Nilasari *et al.*, 2012), introduces a pathway that directly drains the pool of available pyruvate in *E. coli* DH5α. Overproduction of ALDC also depletes the native pool of α-acetolactate that can be used for biosynthesis of branched amino acids (Chiarla *et al.*, 1997).

Thus, a hypothesis was established. Background expression of the *alsSD* operons in introduced expression constructs may impose a significant level of metabolic burden that severely hinders cell growth, which could explain the observed increased mutation rate of the inserts in transformed plasmids. The base substitutions in the -10 and -35 promoter regions or loss of ORFs likely relieves a significant portion the construct-induced metabolic burden, lowering it below a "threshold level" where cell growth is not significantly hindered. This is likely the driving force for the selective propagation of transformants with detrimentally mutated constructs.

However, plasmid constructs pTH1mp-*budC*_Bl, pTH1mp-*bdhA*_Bs and pTH1mp-*bdhA*_Pp were successfully transformed into *E. coli* DH5α free of deleterious mutations (data not shown). For constructs harbouring *bdhA*, *budC* or *gdh*, the metabolic burden is likely lower compared to the *alsSD* operon-harbouring constructs in *E. coli* DH5α as it does not naturally overproduce acetoin, a substrate of 2,3-BDH (Xu *et al.*, 2014).

As mentioned above however, even the overproduction of benign proteins has been shown to cause promoter deletions and still depletes host cell resources (Kawe, Horn and Plückthun, 2009), as sequencing of purified plasmids pTH1mp-*gdh*_Bl and pTH1mp-*budC*_Ec did have detrimental mutations (data not shown).

In summary, the sequencing results suggest that the plasmid constructs experienced high mutation rate when transformed into *E. coli* DH5α host; hypothesized to be caused by background expression ("leaky" expression) of the plasmid constructs, given that the *mdh* promoter is constitutively active in *E. coli* (Nilasari *et al.*, 2012). With this in mind, reducing the background expression of the recombinant gene/operon could potentially increase the stability of the plasmid.

4.1.2 Exploiting the *lac* operon regulatory mechanism to lower background expression

In *E. coli*, the *lac* operon encodes all the genes required for catabolism of lactose. The operon is regulated by the *lac* repressor protein (LacI) which may interact with three operators found in the lac operon: the primary *lac O1* operator (*lacO*) and two auxiliary operators, O2 and O3. *LacO* contains the consensus sequence 5'- AATTGTGAGCGGATAACAATT-3'(Müller *et al.*, 1998) which is the binding site of LacI. Binding of LacI to *lacO* represses the expression of the *lac* operon by inhibiting transcription initiation (Oehler *et al.*, 1990). *In vivo* expression experiments have shown that in the absence an auxiliary operator, *lacO* alone leads to 100-fold gene repression compared to induced state. If *lacO* is deleted, repression is completely abolished even if the auxiliary operators are present (Müller *et al.*, 1998). However, loss of one of the auxiliary operators leads to a 2- to 3- fold reduction in repression, while the loss of both operators lead to a 50-fold reduction in repression, demonstrating the supporting roles of the O2 and O3 operators (Oehler *et al.*, 1990). The binding of allolactose or the lactose structural analogue, isopropyl

β-D-1-thiogalactopyranoside (IPTG), to LacI causes a conformational change in the repressor's structure, preventing it from binding to the *lacO* recognition sequence (Ullmann, 2009).

The use of an IPTG-inducible promoter to heterologously express toxic gene products in *E. coli* has been previously demonstrated (Simons *et al.*, 1984; Hashemzadeh-Bonehi *et al.*, 1998; Warren *et al.*, 2000). For instance, Yansura and Hennert (1984) created a hybrid IPTG-inducible system in *B. subtilis* 168. Briefly, when the penicillinase gene was cloned into a plasmid heterologously expressing the *E. coli* gene encoding LacI, and placed under control of a promoter containing the *lacO* sequence, the expression of penicillinase was inducible by the presence of IPTG, with up to 100-fold difference between induced and uninduced state. In addition, Brosius (1984) succeeded in expressing a toxic rat insulin gene by placing it under control of the synthetic *tac* promoter (containing the *lacO* consensus sequence), and transforming the construct into a LacI-overproducing *E. coli* strain (*E. coli* RB791).

Hence, in hope of lowering background expression of the remaining plasmid constructs, the 21 bp *lacO* consensus sequence was inserted between the *mdh* promoter and RBS in the constructs by Gibson Assembly. To accomplish this, a 72 bp fragment containing the *lacO* sequence was designed (**Figure 4.1**).

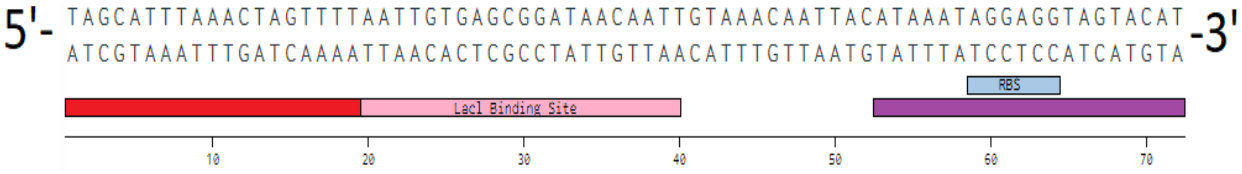

Figure 4.1. The 72 bp *lacO* fragment containing the *lacO* sequence. 21 bp *lacO* consensus sequence (LacI binding site) (pink) and *B. methanolicus* MGA3 RBS (blue) are indicated. Red bar, 5'-terminal region overlapping with the 3'-end of linear pTH1mp amplified with primer pair TDBF/THBR; Purple bar, 3'-terminal region overlapping with the 5'-end PCR amplified gene inserts using specifically designed primers.

The fragment consists of the 51 base pairs upstream of the *Pci*I restriction site in pTH1mp, with the 21 bp *lacO* consensus sequence inserted between the 19th and 20th base pairs. Linear pTH1mp with truncated 3'-end overlapping with the 5'-end of the *lacO* fragment was PCR amplified using the primer pair TDBF/THBR and already linearized pTH1mp as template. The 3' terminal-end of the *lacO* fragment restores the truncated terminal 3'-end of pTH1mp.

The TDBF/THBR-amplified pTH1mp vector, *lacO* fragment and desired gene insert were assembled into a single construct by Gibson Assembly (**Figure 4.2**). The presence of l*acO* in the plasmid constructs allow binding of the constitutively produced Lacl protein natively present in *E. coli* DH5α (Barker *et al.*, 1998) and was hypothesized to lower background expression. This should in turn lower the metabolic burden imposed by the plasmids below the threshold level, permitting the cell to grow while maintaining the correct insert sequence in the plasmid. BLAST search of the *B. methanolicus* MGA3 genome with sequences of gene encoding Lacl from *E. coli* as template did not reveal any sequences with significant similarity, suggesting the *lacO* binding sequence should not significantly affect expression in *B. methanolicus* MGA3 (data not shown).

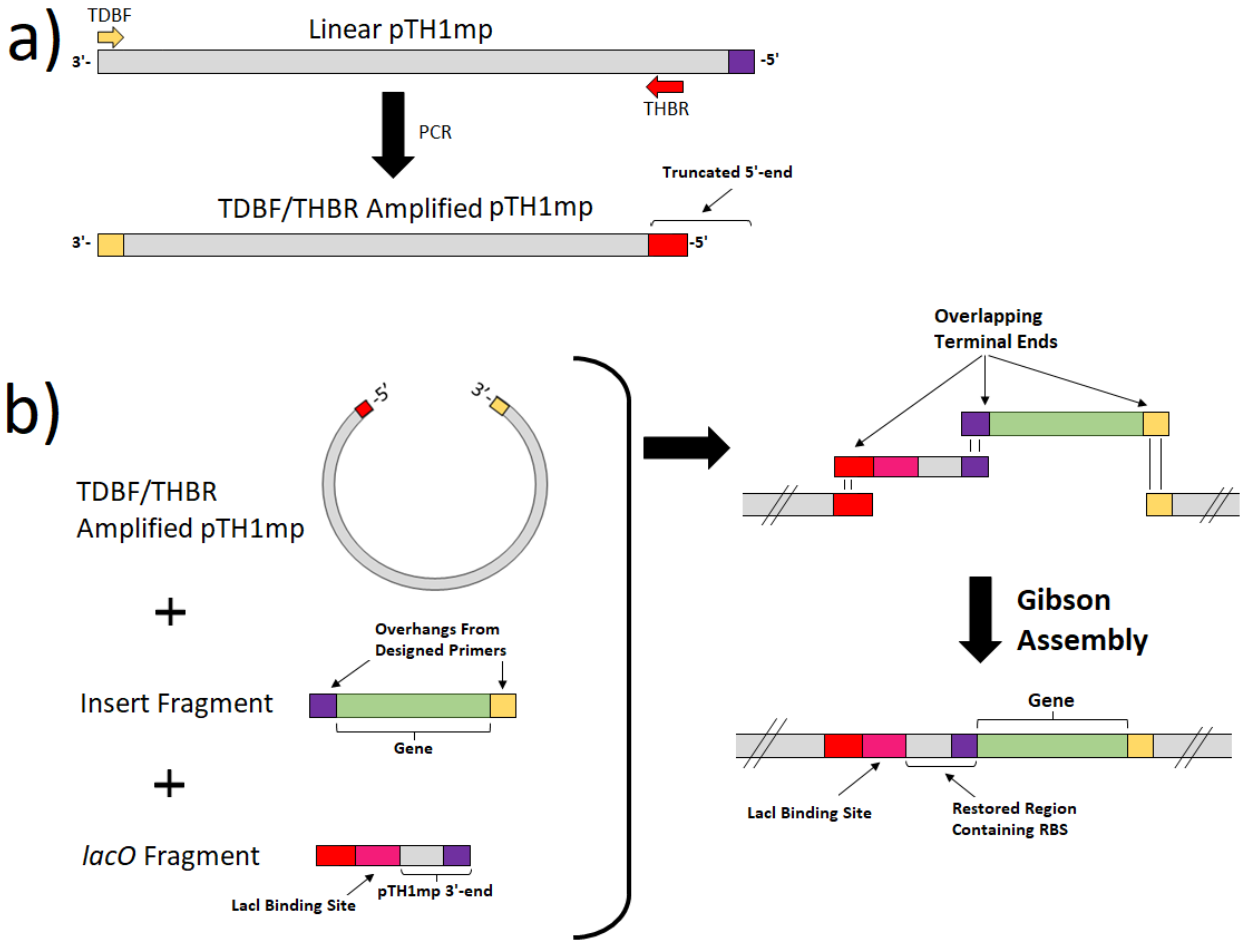

Figure 4.2. Cloning procedure of TDFB/THBR amplified pTH1mp backbone, *lacO* fragment and gene insert. a), PCR amplification of pTH1mp with TDBF (yellow arrow) /THBR (red arrow) primer pair to produce the 5'-end truncated pTH1mp backbone with overlapping region to *lacO* fragment. b), Schematic overview of the cloning procedure of pTH1mpLacO-"Gene Insert" constructs by Gibson Assembly, using DNA fragments with overlapping terminal ends. Truncated 5'-end of pTH1mp containing the RBS (not indicated) is restored by the *lacO* fragment.

Using this strategy, the plasmids pTH1mpLacO-*alsSD*_Pp, pTH1mpLacO-gdh_Bl and pTH1mpLacO-*budC*_Ec, pTH1mpLacO-*alsSD*_Bl and pTH1mpLacO-*alsSD*_Bs were created.

However, only the three former plasmids were successfully transformed in DH5α free of detrimental mutations (data not shown), yielding strains DH5α (pTH1mpLacO-gdh_Bl), DH5α (pTH1mpLacO-*budC*_Ec) and DH5α (pTH1mpLacO-*alsSD*_Pp).

Sequencing results of plasmids pTH1mpLacO-alsSD_Bl and pTH1mpLacO-alsSD_Bs purified from transformed culture still revealed detrimental mutations (specifically base-substitution of the -10 and -35 consensus sequences, data not shown)

4.1.3 GTG start codon substitution to further lower background expression

The persistent occurrence of mutations in of the plasmid constructs pTH1mpLacO-*alsSD*_Bl and pTH1mpLacO-*alsSD*_Bs suggests still lethal-level of background expression. This could be due to saturation of the natively-present LacI proteins within the DH5α host cell. In addition, as the auxiliary operators are not present in the plasmid, repression by LacI is likely not optimal (Warren *et al.*, 2000).

With this in mind, an additional method was employed to further lower gene expression. The expression level of a gene generally decreases when the ATG start codon is substituted with GTG, which has been well documented in *E. coli* and other bacteria (Reddy, Peterkofsky and McKenney, 1985; Blattner and al., 1997; Donnell and Janssen, 2001). Thus, to further lower background expression of the *alsSD* operon, the ATG start codon of the *alsSD* was changed to GTG by PCR amplification using primer pairs D028/D023 and D029/D026 with isolated gDNA from *B. licheniformis* DSM13 and *B. subtilis* 168 as template, respectively.

While this strategy might be sub-optimal if high level expression in the final host strain is desired, it is a compromise for the expression of a potentially toxic operon. The plasmids pTH1mp-*alsSD*_Bl(GTG) and pTH1mp-*alsSD*_Bs(GTG) were constructed and transformed into *E. coli* DH5α, resulting in the DH5α (pTH1mp-*alsSD*_Bl(GTG)) and DH5α (pTH1mp-*alsSD*_Bs(GTG)) strains. The purified plasmids were sequenced and confirmed for the GTG start codon substitution, and the fact that the plasmids were free of detrimental mutations.

The plasmid constructs pTH1mp-*alsSD*_Ec, pTH1mpLacO-*alsSD*_Ec and pTH1mpLacO-*alsSD*_Ec(GTG), all harbouring the *alsSD* operon from *E. cloacae* SDM, were created in a Gibson Assembly reaction, but in all of those attempts mutations occurred after transformation into respective *E. coli* DH5α. A *B. methanolicus* MGA3 strain expressing the *alsSD* operon from *E. cloacae* SDM is thus missing.

4.2 Transformation of *Bacillus methanolicus* MGA3 with Cloned Constructs

Five of the eight constructed plasmids were successfully transformed into electrocompetent *B. methanolicus* MGA3 cells, yielding the strains MGA3 (pTH1mpLacO-*alsSD*_Bl(GTG)), MGA3 (pTH1mpLacO-*alsSD*_Bs(GTG)), MGA3 (pTH1mp-*budC*_Bl), MGA3 (pTH1mp-*gdh*_Bl) and MGA3 (pTH1mpLacO-*bdhA*_Bs) (**Table 3.2**).

No colonies were obtained after transformation with plasmids pTH1mpLacO-*alsSD*_Pp, pTH1mp-*bdhA*_Pp and pTH1mpLacO-*budC*_Ec into *B. methanolicus* MGA3 despite several attempts. The GTG-start codon replacement strategy was not attempted as the copy number of pTH1mp plasmid in *B. methanolicus* is low (5 copies per cell) (Irla *et al.*, 2016) and hence toxic levels of overproduced proteins was not expected. Nonetheless, expression of the recombinant genes from these three untransformable plasmids might impose a toxic effect on cells as previously discussed, resulting in severely hindered growth or even cell death, which could explain the absence of colony formation during transformation.

4.3 Activities of Recombinant Enzymes in Available *Escherichia coli* DH5α and *Bacillus methanolicus* MGA3 Strains.

The activities of ALS and ALDC were assayed simultaneously by monitoring the production of acetoin from pyruvate, while 2,3-BDHs and GDH activity was assayed by monitoring the consumption of NADH for the conversion of acetoin to 2,3-BD. Crude extracts of the available recombinant DH5α and MGA3 strains were prepared and assayed to evaluate their functional activity within respective strains. Protein concentration in crude extract was determined by Bradford Assay (Harlow and Lane, 2006).

Notably, crude extract prepared from DH5α strains cultivated without IPTG induction still showed significantly high enzyme activity (**Figure 3.5** and **Figure 3.7**) compared to activity in the crude extract of control. This indicates that the addition of the *lacO* consensus sequence did not result in tight regulation recombinant gene, discouraging the use of this method. Warren *et al.* (2000) created three highly regulated IPTG-inducible plasmids, but these plasmids contained the entire region between O3 operator and *lacO* of the *lac* operon. The "leaky" expression of the pTH1mpLacO constructs could be corrected by addition of an auxiliary *lac* operators, an interesting future prospect. No IPTG-induction experiment was done to examine the impact of the inserted *lacO* consensus sequence in the recombinant DH5α strains.

4.3.1 Activity of the *alsSD* operon-encoded enzymes in recombinant MGA3 strains

Significant acetoin-synthesising activity was observed in all crude extracts collected from the recombinant MGA3 strains (**Figure 3.6**). The specific activity of the *alsSD* operon-encoded enzymes in crude extract of MGA3 (pTH1mpLacO-*alsSD*_Bl(GTG)) was 17.8 ± 0.1 U/mg at 50 °C, higher than specific activity in crude extract of MGA3 (pTH1mp-*alsSD*LacO_Bs(GTG)) which was 12.0 ± 0.7 U/mg. Interestingly, crude extract from MGA3 (pTH1mp) displayed a specific activity of 2.7 ± 0.4 U/mg. This relatively high specific activity in control could be due to the fact that the Voges-Proskauer colorimetric method used to determine acetoin concentrations in this thesis (**Chapter 2.16**), is also sensitive to diacetyl (Sylvia, 2009). Inspection of the *B. methanolicus* butanoate metabolic pathway in the Kyoto Encyclopaedia of Genes and Genomes (KEGG) revealed the presence of a putative AHAS encoded by a putative *ilvH* gene (BMMGA3_12760).

The accumulation of acetoin observed in the crude extract from MGA3 (pTH1mp) could be due to the presence of diacetyl produced un-specifically by non-enzymatic oxidation of α-acetolactate, synthesised in the reaction catalysed by *ilvH*-encoded enzyme which belongs to the biosynthesis pathway of branched amino acids. The higher enzymatic activity observed in the crude extract from MGA3 (pTH1mpLacO-*alsSD*_Bl(GTG) strain in comparison to MGA3 (pTH1mpLacO-*alsSD*_BS(GTG) could be attributed to the thermophilic nature of *B. licheniformis*. Previous studies have reported numerous *B. licheniformis* strains (such as BL1 and 10-1-A) capable of thermophilically producing 2,3-BD, with optimal production at 50 °C, (Wang *et al.*, 2012; Li *et al.*, 2013b; Ge, Li, Li, *et al.*, 2016). On the other hand, 2,3-BD or acetoin producing *B. subtilis* strains are optimally cultivated at 37 °C for production (Z. Liu *et al.*, 2011; Zhang *et al.*, 2011; M. Wang *et al.*, 2012; Dai *et al.*, 2015; Hao *et al.*, 2017). This could suggest that *B. licheniformis*-derived enzymes have higher thermal stability than those derived from mesophilic *B. subtilis*.

Interestingly, Fu *et al.* (2016c) tested the production of meso-2,3-BD in their mutant *B. subtilis* BSF9 strain at temperatures 37, 42, 46 and 50 °C. *B. subtilis* BSF9 cultures were grown in 100 mL minimum media supplemented with 10 g/L glucose in 250-mL shake-flask at 100 rpm. They report no significant difference in meso-2,3-BD titer nor productivity at 37, 42 and 46 °C. At 50 °C however, titer and productivity decreased by 28.6 % and 36.3 % compared to those at 37 °C, respectively. The authors attribute this to the lower biomass yield observed at 50 °C and not necessarily to lower enzymatic activity. Thus, while *B. subtilis* may grow and produce acetoin and 2,3-BD at temperatures higher than 37 °C, it appears to not do so optimally at 50 °C, compared to *B. licheniformis*. It seems likely that native proteins in *B. licheniformis* strains are more thermostable than proteins in *B. subtilis*.

4.3.2 Activity of 2,3-butanediol dehydrogenases in recombinant MGA3 strains

The recombinant strains MGA3 (pTH1mpLacO-*bdhA*_Bs), MGA3 (pTH1mp-*budC*_Bl) and MGA3 (pTH1mpLacO-*gdh*_Bl) all showed significant activity compared to control strain (**Figure 3.8**). Specific activity was defined as the amount of NADH (mM) consumed per minute, per mg of protein in crude extract.

Among the recombinant *E. coli* DH5α strains, crude extract from DH5α (pTH1mpLacO-*budC*_Ec) displayed the highest acetoin reducing activity at both 37 °C and 45 °C (**Figure 3.7**), but transformation of pTH1mpLacO-*budC*_Ec into *B. methanolicus* MGA3 resulted in no colonies despite several attempts.

Crude extract from MGA3 (pTH1mpLacO-*bdhA*_Bs) displayed highest activity of 1.47 ± 0.02 U/mg, 4.2-fold and 6.4-fold higher than the activity assayed in the crude extract from MGA3 (pTH1mp-*budC*_Bl) (0.35 ± 0.02 U/mg) and MGA3 (pTH1mpLacO-*gdh*_Bl) (0.23 ± 0.02 U/mg), respectively. Control strain MGA3 (pTH1mp) displayed an activity of 0.05 ± 0.04 U/mg, while MGA3 (pTH1mpLacO-*budC*_Ec) and MGA3 (pTH1mp-*bdhA*_Pp) strains are missing.

The acetoin-reducing activity observed in the three available MGA3 strains indicates possibility of *in vivo* 2,3-BD production in *B. methanolicus* MGA3. However, due to incompatibility of two expression vectors sharing the same origin of replication (Velappan *et al.*, 2007), creating a co-expressing recombinant 2,3-BD-producing *B. methanolicus* MGA3 strain was not possible with the available constructs. A strategy to establish such a strain would be to clone the desired gene into a suitable plasmid compatible with pTH1mp, such as the previously described pUB110Smp. The high copy number of pUB110Smp in *B. methanolicus* MGA3 (25 ± 1) (Irla *et al.*, 2016) could bestow upon even higher degree of metabolic burden to transformed cells; considering the problems already faced with pTH1mp, which has a lower copy number (5 ± 1) (Irla *et al.*, 2016). Use of an efficient inducible promoter to lower background expression is a possible solution. The previously established pTH1xpx inducible plasmid (Irla *et al.*, 2016) is also an option (discussed below).

Based on the available enzyme assay results, the *alsSD* operon from *B. licheniformis* and *bdhA* gene from *B. subtilis* 168 are the most optimal combination of genes for the potential production of 2R,3R-BD. Meso-2,3-BDH encoded by *budC* gene from *B. licheniformis* DSM13 has been identified to be responsible for production of both meso-2,3-BDH from 3R-acetoin (Qi *et al.*, 2014) and 2S,3S-BDH from DA (Xu *et al.*, 2016). For production of enantiopure 2,3-BDH in *B. methanolicus* MGA3, additional engineering effort to accumulate the respective precursor metabolite would likely be required.

4.4 Characterization of Transformed Acetoin-Producing MGA3 Strains

Basic Local Alignment Search Tool (BLAST) was used to determine the presence or absence of genes encoding enzymes involved in the biosynthesis of acetoin in the *B. methanolicus* MGA3 genome. The nucleotide sequences of the *alsSD* operon of *B. licheniformis* DSM13 and *B. subtilis* 168 were used as template to search the NCBI non-redundant protein sequences database using a translated nucleotide query (BLASTX). No sequences of significant similarity were found, concluding that *B. methanolicus* MGA3 does not possess *alsS* or *alsD* in its genome.

In addition, BLAST analysis with the *acoA*, *acoB* and *acoR* gene sequences found in *B. subtilis* 168 genome suggest that *B. methanolicus* MGA3 genome does not encode an acetoin dehydrogenase complex as in *B. subtilis* 168 and *B. licheniformis* DSM3. To further evaluate the potential of *B. methanolicus* MGA3 as a potential acetoin producer, an acetoin tolerance experiment was conducted. MGA3 (pTH1mp) was cultivated at different increasing concentrations of acetoin in MVcM medium supplemented with 0.2 M methanol and additives supporting growth. No growth was observed at 50 g/L, and the IC_{50} of acetoin for MGA3 (pTH1mp) was determined to be 25.8 g/L acetoin. The mechanism of acetoin toxicity to microorganisms is not known.

MGA3 (pTH1mpLacO-*alsSD*_Bl(GTG)) and MGA3 (pTH1mpLacO-*alsSD*_Bs(GTG)) was characterized in terms of growth rate and acetoin production by batch-cultivation in 25 mL MVcM media supplemented with 0.2 M methanol and additives at 50 °C, 200 rpm for 24 hours. Acetoin concentration in supernatant was measured at the end of experiment. *B. methanolicus* MGA3 does not accumulate acetoin in the growth medium to significant levels, as the acetoin titer in supernatant from control strain MGA3 (pTH1mp) was 0.02 ± 0.01 (**Table 3.3**), with a specific growth rate of 0.36 ± 0.00 h^{-1}.

Specific growth rate of MGA3 (pTH1mpLacO-*alsSD*_Bl(GTG)) was 0.09 ± 0.01 h^{-1}, 75 % lower than control strain, but the strain achieved the highest acetoin titer of 1.48 ± 0.24 g/L, 74-fold higher compared to control strain and equal to a yield of 0.23 ± 0.04 g/g.

Supernatant in growth medium of MGA3 (pTH1mpLacO-*alsSD*_Bs(GTG)) had an acetoin titer of 0.62 ± 0.00 g/L, equal to a yield 0.10 ± 0.00 g/g which is 2.3-times lower than yield achieved

by MGA3 (pTH1mpLacO-*alsSD*_Bl(GTG)). Remarkably, the growth rate of MGA3 (pTH1mpLacO-*alsSD*_Bs(GTG)) was comparable to the control strain at 0.35 ± 0.010 h^{-1}.

The respective acetoin titers and yields reached by the three strains is consistent with the enzymatic activity observed in their crude extracts at 50 °C, which is attributed to the different optimal temperature of the enzymes. High enzymatic activity of ALS and ALDC likely results in increased energy requirement as the pool of available pyruvate and α-acetolactate are shunted off for the production of acetoin, which could explain the significantly lower growth rate of MGA3 (pTH1mpLacO-*alsSD*_Bl(GTG)). Productivity of MGA3 (pTH1mpLacO-*alsSD*_Bl(GTG)) and MGA3 (pTH1mpLacO-*alsSD*_sl(GTG)) was not determined, but in general, a low growth rate limits a strains economic viability, as it leads to lower productivity at an industrial scale. A solution to overcome the poor growth of MGA3 (pTH1mpLacO-*alsSD*_Bl(GTG)) would be the use of an inducible promoter to tightly regulate the expression of the *alsSD* operon, and to only induce when OD_{600} is high and cells are in exponential growth phase (Comba, Arabolaza and Gramajo, 2012). Irla *et al.* (2016) developed the pTH1xpx plasmid with the xylose inducible promoter originally from *B. megaterium*. The plasmid demonstrated low background expression in absence of xylose, a titratable induction, and a 75-fold induction difference between uninduced and fully induced state. As an already established plasmid in *B. methanolicus* MGA3, pTH1xpx could be suitable host for harbouring the *alsSD* operon from *B. licheniformis* DSM13.

4.5 Evaluating *Bacillus methanolicus* MGA3 as a Potential Acetoin Producer

For the narrow metabolic engineering work performed in this thesis, a relatively high acetoin yield was achieved in comparison to previous more extensive engineering efforts for acetoin production in a heterologous host. For instance, Li *et al.* (2014) engineered *Candida glabrata* (*C. glabrate*) by a systematic approach by evaluating the activity of ALS and ALDC from four different species. The genes *alsS* from *B. subtilis* and *alsD* from *B. amyloquefaciens* were eventually chosen for heterologous co-expression in *C. glabrate*; three promoters were also evaluated. The resulting *C. glabrata* MuA13 strain (harbouring plasmid pY26-TEF-ALS-GPD-ALDC) achieved acetoin titer of 1.96 g/L, but produced ethanol as a major by-product. Further engineering by deletion of the gene encoding ethanol dehydrogenase and addition of nicotinic acid (precursor to NAD^+) to lower NADH/NAD^+ ratio resulted in an acetoin titer of 3.67 g/L by the final mutant strain *C. glabrata* MuA15 growing on 120 g/L glucose (Li *et al.*, 2014), a titer in similar range to MGA3 (pTH1mpLacO-*alsSD*_Bl(GTG)).

Many parameters describing acetoin production of MGA3 (pTH1mpLacO-*alsSD*_Bl(GTG)) and MGA3 (pTH1mpLacO-*alsSD*_Bs(GTG)) are yet to be determined, such as the rate of methanol consumption, productivity and by-product formation. Insight into these parameters would be the starting point for inspiration of future engineering strategies. Some of the engineering strategies employed for *C. glabrata* MuA15 are potential strategies for MGA3 (pTH1mp-*alsSD*_Bl(GTG)) and MGA3 (pTH1mp-*alsSD*_Bs(GTG)) as well.

Co-factor engineering strategies for acetoin or 2,3-BD production generally involves regulating the intracellular NADH/NAD^+ ratio. Employing the water-forming NADH oxidase to regulate the intracellular NAD^+ was deemed effective in elevating acetoin yield in use in *S. marcescens* (J. A. Sun *et al.*, 2012; Ji *et al.*, 2013). However, wild type *B. methanolicus* MGA3 cannot naturally convert acetoin to 2,3-BDH, deeming this strategy is inapplicable.

In comparison to the performance of native 2,3-BD producers (under adequately comparable conditions), the acetoin yield of MGA3 (pTH1mpLacO-*alsSD*_Bl(GTG)) and MGA3 (pTH1mpLacO-*alsSD*_Bs(GTG)) is relatively low. For example, the isolated *B. subtilis* JNA3-10 strain was cultivated in experimentally optimized conditions (pH and temperature was tested).

The highest titer achieved was 42.2 g/L after 132 hours shake-flask fermentation in 50 mL medium at 37 °C, pH = 4, growing on 150 g/L glucose. Interestingly, the authors observed reverse 2,3-BD transformation, where acetoin titers began increasing during stationary phase after glucose was completely depleted, hence the long cultivation time. The titer was achieved however, without any metabolic engineering efforts (Zhang *et al.*, 2011). Furthermore, a *bdhA* and *acoA* double-knockout *B. subtilis* strain was created. Subsequent overexpression of the *B. subtilis* 168 *alsSD* operon created strain BSUW06. BSUW06 grown by shake-flask cultivation in 100 mL LB medium at 37 °C, 220 rpm achieved a titer of 19.1 g/L with yield 0.38 g/g, after 62 hours, which was reported to be 26 % higher than wild type *B. subtilis* 168 under same conditions (M. Wang *et al.*, 2012).

While there are numerous reports of achieved acetoin titers substantially higher than those reported here by MGA3 (pTH1mp-*alsSD*_Bl(GTG)) and MGA3 (pTH1mp-*alsSD*_Bs(GTG)) (**Table 1.1**), the differences in fermentation conditions such as substrate supply, medium volume, operation mode, etc. makes the results incomparable. It is important to note that glucose is the raw material often employed to achieve high acetoin titers, which is not ideal given its rising price, and that it is a food-commodity (Haley, 2015). Hence, the ability of MGA3 (pTH1mp-*alsSD*_Bl(GTG)) and MGA3 (pTH1mp-*alsSD*_Bs(GTG)) to convert inexpensive, renewable and pure methanol to acetoin is a unique and dominating advantage. In addition, *B. methanolicus* grows optimally at temperatures between 50-53 °C on methanol, which are conditions unfavourable for growth of most mesophilic bacteria, thus lowering risk of costly production delays/shut-downs cause by contamination (Beckner, Ivey and Phister, 2011).

B. methanolicus MGA3 shows promise as a candidate for industrial production of acetoin, and possibly 2,3-BD. Much of the bacterium's capability remains unexplored, prompting inquiry into future engineering strategies. In addition, to engineering strategies, process control variables can also be employed to optimize acetoin yield, as reviewed by Xiao and Lu (2014). A few of such strategies possibly applicable to *B. methanolicus* are discussed below.

4.5.1 Process Control Variables for Optimization of Acetoin Production in *Bacillus methanolicus* MGA3

In general, high oxygen supply favours acetoin formation and decreases 2,3-BD final titre in native 2,3-BD producers, although abundance of oxygen may also lead to generation of excess biomass and CO_2. To achieve highest yield, a balance of resources dedicated for acetoin production and cell growth needs to be achieved, which can be done by careful control of oxygen supply (Moes *et al.*, 1985; Zeng *et al.*, 1994; Zhang *et al.*, 2010; Häßler *et al.*, 2012). Simple two-stage agitation control strategies have seen success in increasing 2,3-BD titers, although the use of slow-fast or fast-slow agitation scheme appears to be species dependent, as studies report success with both in different microorganisms (Ji *et al.*, 2009; Sun *et al.*, 2012; Zhang *et al.*, 2013).

The ALS from *E. aerogenes* (Perego *et al.*, 2000; Converti *et al.* 2003), *L. lactis* (Lopez De Felipe *et al.* 1997) and *P. polymyxa* (Zhang *et al.*, 2012) functions optimally at a pH between 5.5 to 6. Acetoin production in these bacteria were favoured in acidic pH and excess of pyruvate. Acetate supplementation of growth medium has been reported to induce expression of the three key enzymes in 2,3-BD pathway and increasing product titers in *E. aerogenes* (Lee *et al.*, 2016, 2017) and *P. polymyxa* (Akhtar, 2007). The mechanism of acetate induction is however, unclear. Whether this strategy is applicable to the acetoin-producing *B. methanolicus* MGA3 strains created here, whose *alsSD* operon is under control of the *mdh* promoter, is to be determined.

B. methanolicus MGA3 tolerates relatively low acetoin concentrations (IC_{50} = 25.8 g/L) in growth medium before growth is reduced by 50%. Remarkably, acetoin tolerance can be increased, as demonstrated by Luo *et al.* (2014). Adaptive evolution using acetoin stress as the selection pressure to screen for acetoin tolerant strains led to the isolation of the *B. amyloliquefaciens* E-11 strain, which exhibited increased acetoin resistance compared to parent strain. The bacterium also achieved higher acetoin titers, yields and productivity, although the exact mechanism of elevated acetoin resistance was undetermined.

5 Conclusion

B. methanolicus shows promise as microbial producer, being able to grow exclusively on methanol as carbon and energy source. Heterologous expression of *alsSD* operons derived from native 2,3-BD producers in *B. methanolicus* MGA3 appears to have an adverse effect on growth, which was attributed to high background expression from plasmid constructs. Efforts to lower background expression involved cloning the *LacO* consensus sequence into pTH1mp and by changing the start codon to sub-optimal GTG start codon. Both strategies were employed to create two acetoin-producing strains, *B.* MGA3 (pTH1mpLacO-*alsSD*_Bl(GTG)) and MGA3 (pTH1mpLacO-*alsSD*_Bs(GTG)), which differed greatly in growth characteristics.

Enzyme assay of the crude extracts harvest from non-induced DH5α cultures displayed significant acetoin-synthesising activity, suggesting that the addition of the *LacO* consensus sequence did not lead to tight regulation.

As acetoin is the direct precursor to 2,3-BD, the activity of 2,3-BDHs from the same native 2,3-BD producers were assayed in *B. methanolicus* MGA3. The strains MGA3 (pTH1mp-*budC*_Bl), MGA3 (pTH1mp-gdh_Bl) and MGA3 (pTH1mp-*bdhA*_Bs) were created, overexpressing meso-2,3-BDH, GDH and 2R,3R-BDH respectively. Enzymatic assay of crude extract from the respective strains revealed significant acetoin-reducing activity in all three strains, suggesting potential to produce all three stereoisomeric forms of 2,3-BD in *B. methanolicus* MGA3. I*n vivo* production of 2,3-BDH was not attempted.

MGA3 (pTH1mpLacO-*alsSD*_Bl(GTG)) achieved an acetoin titer of 1.48 ± 0.24 g/L after 24-hour batch-fermentation at 50 °C, and a yield of 0.23 ± 0.04 g/g. The specific growth rate (0.09 ± 0.01) was however, 75 % lower compared to control strain. MGA3 (pTH1mpLacO-*alsSD*_Bs(GTG)) achieved an acetoin titer of 0.62 ± 0.00 g/L, with a specific growth rate (0.35 h^{-1}) comparable to growth rate of control strain (0.36 h^{-1}). The titer and yield of the two trains is consistent with the specific enzyme activity observed, which was 17.8 ± 0.1 and 12.0 ± 0.7 U/mg for MGA3 (pTH1mpLacO-*alsSD*_Bl(GTG)) and MGA3 (pTH1mpLacO-*alsSD*_Bs(GTG)), respectively.

Ultimately, the ability to use methanol as substrate for acetoin production is a dominating advantage, and the relatively low engineering effort performed, yet relatively high achieved

yields iin this thesis show promise for *B. methanolicus* MGA3 as a candidate for acetoin production. The characterization of acetoin production by the two MGA3 strains is lacking, leaving much room for further metabolic engineering to optimize acetoin yields. To date, this is the first report of metabolically engineering *B. methanolicus* MGA3 for the production of a non-amino acid specialty compound, and the first reported demonstration of the bioconversion of inexpensive methanol to valuable acetoin.

6 Literature

Aasberg-Petersen, K. *et al.* (2008) 'Large scale methanol production from natural gas', *Haldor Topsoe*, p. 22. Available at: http://www.topsoe.com/sites/default/files/topsoe_large_scale_methanol_prod_paper.ashx_.pdf.

Akhtar, M. S. (2007) 'Enhanced 2,3-Butanediol Production by Addition of Acetic Acid in Paenibacillus polymyxa', *Australasian Plant Pathology*, 1(2), p. 293. doi: 10.1071/AP07006.

Ali, N. O. *et al.* (2001) 'Regulation of the acetoin catabolic pathway is controlled by sigma L in Bacillus subtilis', *Journal of Bacteriology*, 183(8), pp. 2497–2504. doi: 10.1128/JB.183.8.2497-2504.2001.

Arfman, N. *et al.* (1992) 'Bacillus methanolicus sp. nov., a New Species of Thermotolerant, Methanol-Utilizing, Endospore-Forming Bacteria', *International Journal of Systematic Bacterioldgy*, (July), pp. 439–445. Available at: http://www.microbiologyresearch.org/docserver/fulltext/ijsem/42/3/ijs-42-3-439.pdf?expires=1515406317&id=id&accname=guest&checksum=2CD9F355F8893AF116BB3773A69C4734.

Bais, A. F. *et al.* (2018) 'Environmental effects of ozone depletion, UV radiation and interactions with climate change: UNEP Environmental Effects Assessment Panel, update 2017', *Photochemical & Photobiological Sciences*. Royal Society of Chemistry, 17(2), pp. 127–179. doi: 10.1039/C7PP90043K.

Bao, T. *et al.* (2015) 'Regulation of the NADH pool and NADH/NADPH ratio redistributes acetoin and 2,3-butanediol proportion in Bacillus subtilis', *Biotechnology Journal*, 10(8), pp. 1298–1306. doi: 10.1002/biot.201400577.

Barbir, F., Veziroğlu, T. N. and Plass, H. J. (1990) 'Environmental damage due to fossil fuels use', *International Journal of Hydrogen Energy*, 15(10), pp. 739–749. doi: 10.1016/0360-3199(90)90005-J.

Barker, A. *et al.* (1998) 'Operator search by mutant Lac repressors', *Journal of Molecular Biology*, 278(3), pp. 549–558. doi: 10.1006/jmbi.1998.1729.

Bartowsky, E. J. and Henschke, P. A. (2004) 'The "buttery" attribute of wine—diacetyl—desirability, spoilage and beyond', *International Journal of Food Microbiology*, 96(3), pp. 235–252. doi: 10.1016/j.ijfoodmicro.2004.05.013.

Beckner, M., Ivey, M. L. and Phister, T. G. (2011) 'Microbial contamination of fuel ethanol fermentations', *Letters in Applied Microbiology*, 53(4), pp. 387–394. doi: 10.1111/j.1472-765X.2011.03124.x.

Bentley, W. E. *et al.* (1990) 'Plasmid-encoded protein: The principal factor in the "metabolic burden" associated with recombinant bacteria', *Biotechnology and Bioengineering*, 35(7), pp. 668–681. doi: 10.1002/bit.260350704.

Bernt, E. and Hess, B. (1965) *Methods of Enzymatic Analysis*, *Methods of Enzymatic Analysis*. doi: 10.1016/B978-0-12-395630-9.50134-1.

Bertau, M. *et al.* (2014) 'Methanol: The basic chemical and energy feedstock of the future: Asinger's vision today (Chapter 1: Introduction)', *Methanol: The Basic Chemical and Energy Feedstock of the Future: Asinger's Vision Today*, pp. i–xxxi. doi: 10.1007/978-3-642-39709-7.

Bethesda Research Laboratories (1986) 'E. coli DH5 alpha competent cells', *FOCUS - Bethesda Research Laboratories*, 8, p. 9.

Biswas, R. *et al.* (2012) 'Enhanced production of 2,3-butanediol by engineered Bacillus subtilis', *Applied Microbiology and Biotechnology*, 94(3), pp. 651–658. doi: 10.1007/s00253-011-3774-5.

Blattner, F. R. and al., et (1997) 'The complete genome sequence of Escherichia coli K-12', *Science*, 277(September), pp. 1453–1462.

Blomqvist, K. *et al.* (1993) 'Characterization of the genes of the 2,3-butanediol operons from Klebsiella terrigena and Enterobacter aerogenes', *Journal of Bacteriology*, 175(5), pp. 1392–1404. doi: 10.1128/jb.175.5.1392-1404.1993.

Bozdag, A., Komives, C. and Flickinger, M. C. (2015) 'Growth of Bacillus methanolicus in 2 M methanol at 50 °C: the effect of high methanol concentration on gene regulation of enzymes involved in formaldehyde detoxification by the ribulose monophosphate pathway', *Journal of Industrial Microbiology and Biotechnology*. Springer Berlin Heidelberg, 42(7), pp. 1027–1038. doi: 10.1007/s10295-015-1623-8.

Bradford, M. M. (1976) 'A rapid and sensitive method for the quantitation of microgram quantities of protein utilizing the principle of protein-dye binding', *Analytical Biochemistry*, 72(1–2), pp. 248–254. doi: 10.1016/0003-2697(76)90527-3.

Brautaset, T. *et al.* (2003) 'Role of the *Bacillus methanolicus* citrate synthase II gene, *citY*, in regulating the secretion of glutamate in L-lysine-secreting mutants', *Appl Environ Microbiol*, 69(7), pp. 3986–3995. doi: 10.1128/AEM.69.7.3986.

Brautaset, T. *et al.* (2004) 'Plasmid-Dependent Methylotrophy in Thermotolerant Bacillus methanolicus', *Journal of Bacteriology*, 186(5), pp. 1229–1238. doi: 10.1128/JB.186.5.1229-1238.2004.

Brautaset, T. *et al.* (2007) 'Bacillus methanolicus: A candidate for industrial production of amino acids from methanol at 50°C', *Applied Microbiology and Biotechnology*. doi: 10.1007/s00253-006-0757-z.

Brautaset, T. *et al.* (2010) 'Bacillus methanolicus pyruvate carboxylase and homoserine dehydrogenase I and II and their roles for L-lysine production from methanol at 50°C', *Applied Microbiology and Biotechnology*, 87(3), pp. 951–964. doi: 10.1007/s00253-010-2559-6.

Brosius, J. (1984) 'Toxicity of an overproduced foreign gene product in Escherichia coli and its use in plasmid vectors for the selection of transcription terminators', *Gene*, 27(2), pp. 161–172. doi: 10.1016/0378-1119(84)90137-9.

Burdock, G. A. (2005) 'Fenaroli's Handbook of Flavor Ingredients, Fifth Edition', in *Fenaroli's Handbook of Flavor Ingredients, FifthEdition*, p. 147. doi: 10.1201/NOE0849309465.fmatt.

Burkholder, P. R. and Giles, N. H. (1947) 'Induced biochemical mutations in Bacillus subtilis', *American journal of botany*, 34(6), pp. 345–348. doi: 10.2307/2437147.

Chaudhari, S. S. *et al.* (2016) 'The LysR-type transcriptional regulator, CidR, regulates stationary phase cell death in Staphylococcus aureus', *Molecular Microbiology*, 101(6), pp. 942–953. doi: 10.1111/mmi.13433.

Chen, C. *et al.* (2014) 'Mechanism of 2,3-butanediol stereoisomer formation in Klebsiella pneumoniae', *Applied Microbiology and Biotechnology*, 98(10), pp. 4603–4613. doi: 10.1007/s00253-014-5526-9.

Chen, N. H. *et al.* (2016) 'Formaldehyde stress responses in bacterial pathogens', *Frontiers in Microbiology*, 7(MAR), pp. 1–17. doi: 10.3389/fmicb.2016.00257.

Chen, R. zhao and Li, yu (2011) 'A novel plant volatile attractant scheme to protect corn in China from the white-spotted flower chafer (Coleoptera: Scarabaeidae: Cetoniinae)', *Journal of Pest Science*, 84(3), pp. 327–335. doi: 10.1007/s10340-011-0353-6.

Chiarla, C. *et al.* (1997) 'The branched-chain amino acids', *Minerva gastroenterologica e dietologica*, 43(4), pp. 189–196. doi: 10.1007/7171.

Cho, S. *et al.* (2015) 'Enhanced 2,3-butanediol production by optimizing fermentation conditions and engineering klebsiella oxytoca M1 through overexpression of acetoin reductase', *PLoS ONE*, 10(9), pp. 1–16. doi: 10.1371/journal.pone.0138109.

Comba, S., Arabolaza, A. and Gramajo, H. (2012) 'Emerging Engineering Principles for Yield Improvement in Microbial Cell Design', *Computational and Structural Biotechnology Journal*. Research Network of Computational and Structural Biotechnology, 3(4), p. e201210016. doi: 10.5936/csbj.201210016.

Converti, A., Perego, P. and Del Borghi, M. (2003) 'Effect of specific oxygen uptake rate on Enterobacter aerogenes energetics: Carbon and reduction degree balances in batch cultivations', *Biotechnology and Bioengineering*, 82(3), pp. 370–377. doi: 10.1002/bit.10570.

Cook, L. K. N. (1996) 'Optimizing Culturing Conditions for Bacillus Subtilis', *South African Avocado Growers' Association Yearbook*, pp. 54–58.

Cue, D. *et al.* (1997) 'Genetic manipulation of Bacillus methanolicus, a gram-positive, thermotolerant methylotroph', *Applied and Environmental Microbiology*, 63(4), pp. 1406–1420.

Cue, D., Lam, H. and Hanson, R. S. (1996) 'Characterization of a Restriction-Modification System of the Thermotolerant Methylotroph Bacillus methanolicus', 62(3), pp. 1107–1111.

Dagert, M. and Ehrlich, S. D. (1979) 'Prolonged incubation in calcium chloride improves the competence of Escherichia coli cells', *Gene*, 6(1), pp. 23–38. doi: 10.1016/0378-1119(79)90082-9.

Dai, J. Y. *et al.* (2015) 'High acetoin production by a newly isolated marine Bacillus subtilis strain with low requirement of oxygen supply', *Process Biochemistry*, 50(11), pp. 1730–1734. doi: 10.1016/j.procbio.2015.07.010.

Dalton, H. (1983) *The biochemistry of methylotrophs, Trends in Biochemical Sciences*. doi: 10.1016/0968-0004(83)90116-0.

Dijkhuizen, L. *et al.* (1988) 'Isolation and initial characterization of thermotolerant

methylotrophic Bacillus strains', *FEMS Microbiology Letters*, 52(3), pp. 209–214.

Donnell, S. M. O. and Janssen, G. R. (2001) 'The Initiation Codon Affects Ribosome Binding and Translational Efficiency in Escherichia coli of c I mRNA with or without the 5 ′ Untranslated Leader The Initiation Codon Affects Ribosome Binding and Translational Efficiency in Escherichia coli of cI mRN', *Journal of Bacteriology*, 183(4), pp. 1277–1283. doi: 10.1128/JB.183.4.1277.

Ebel, K. *et al.* (1998) 'Process for the preparation of acyloins'. Germany, BASF Aktiengesellschaft: Patent US5831097 A.

Eikmanns, B. J. *et al.* (1994) 'Nucleotide sequence, expression and transcriptional analysis of the Corynebacterium glutamicum gltA gene encoding citrate synthase', *Microbiology*, 140(Pt 8), pp. 1817–1828. doi: 10.1099/13500872-140-8-1817.

el-Helow, E. R. and Khattab, A. A. (1996) 'The development of a Bacillus subtilis 168 culture condition for enhanced and accelerated beta-mannanase production', *Acta Microbiol Immunol Hung*, 43(4), pp. 289–299. Available at: http://www.ncbi.nlm.nih.gov/entrez/query.fcgi?cmd=Retrieve&db=PubMed&dopt=Citation&list_uids=9147720.

Feng, W. *et al.* (2011) 'Analysis of Methanol Production from Biomass Gasification', *Chemical Engineering and Technology*, 34(2), pp. 307–317. doi: 10.1002/ceat.201000346.

Fernie, A. R., Carrari, F. and Sweetlove, L. J. (2004) 'Respiratory metabolism: Glycolysis, the TCA cycle and mitochondrial electron transport', *Current Opinion in Plant Biology*, pp. 254–261. doi: 10.1016/j.pbi.2004.03.007.

Flickinger, M. C. (1980) 'CURRENT BIOLOGICAL RESEARCH IN CONVERSION OF CELLULOSE CARBOHYDRATES INTO LIQUID FUELS - HOW FAR HAVE WE COME?', *Biotechnology and Bioengineering*, 22 Suppl 1, pp. 27–48. Available at: https://www.scopus.com/inward/record.uri?eid=2-s2.0-0019090663&partnerID=40&md5=00a6b2a2e2eeacca2dbf08aa6ee04a56.

Forlani, G., Mantelli, M. and Nielsen, E. (1999) 'Biochemical evidence for multiple acetoin-forming enzymes in cultured plant cells', *Phytochemistry*, 50(2), pp. 255–262. doi: 10.1016/S0031-9422(98)00550-0.

Frackman, B. S. *et al.* (1998) 'Betaine and DMSO : Enhancing Agents for PCR', *Promega Notes*, 65(65), pp. 9–12. Available at: http://taq.ch/pnotes/65/6921_27/6921_27_core.pdf.

Frädrich, C. *et al.* (2012) 'The transcription factor alsr binds and regulates the promoter of the alssd operon responsible for acetoin formation in bacillus subtilis', *Journal of Bacteriology*, 194(5), pp. 1100–1112. doi: 10.1128/JB.06425-11.

Fu, J. *et al.* (2016a) 'Metabolic engineering of Bacillus subtilis for chiral pure meso-2,3-butanediol production', *Biotechnology for Biofuels*, 9(1). doi: 10.1186/s13068-016-0502-5.

Fu, J. *et al.* (2016b) 'Metabolic engineering of Bacillus subtilis for chiral pure meso-2,3-butanediol production', *Biotechnology for Biofuels*. doi: 10.1186/s13068-016-0502-5.

Fu, J. *et al.* (2016c) 'Metabolic engineering of Bacillus subtilis for chiral pure meso-2,3-

butanediol production', *Biotechnology for Biofuels*. BioMed Central, 9(1), pp. 1–14. doi: 10.1186/s13068-016-0502-5.

von Gabain, A. and Bujard, H. (1979) 'Interaction of Escherichia coli RNA polymerase with promoters of several coliphage and plasmid DNAs.', *Proceedings of the National Academy of Sciences of the United States of America*, 76(1), pp. 189–93. doi: 10.1073/pnas.76.1.189.

Gao, J. *et al.* (2013) 'A 2,3-butanediol dehydrogenase from paenibacillus polymyxa ZJ-9 for mainly producing R,R-2,3-butanediol: Purification, characterization and cloning', *Journal of Basic Microbiology*, 53(9), pp. 733–741. doi: 10.1002/jobm.201200152.

Garg, S. K. and Jain, A. (1995) 'Fermentative production of 2,3-butanediol: A review', *Bioresource Technology*, pp. 103–109. doi: 10.1016/0960-8524(94)00136-O.

Ge, L. *et al.* (2011a) 'A New Method for Industrial Production of 2,3-butanediol', *Journal of Biomaterials and Nanobiotechnology*, 2, pp. 335–336. doi: 10.1007/s002530000486.

Ge, L. *et al.* (2011b) 'A New Method for Industrial Production of 2,3-Butanediol', *Journal of Biomaterials and Nanobiotechnology*, (2), pp. 335–336. doi: 10.1007/s002530000486.

Ge, Y., Li, K., Li, L., *et al.* (2016) 'Contracted but effective: production of enantiopure 2,3-butanediol by thermophilic and GRAS Bacillus licheniformis', *Green Chem.*, pp. 4693–4703. doi: 10.1039/C6GC01023G.

Ge, Y., Li, K., Gao, L., *et al.* (2016) 'Contracted but effective: production of enantiopure 2,3-butanediol by thermophilic and GRAS Bacillus licheniformis', *Green Chemistry*, 18, pp. 4693–4703. Available at: http://pubs.rsc.org/en/content/articlelanding/2016/gc/c6gc01023g#!divAbstract.

Gibson, D. G. *et al.* (2009) 'Enzymatic assembly of DNA molecules up to several hundred kilobases', *Nature Methods*, 6(5), pp. 343–345. doi: 10.1038/nmeth.1318.

Gill, C. O. and Suisted, J. R. (1978) 'The effects of temperature and growth rate on the proportion of unsaturated fatty acids in bacterial lipids.', *Journal of general microbiology*, 104(1), pp. 31–6. doi: 10.1099/00221287-104-1-31.

Gillberg, B. O. (2009) *Memorandum: Methanol factory in Hagfors*. VärmlandsMetanol AB/Miljöcentrum.

Glick, B. R. (1995) 'Metabolic load and heterologous gene expression', *Biotechnology Advances*, pp. 247–261. doi: 10.1016/0734-9750(95)00004-A.

Glick, B. R., Brooks, H. E. and Pasternak, J. J. (1986) 'Physiological effects of plasmid DNA transformation on Azotobacter vinelandii', *Canadian Journal of Microbiology*, 32(2), pp. 145–148. doi: 10.1139/m86-028.

Gräfje, H. *et al.* (2012) 'Butanediols, Butenediol, and Butynediol', in *Ullmann's Encyclopedia of Industrial Chemistry*, pp. 407–415. doi: 10.1002/14356007.a04_455.

Green, M. R. and Sambrook, J. (2012) *Molecular Cloning: A Laboratory Manual (Fourth Edition), Cold Spring Harbor Laboratory Press; 4th edition (June 15, 2012)*. Available at: http://www.amazon.com/Molecular-Cloning-Laboratory-Edition-Three/dp/1936113422.

Haley, S. (2015) ‘Projecting World Raw Sugar Prices’, *Economic Research Service*.

Hamelinck, C. N. and Faaij, A. P. C. (2002) ‘Future prospects for production of methanol and hydrogen from biomass’, *Journal of Power Sources*, 111(1), pp. 1–22. doi: 10.1016/S0378-7753(02)00220-3.

Hanson, R.S., Dillingham, R., Olson, P., Lee, G.H., Cue, D., Schendel, F.J., Bremmon, C., Flickinger, M. C. (1996) ‘Production of L-Lysine and Some Other Amino Acids by Mutants of B. methanolicus.’, *Microbial Growth on C1 Compounds*, pp. 227–236.

Hao, W. *et al.* (2017) ‘Metabolic engineering of Bacillus sp. for diacetyl production’, *Process Biochemistry*. Elsevier, 58(2), pp. 69–77. doi: 10.1016/j.procbio.2017.04.015.

Harden, A. and Walpole, G. (1906) ‘2,3-Butylene glycol fermentation by Aerobacter aerogenes.’, *Proceedings of the Royal Society of London B.*, 77, pp. 399–405.

Harlow, E. and Lane, D. (2006) ‘Bradford Assay’, *Cold Spring Harbor Protocols*, 2006(6), p. pdb.prot4644-pdb.prot4644. doi: 10.1101/pdb.prot4644.

Hashemzadeh-Bonehi, L. *et al.* (1998) ‘Importance of using lac rather than ara promoter vectors for modulating the levels of toxic gene products in Escherichia coli’, *Molecular Microbiology*, 30(3), pp. 676–678.

Häßler, T. *et al.* (2012) ‘Enhanced fed-batch fermentation of 2,3-butanediol by Paenibacillus polymyxa DSM 365’, *Bioresource Technology*, 124, pp. 237–244. doi: 10.1016/j.biortech.2012.08.047.

van Haveren, J., Scott, E. L. and Sanders, J. (2008) ‘Bulk chemicals from biomass’, *Biofuels, Bioproducts and Biorefining*, pp. 41–57. doi: 10.1002/bbb.43.

Heggeset, T. M. B. *et al.* (2012) ‘Genome sequence of thermotolerant Bacillus methanolicus: Features and regulation related to methylotrophy and production of L-lysine and L-glutamate from methanol’, *Applied and Environmental Microbiology*, 78(15), pp. 5170–5181. doi: 10.1128/AEM.00703-12.

Heggeset, T. M. B. *et al.* (2012) ‘Genome sequence of thermotolerant Bacillus methanolicus: Features and regulation related to methylotrophy and production of L-lysine and L-glutamate from methanol’, *Applied and Environmental Microbiology*. doi: 10.1128/AEM.00703-12.

Hong, Y., Pasternak, J. J. and Glick, B. R. (1991) ‘Biological consequences of plasmid transformation of the plant growth promoting rhizobacterium Pseudomonas putida GR12-2’, *Canadian Journal of Microbiology*, 37(10), pp. 796–799. doi: 10.1139/m91-137.

Huang, M., Oppermann-Sanio, F. B. and Steinbüchel, a (1999) ‘Biochemical and molecular characterization of the Bacillus subtilis acetoin catabolic pathway.’, *Journal of bacteriology*, 181(12), pp. 3837–3841.

Huo, Y. *et al.* (2018) ‘Acetolactate synthase (AlsS) in Bacillus licheniformis WX-02: enzymatic properties and efficient functions for acetoin/butanediol and l-valine biosynthesis’, *Bioprocess and Biosystems Engineering*, 41(1), pp. 87–96. doi: 10.1007/s00449-017-1847-2.

Ikeda, M. and Takeno, S. (2013) *Amino Acid Production by Corynebacterium glutamicum*,

Corynebacterium glutamicum. Biology and Biotechnology. doi: 10.1007/978-3-642-29857-8.

Irla, M. *et al.* (2015) 'Transcriptome analysis of thermophilic methylotrophic Bacillus methanolicus MGA3 using RNA-sequencing provides detailed insights into its previously uncharted transcriptional landscape', *BMC Genomics*. doi: 10.1186/s12864-015-1239-4.

Irla, M. *et al.* (2016) 'Genome-based genetic tool development for Bacillus methanolicus: Theta- and rolling circle-replicating plasmids for inducible gene expression and application to methanol-based cadaverine production', *Frontiers in Microbiology*. doi: 10.3389/fmicb.2016.01481.

Irla, M. *et al.* (2017) 'Methanol-based γ-aminobutyric acid (GABA) production by genetically engineered Bacillus methanolicus strains', *Industrial Crops and Products*, 106, pp. 12–20. doi: 10.1016/j.indcrop.2016.11.050.

Jakobsen, Ø. M. *et al.* (2006) 'Upregulated Transcription of Plasmid and Chromosomal Ribulose Monophosphate Pathway Genes Is Critical for Methanol Assimilation Rate and Methanol Tolerance in the Methylotrophic Bacterium Bacillus methanolicus', 188(8), pp. 3063–3072. doi: 10.1128/JB.188.8.3063.

Jakobsen, Ø. M. *et al.* (2009) '(HAS IC50) Overexpression of wild-type aspartokinase increases L-lysine production in the thermotolerant methylotrophic bacterium Bacillus methanolicus', *Applied and Environmental Microbiology*, 75(3), pp. 652–661. doi: 10.1128/AEM.01176-08.

Jensen, P. R. and Hammer, K. (1998) 'The sequence of spacers between the consensus sequences modulates the strength of prokaryotic promoters', *Applied and Environmental Microbiology*, 64(1), pp. 82–87. doi: 10.1002/bies.950100409.

Jeon, Y. H. *et al.* (2010) 'Effects of initial inoculation density of Paenibacillus polymyxa on colony formation and starch-hydrolytic activity in relation to root rot in ginseng', *Journal of Applied Microbiology*, 109(2), pp. 461–470. doi: 10.1111/j.1365-2672.2010.04674.x.

Ji, X. J. *et al.* (2008) 'Enhanced 2,3-butanediol production by altering the mixed acid fermentation pathway in Klebsiella oxytoca', *Biotechnology Letters*, 30(4), pp. 731–734. doi: 10.1007/s10529-007-9599-8.

Ji, X. J., Huang, H., Du, J., Zhu, J. G., Ren, L. J., Li, S., *et al.* (2009) 'Development of an industrial medium for economical 2,3-butanediol production through co-fermentation of glucose and xylose by Klebsiella oxytoca', *Bioresource Technology*, 100(21), pp. 5214–5218. doi: 10.1016/j.biortech.2009.05.036.

Ji, X. J., Huang, H., Du, J., Zhu, J. G., Ren, L. J., Hu, N., *et al.* (2009) 'Enhanced 2,3-butanediol production by Klebsiella oxytoca using a two-stage agitation speed control strategy', *Bioresource Technology*, 100(13), pp. 3410–3414. doi: 10.1016/j.biortech.2009.02.031.

Ji, X. J. *et al.* (2010) 'Engineering Klebsiella oxytoca for efficient 2, 3-butanediol production through insertional inactivation of acetaldehyde dehydrogenase gene', *Applied Microbiology and Biotechnology*, 85(6), pp. 1751–1758. doi: 10.1007/s00253-009-2222-2.

Ji, X. J. *et al.* (2013) 'Cofactor engineering through heterologous expression of an NADH oxidase and its impact on metabolic flux redistribution in Klebsiella pneumoniae', *Biotechnology for Biofuels*, 6(1). doi: 10.1186/1754-6834-6-7.

Ji, X. J. *et al.* (2015) 'Constructing a synthetic metabolic pathway in Escherichia coli to produce the enantiomerically pure (R, R)-2,3-butanediol', *Biotechnology and Bioengineering*, 112(5), pp. 1056–1059. doi: 10.1002/bit.25512.

Ji, X. J., Huang, H. and Ouyang, P. K. (2011) 'Microbial 2,3-butanediol production: A state-of-the-art review', *Biotechnology Advances*. Elsevier B.V., 29(3), pp. 351–364. doi: 10.1016/j.biotechadv.2011.01.007.

Johansen, L., Bryn, K. and Stormer, F. C. (1975) 'Physiological and biochemical role of the butanediol pathway in Aerobacter (Enterobacter) aerogenes', *Journal of Bacteriology*, 123(3), pp. 1124–1130.

Jung, M. Y. *et al.* (2012) 'Deletion of lactate dehydrogenase in Enterobacter aerogenes to enhance 2,3-butanediol production', *Applied Microbiology and Biotechnology*, 95(2), pp. 461–469. doi: 10.1007/s00253-012-3883-9.

Jurchescu, I. M. *et al.* (2013) 'Enhanced 2,3-butanediol production in fed-batch cultures of free and immobilized Bacillus licheniformis DSM 8785', *Applied Microbiology and Biotechnology*, 97(15), pp. 6715–6723. doi: 10.1007/s00253-013-4981-z.

Kamarudin, S. K. *et al.* (2013) 'Production of methanol from biomass waste via pyrolysis', *Bioresource Technology*, 129, pp. 463–468. doi: 10.1016/j.biortech.2012.11.016.

Kato, N., Yurimoto, H. and Thauer, R. K. (2006) 'The Physiological Role of the Ribulose Monophosphate Pathway in Bacteria and Archaea', *Bioscience, Biotechnology, and Biochemistry*, 70(1), pp. 10–21. doi: 10.1271/bbb.70.10.

Kawe, M., Horn, U. and Plückthun, A. (2009) 'Facile promoter deletion in Escherichia coli in response to leaky expression of very robust and benign proteins from common expression vectors', *Microbial Cell Factories*, 8, pp. 1–8. doi: 10.1186/1475-2859-8-8.

Keller, R. *et al.* (1998) 'Occurrence of virulence-associated properties in Enterobacter cloacae', *Infection and Immunity*, 66(2), pp. 645–649.

Kim, Y. S. *et al.* (2016) 'Biological characteristics of paenibacillus polymyxa GBR-1 involved in root rot of stored Korean ginseng', *Journal of Ginseng Research*. Elsevier Ltd, 40(4), pp. 453–461. doi: 10.1016/j.jgr.2015.09.003.

Kralj, A. K. and Kralj, D. (2010) 'Methanol production from biogas', *International Journal of Mathematics and Computers in Simulation*, 4(2), pp. 34–41.

Krog, A., Heggeset, T. M. B., *et al.* (2013) 'Functional characterization of key enzymes involved in l-glutamate synthesis and degradation in the thermotolerant and methylotrophic bacterium bacillus methanolicus', *Applied and Environmental Microbiology*, 79(17), pp. 5321–5328. doi: 10.1128/AEM.01382-13.

Krog, A., Heggeset, T. M. B., *et al.* (2013) 'Methylotrophic Bacillus methanolicus Encodes Two Chromosomal and One Plasmid Born NAD+ Dependent Methanol Dehydrogenase Paralogs with Different Catalytic and Biochemical Properties', *PLoS ONE*, 8(3). doi: 10.1371/journal.pone.0059188.

Lee, S. J. *et al.* (2016) 'Stimulation of 2,3-butanediol production by upregulation of alsR gene

transcription level with acetate addition in Enterobacter aerogenes ATCC 29007', *Process Biochemistry*, 51(12), pp. 1904–1910. doi: 10.1016/j.procbio.2016.09.008.

Lee, S. J. *et al.* (2017) 'Process strategy for 2,3-butanediol production in fed-batch culture by acetate addition', *Journal of Industrial and Engineering Chemistry*, 56, pp. 157–162. doi: 10.1016/j.jiec.2017.07.008.

Li, J. and Zhang, Y. (2014) 'Relationship between promoter sequence and its strength in gene expression', *European Physical Journal E*, 37(9), pp. 1–6. doi: 10.1140/epje/i2014-14086-1.

Li, L. *et al.* (2013a) 'A newly isolated Bacillus licheniformis strain thermophilically produces 2,3-butanediol, a platform and fuel bio-chemical', *Biotechnology for Biofuels*, 6(1), pp. 1–13. doi: 10.1186/1754-6834-6-123.

Li, L. *et al.* (2013b) 'A newly isolated Bacillus licheniformis strain thermophilically produces 2,3-butanediol, a platform and fuel bio-chemical', *Biotechnology for Biofuels*, 6(1). doi: 10.1186/1754-6834-6-123.

Li, L. *et al.* (2015) 'Metabolic engineering of Enterobacter cloacae for high-yield production of enantiopure (2R,3R)-2,3-butanediol from lignocellulose-derived sugars', *Metabolic Engineering*. Elsevier, 28, pp. 19–27. doi: 10.1016/j.ymben.2014.11.010.

Li, N. *et al.* (2016) 'Direct C–C coupling of bio-ethanol into 2,3-butanediol by photochemical and photocatalytic oxidation with hydrogen peroxide', *Green Chem.*, 18(22), pp. 6029–6034. doi: 10.1039/x0xx00000x.

Li, S. *et al.* (2014) 'Enhancement of acetoin production in Candida glabrata by in silico-aided metabolic engineering', *Microbial Cell Factories*, 13(1), pp. 1–11. doi: 10.1186/1475-2859-13-55.

Liang, K. and Shen, C. R. (2017) 'Engineering cofactor flexibility enhanced 2,3-butanediol production in Escherichia coli', *Journal of Industrial Microbiology and Biotechnology*, 44(12), pp. 1605–1612. doi: 10.1007/s10295-017-1986-0.

Liao, J. C. *et al.* (2016) 'Fuelling the future: Microbial engineering for the production of sustainable biofuels', *Nature Reviews Microbiology*, pp. 288–304. doi: 10.1038/nrmicro.2016.32.

Liu, Y. *et al.* (2011) 'Efficient production of acetoin by the newly isolated Bacillus licheniformis strain MEL09', *Process Biochemistry*, 46(1), pp. 390–394. doi: 10.1016/j.procbio.2010.07.024.

Liu, Z. *et al.* (2011) 'Production of (2S,3S)-2,3-butanediol and (3S)-acetoin from glucose using resting cells of Klebsiella pneumonia and Bacillus subtilis', *Bioresource Technology*. Elsevier Ltd, 102(22), pp. 10741–10744. doi: 10.1016/j.biortech.2011.08.110.

Lopez De Felipe, F., Starrenburg, M. J. C. and Hugenholtz, J. (1997) 'The role of NADH-oxidation in acetoin and diacetyl production from glucose in Lactococcus lactis subsp. lactis MG1363', *FEMS Microbiology Letters*, 156(1), pp. 15–19. doi: 10.1016/S0378-1097(97)00394-7.

Luo, Q., Wu, J. and Wu, M. (2014) 'Enhanced acetoin production by Bacillus amyloliquefaciens through improved acetoin tolerance', *Process Biochemistry*. Elsevier Ltd, 49(8), pp. 1223–1230. doi: 10.1016/j.procbio.2014.05.005.

Ma, C. *et al.* (2009) ‘Enhanced 2,3-butanediol production by Klebsiella pneumoniae SDM’, *Applied Microbiology and Biotechnology*, 82(1), pp. 49–57. doi: 10.1007/s00253-008-1732-7.

Mabro, R. (2012) ‘The future of oil’, *The Future of Oil as a Source of Energy*, pp. 3–11. doi: 10.4324/9780203059760.

Magee, R. J. and Kosaric, N. (1987) ‘The Microbial Production of 2,3-Butanediol’, *Advances in Applied Microbiology*, 32(C), pp. 89–161. doi: 10.1016/S0065-2164(08)70079-0.

De Mas, C., Jansen, N. B. and Tsao, G. T. (1988) ‘Production of optically active 2,3-butanediol by Bacillus polymyxa’, *Biotechnology and Bioengineering*, 31(4), pp. 366–377. doi: 10.1002/bit.260310413.

Mayer, D., Schlensog, V. and Bock, A. (1995) ‘Identification of the transcriptional activator controlling the butanediol fermentation pathway in Klebsiella terrigena’, *Journal of Bacteriology*, 177(18), pp. 5261–5269. doi: 10.1128/jb.177.18.5261-5269.1995.

Mingchao, M. *et al.* (2011) ‘Complete genome sequence of Paenibacillus polymyxa SC2, a strain of plant growth-promoting rhizobacterium with broad-spectrum antimicrobial activity’, *Journal of Bacteriology*, 193(1), pp. 311–312. doi: 10.1128/JB.01234-10.

Moes, J. *et al.* (1985) ‘A microbial culture with oxygen-sensitive product distribution as a potential tool for characterizing bioreactor oxygen transport’, *Biotechnology and Bioengineering*, 27(4), pp. 482–489. doi: 10.1002/bit.260270413.

Müller, J. *et al.* (1998) ‘Dimeric Lac repressors exhibit phase-dependent co-operativity’, *Journal of Molecular Biology*, 284(4), pp. 851–857. doi: 10.1006/jmbi.1998.2253.

Müller, J. *et al.* (2015) ‘Core pathways operating during methylotrophy of Bacillus methanolicusMGA3 and induction of a bacillithiol-dependent detoxification pathway upon formaldehyde stress’, *Molecular Microbiology*, 98(6), pp. 1089–1100. doi: 10.1111/mmi.13200.

Müller, J. E. N. *et al.* (2015) ‘Engineering Escherichia coli for methanol conversion.’, *Metabolic engineering*, 28, pp. 190–201. doi: 10.1016/j.ymben.2014.12.008.

Nærdal, I. *et al.* (2014) ‘Methanol-based cadaverine production by genetically engineered Bacillus Methanolicus strains’, *Microbial Biotechnology*, 8(2), pp. 342–350. doi: 10.1111/1751-7915.12257.

Nærdal, I. *et al.* (2017) ‘L-lysine production by Bacillus methanolicus: Genome-based mutational analysis and L-lysine secretion engineering’, *Journal of Biotechnology*. Elsevier B.V., 244, pp. 25–33. doi: 10.1016/j.jbiotec.2017.02.001.

Nakashima, N., Akita, H. and Hoshino, T. (2014) ‘Establishment of a novel gene expression method, BICES (biomass-inducible chromosome-based expression system), and its application to the production of 2,3-butanediol and acetoin’, *Metabolic Engineering*, 25, pp. 204–214. doi: 10.1016/j.ymben.2014.07.011.

Nicholson, W. L. (2008a) ‘The Bacillus subtilis ydjL (bdhA) gene encodes acetoin reductase/2,3-butanediol dehydrogenase’, *Applied and Environmental Microbiology*, 74(22), pp. 6832–6838. doi: 10.1128/AEM.00881-08.

Nicholson, W. L. (2008b) 'The Bacillus subtilis ydjL (bdhA) gene encodes acetoin reductase/2,3- butanediol dehydrogenase', *Applied and Environmental Microbiology*, 74(22), pp. 6832–6838. doi: 10.1128/AEM.00881-08.

Nilasari, D. *et al.* (2012) 'Expression of recombinant green fluorescent protein in Bacillus methanolicus', *Biotechnology Progress*, 28(3), pp. 662–668. doi: 10.1002/btpr.1522.

Nilegaonkar, S. *et al.* (1992) 'Production of 2, 3-butanediol from glucose by Bacillus licheniformis', *World Journal of Microbiology & Biotechnology*, 8, pp. 378–381. Available at: http://www.springerlink.com/index/VN5R5HJNP221P336.pdf.

O'Neil, M. J. (2013) *The Merck Index - An Encyclopedia of Chemicals, Drugs, and Biologicals*, *Royal Society of Chemistry*. doi: 10.1007/s13398-014-0173-7.2.

Oehler, S. *et al.* (1990) 'The three operators of the lac operon cooperate in repression.', *The EMBO journal*, 9(4), pp. 973–979. doi: 10.1016/0168-9525(90)90165-3.

Ohya, T. *et al.* (2002) 'Effect of α-hydroxyketones as chelate ligands on dip-coating of zirconia thin films', *Journal of Sol-Gel Science and Technology*, 25(1), pp. 43–50. doi: 10.1023/A:1016088926878.

Olah, G. A. (2003) 'The Methanol Economy', *Chemical & Engineering News Archive*, 81(38), p. 5. doi: 10.1021/cen-v081n038.p005.

Olah, G. A., Goeppert, A. and Prakash, G. K. S. (2009) *Beyond Oil and Gas: The Methanol Economy: Second Edition*, *Beyond Oil and Gas: The Methanol Economy: Second Edition*. doi: 10.1002/9783527627806.

Oppermann, F. B., Schmidt, B. and Steinbuchel, A. (1991) 'Purification and characterization of acetoin:2,6-dichlorophenolindophenol oxidoreductase, dihydrolipoamide dehydrogenase, and dihydrolipoamide acetyltransferase of the Pelobacter carbinolicus acetoin dehydrogenase enzyme system', *Journal of Bacteriology*, 173(2), pp. 757–767. doi: 10.1128/jb.173.2.757-767.1991.

Ott, J. *et al.* (2012) 'Methanol', *Ullmann's Encyclopedia of Industrial Chemistry*.

Pandey, A. and Palni, L. M. S. (1997) 'Bacillus species: The dominant bacteria of the rhizosphere of established tea bushes', *Microbiological Research*, 152(4), pp. 359–365. doi: 10.1016/S0944-5013(97)80052-3.

Perego, P. *et al.* (2000) '2,3-Butanediol production by Enterobacter aerogenes: Selection of the optimal conditions and application to food industry residues', *Bioprocess Engineering*, 23(6), pp. 613–620. doi: 10.1007/s004490000210.

Phalip, V. *et al.* (1994) 'Purification and properties of the α-acetolactate decarboxylase from Lactococcus lactis subsp. lactis NCDO 2118', *FEBS Letters*, 351(1), pp. 95–99. doi: 10.1016/0014-5793(94)00820-5.

Pluschkell, S. B. and Flickinger, M. C. (2002) 'Dissimilation of [13 C] methanol by continuous cultures of Bacillus methanolicus MGA3 at 50 S C studied by 13 C NMR and isotope-ratio mass spectrometry', *Microbiology*, 148(2002), pp. 3223–3233. doi: 10.1099/00221287-148-10-3223.

Qi, G. *et al.* (2014) 'Deletion of meso-2,3-butanediol dehydrogenase gene budC for enhanced D-

2,3-butanediol production in Bacillus licheniformis', *Biotechnology for Biofuels*, 7(1), pp. 1–12. doi: 10.1186/1754-6834-7-16.

Qin, Y. J., Gao, D. and Wang, Z. N. (2000) '[Alpha-acetolactate decarboxylase from B. licheniformis AS10106: cloning and expression gene in E. coli and S. cerevisiae].', *Yi chuan xue bao = Acta genetica Sinica*, 27(2), pp. 165–169.

Raedts, J. *et al.* (2014) 'Molecular characterization of an NADPH-dependent acetoin reductase/2,3-butanediol dehydrogenase from Clostridium beijerinckii NCIMB 8052', *Applied and Environmental Microbiology*, 80(6), pp. 2011–2020. doi: 10.1128/AEM.04007-13.

Reddy, P., Peterkofsky, a and McKenney, K. (1985) 'Translational efficiency of the Escherichia coli adenylate cyclase gene: mutating the UUG initiation codon to GUG or AUG results in increased gene expression.', *Proceedings of the National Academy of Sciences of the United States of America*, 82(17), pp. 5656–5660. doi: 10.1073/pnas.82.17.5656.

Renna, M. C. *et al.* (1993) 'Regulation of the Bacillus subtilis alsS, alsD, and alsR genes involved in post-exponential-phase production of acetoin', *Journal of Bacteriology*, 175(12), pp. 3863–3875. doi: 10.1128/jb.175.12.3863-3875.1993.

Rozkov, A. *et al.* (2004) 'Characterization of the Metabolic Burden on Escherichia coli DH1 Cells Imposed by the Presence of a Plasmid Containing a Gene Therapy Sequence'. doi: 10.1002/bit.20327.

Rudrappa, T. *et al.* (2010) 'The rhizobacterial elicitor acetoin induces systemic resistance in Arabidopsis thaliana', *Communicative and Integrative Biology*, 3(2), pp. 130–138. doi: 10.4161/cib.3.2.10584.

Sadaharu, U. I. *et al.* (1997) 'Molecular generation of an Escherichia coli strain producing only the meso-isomer of 2,3-butanediol', *Journal of Fermentation and Bioengineering*, 84(3), pp. 185–189. doi: 10.1016/S0922-338X(97)82052-1.

Saida, F. *et al.* (2006) 'Expression of Highly Toxic Genes in E. coli: Special Strategies and Genetic Tools', *Current Protein and Peptide Science*, 7(1), pp. 47–56. doi: 10.2174/138920306775474095.

Sajna, K. V., Gottumukkala, L. D. and Sukumaran, R. K. (2015) *Industrial Biorefineries & White Biotechnology*, *Industrial Biorefineries & White Biotechnology*. doi: 10.1016/B978-0-444-63453-5.00020-3.

Sanderson, B. A. *et al.* (2014) 'Modification of gel architecture and TBE/TAE buffer composition to minimize heating during agarose gel electrophoresis', *Analytical Biochemistry*, 454(1), pp. 44–52. doi: 10.1016/j.ab.2014.03.003.

Schendel, F. J. *et al.* (1990) 'L-Lysine Production at 50°C by Mutants of a Newly Isolated and Characterized Methylotrophic Bacillus sp.', 56(4), pp. 963–970.

Seo, J. H. and Bailey, J. E. (1985) 'Effects of recombinant plasmid content on growth properties and cloned gene product formation in Escherichia coli.', *Biotechnology and bioengineering*, 27(12), pp. 1668–74. doi: 10.1002/bit.260271207.

Shin, S. H. *et al.* (2012) 'Complete genome sequence of Klebsiella oxytoca KCTC 1686, used in

production of 2,3-butanediol', *Journal of Bacteriology*, pp. 2371–2372. doi: 10.1128/JB.00026-12.

Shine, J. and Dalgarno, L. (1974) 'The 3'-Terminal Sequence of Escherichia coli 16S Ribosomal RNA: Complementarity to Nonsense Triplets and Ribosome Binding Sites', *Proceedings of the National Academy of Sciences*, 71(4), pp. 1342–1346. doi: 10.1073/pnas.71.4.1342.

Silva, F., Queiroz, J. A. and Domingues, F. C. (2012) 'Evaluating metabolic stress and plasmid stability in plasmid DNA production by Escherichia coli', *Biotechnology Advances*. Elsevier Inc., pp. 691–708. doi: 10.1016/j.biotechadv.2011.12.005.

Simons, A. *et al.* (1984) 'Possible ideal lac operator: Escherichia coli lac operator-like sequences from eukaryotic genomes lack the central G X C pair', *Proceedings of the National Academy of Sciences of the United States of America*, 81(6), pp. 1624–1628. doi: 10.1073/pnas.81.6.1624.

Soltys, K. A., Batta, A. K. and Koneru, B. (2001) 'Successful nonfreezing, subzero preservation of rat liver with 2,3-butanediol and type I antifreeze protein', *Journal of Surgical Research*, 96(1), pp. 30–34. doi: 10.1006/jsre.2000.6053.

Stachiotti, M. G. *et al.* (2005) 'Effects of the Chemical Modifier on the Thermal Evolution of SrBi2Ta2O9 Precursor Powders', *Journal of Sol-Gel Science and Technology*, 36, pp. 53–60. doi: 10.1007/s10971-005-2438-2.

Stolzenberger, J. *et al.* (2013) 'Characterization of fructose 1,6-bisphosphatase and sedoheptulose 1,7-bisphosphatase from the facultative ribulose monophosphate cycle methylotroph Bacillus methanolicus', *Journal of Bacteriology*, 195(22), pp. 5112–5122. doi: 10.1128/JB.00672-13.

Stolzenberger, J., Lindner, S. N. and Wendisch, V. F. (2013) 'The methylotrophic Bacillus methanolicus MGA3 possesses two distinct fructose 1,6-bisphosphate aldolases', *Microbiology (United Kingdom)*, 159(8), pp. 1770–1781. doi: 10.1099/mic.0.067314-0.

Studer, M. and Blaser, H. (1998) 'Hydrogenation of butane-2 , 3-dione with heterogeneous cinchona modified platinum catalysts : a combination of an enantioselective reaction and kinetic resolution', *Chem. Comm.*, pp. 1053–1054. doi: 10.1039/A801390J.

Sun, J. *et al.* (2012) 'Enhanced acetoin production by serratia marcescens H32 using statistical optimization and a two-stage agitation speed control strategy', *Biotechnology and Bioprocess Engineering*, 17(3), pp. 598–605. doi: 10.1007/s12257-011-0587-4.

Sun, J. A. *et al.* (2012) 'Enhanced acetoin production by Serratia marcescens H32 with expression of a water-forming NADH oxidase', *Bioresource Technology*, 119, pp. 94–98. doi: 10.1016/j.biortech.2012.05.108.

Sylvia, M. (2009) 'Methyl Red and Voges-Proskauer Test Protocols', *american society for microbiology*, (December 2009), p. 6. Available at: http://www.microbelibrary.org/component/resource/laboratory-test/3204-methyl-red-and-voges-proskauer-test-protocols.

Takahashi, Y. *et al.* (2000) 'Development of new modifiers for titanium alkoxide-based sol-gel process', *Journal of Sol-Gel Science and Technology*, 17(3), pp. 227–238. doi: 10.1023/A:1008716122654.

Tam, N. K. M. *et al.* (2006) 'The intestinal life cycle of Bacillus subtilis and close relatives', *Journal of Bacteriology*, 188(7), pp. 2692–2700. doi: 10.1128/JB.188.7.2692-2700.2006.

Thanh, T. N. *et al.* (2010) 'Regulation of acetoin and 2,3-butanediol utilization in Bacillus licheniformis', *Applied Microbiology and Biotechnology*, 87(6), pp. 2227–2235. doi: 10.1007/s00253-010-2681-5.

Tibdewal, S., Saxena, U. and Gurumoorthy, A. V. P. (2014) 'Hydrogen economy vs. Methanol economy', *International Journal of Chemical Sciences*, 12(4), pp. 1478–1486.

Timmusk, S. *et al.* (2005) 'Paenibacillus polymyxa Invades Plant Roots and Forms Biofilms', *Appl. Environ. Microbiol.*, 71(11), pp. 274–302. doi: 10.1128/AEM.71.11.7292.

Tong, Y. *et al.* (2013) 'Genome Sequence of Paenibacillus polymyxa ATCC 12321 , a Promising Strain for Optically Active (R , R) -2 , 3-Butanediol Production', *Genome Announcements*, 1(4), pp. 2012–2013. doi: 10.1128/genomeA.00572-13.Copyright.

Tran, A. V. and Chambers, R. P. (1987) 'The dehydration of fermentative 2,3-butanediol into methyl ethyl ketone', *Biotechnology and Bioengineering*, 29(3), pp. 343–351. doi: 10.1002/bit.260290308.

Ullmann, A. (2009) 'Escherichia coli Lactose Operon', *Encyclopedia of Life Sciences*. doi: 10.1002/9780470015902.a0000849.pub2.

Velappan, N. *et al.* (2007) 'Plasmid incompatibility: More compatible than previously thought?', *Protein Engineering, Design and Selection*, 20(7), pp. 309–313. doi: 10.1093/protein/gzm005.

Vivijs, B. *et al.* (2014) 'Acetoin synthesis acquisition favors *Escherichia coli* growth at low pH.', *Applied and environmental microbiology*, 80(19), pp. 6054–6061. doi: 10.1128/AEM.01711-14.

Vojcic, L. *et al.* (2012) 'An efficient transformation method for bacillus subtilis DB104', *Applied Microbiology and Biotechnology*, 94(2), pp. 487–493. doi: 10.1007/s00253-012-3987-2.

Vonck, J. *et al.* (1991) 'Electron microscopic analysis and biochemical characterization of a novel methanol dehydrogenase from the thermotolerant Bacillus sp. C1', *J Biol Chem*, 266(6), pp. 3949–3954. Available at: http://www.ncbi.nlm.nih.gov/pubmed/1995642.

de Vries, G. E., Kües, U. and Stahl, U. (1990) 'Physiology and genetics of methylotrophic bacteria', *FEMS Microbiology Letters*, 75(1). doi: 10.1016/0378-1097(90)90523-S.

Wang, A. *et al.* (2012) 'Efficient 2,3-Butanediol production from Cassava powder by a crop-biomass-utilizer, enterobacter cloacae subsp. dissolvens SDM', *PLoS ONE*, 7(7). doi: 10.1371/journal.pone.0040442.

Wang, M. *et al.* (2012) 'Metabolic engineering of Bacillus subtilis for enhanced production of acetoin.', *Biotechnology letters*, 34(10), pp. 1877–1885. doi: 10.1007/s10529-012-0981-9.

Wang, Q. *et al.* (2012) 'Metabolic engineering of thermophilic Bacillus licheniformis for chiral pure D-2,3-butanediol production', *Biotechnology and Bioengineering*, 109(7), pp. 1610–1621. doi: 10.1002/bit.24427.

Warren, J. W. *et al.* (2000) 'Construction and characterization of a highly regulable expression vector, pLAC11, and its multipurpose derivatives, pLAC22 and pLAC33', *Plasmid*, 44(2), pp.

138–151. doi: 10.1006/plas.2000.1477.

Waschkau, B. *et al.* (2008) ‘Generation of readily transformable Bacillus licheniformis mutants’, *Applied Microbiology and Biotechnology*, 78(1), pp. 181–188. doi: 10.1007/s00253-007-1278-0.

Werpy, T. and Petersen, G. (2004) ‘Top Value Added Chemicals from Biomass Volume I — Results of Screening for Potential Candidates from Sugars and Synthesis Gas Top Value Added Chemicals From Biomass Volume I : Results of Screening for Potential Candidates’, *Other Information: PBD: 1 Aug 2004*, p. Medium: ED; Size: 76 pp. pages. doi: 10.2172/15008859.

Whitaker, W. B. *et al.* (2017) ‘Engineering the biological conversion of methanol to specialty chemicals in Escherichia coli’, *Metabolic Engineering*, 39(October 2016), pp. 49–59. doi: 10.1016/j.ymben.2016.10.015.

Wiegeshoff, F. and Marahiel, M. A. (2007) ‘Characterization of a mutation in the acetolactate synthase of Bacillus subtilis that causes a cold-sensitive phenotype’, *FEMS Microbiology Letters*, 272(1), pp. 30–34. doi: 10.1111/j.1574-6968.2007.00739.x.

Wittmann, C. *et al.* (2007) ‘Response of fluxome and metabolome to temperature-induced recombinant protein synthesis in Escherichia coli’, *Journal of Biotechnology*, 132(4), pp. 375–384. doi: 10.1016/j.jbiotec.2007.07.495.

Woolston, B. M., Edgar, S. and Stephanopoulos, G. (2013) ‘Metabolic Engineering: Past and Future’, *Annu. Rev. Chem. Biomol. Eng*, 4, pp. 259–88. doi: 10.1146/annurev-chembioeng-061312-103312.

Wu, G. *et al.* (2016) ‘Metabolic Burden: Cornerstones in Synthetic Biology and Metabolic Engineering Applications’, *Trends in Biotechnology*. Elsevier Ltd, 34(8), pp. 652–664. doi: 10.1016/j.tibtech.2016.02.010.

Xiao, Z. J. *et al.* (2006) ‘Tetramethylpyrazine production from glucose by a newly isolated Bacillus mutant’, *Applied Microbiology and Biotechnology*, 73(3), pp. 512–518. doi: 10.1007/s00253-006-0491-6.

Xiao, Z. and Lu, J. R. (2014a) ‘Generation of acetoin and its derivatives in foods’, *Journal of Agricultural and Food Chemistry*, 62(28), pp. 6487–6497. doi: 10.1021/jf5013902.

Xiao, Z. and Lu, J. R. (2014b) ‘Strategies for enhancing fermentative production of acetoin: A review’, *Biotechnology Advances*. Elsevier Inc., 32(2), pp. 492–503. doi: 10.1016/j.biotechadv.2014.01.002.

Xiao, Z. and Xu, P. (2007) ‘Acetoin metabolism in bacteria’, *Critical Reviews in Microbiology*, 33(2), pp. 127–140. doi: 10.1080/10408410701364604.

Xie, N. Z. *et al.* (2015) ‘Genome sequence of type strain Paenibacillus polymyxa DSM 365, a highly efficient producer of optically active (R,R)-2,3-butanediol’, *Journal of Biotechnology*, 195, pp. 72–73. doi: 10.1016/j.jbiotec.2014.07.441.

Xu, G. C. *et al.* (2016) ‘Cloning, Expression, and Characterization of budC Gene Encoding meso-2,3-Butanediol Dehydrogenase from Bacillus licheniformis’, *Applied Biochemistry and Biotechnology*, 178(3), pp. 604–617. doi: 10.1007/s12010-015-1897-3.

Xu, Y. *et al.* (2012) 'Genome sequence of Enterobacter cloacae subsp. Dissolvens SDM, an efficient biomass-utilizing producer of platform chemical 2,3-butanediol', *Journal of Bacteriology*, 194(4), pp. 897–898. doi: 10.1128/JB.06495-11.

Xu, Y. *et al.* (2014) 'Systematic metabolic engineering of Escherichia coli for high-yield production of fuel bio-chemical 2,3-butanediol', *Metabolic Engineering*, 23, pp. 22–33. doi: 10.1016/j.ymben.2014.02.004.

Yan, Y., Lee, C.-C. and Liao, J. C. (2009) 'Enantioselective synthesis of pure (R,R)-2,3-butanediol in Escherichia coli with stereospecific secondary alcohol dehydrogenases', *Organic & Biomolecular Chemistry*, 7(19), p. 3914. doi: 10.1039/b913501d.

Yang, T. *et al.* (2013) 'Improved Production of 2,3-Butanediol in Bacillus amyloliquefaciens by Over-Expression of Glyceraldehyde-3-Phosphate Dehydrogenase and 2,3-butanediol Dehydrogenase', *PLoS ONE*, 8(10). doi: 10.1371/journal.pone.0076149.

Yang, T. *et al.* (2015) 'Metabolic engineering of Bacillus subtilis for redistributing the carbon flux to 2,3-butanediol by manipulating NADH levels', *Biotechnology for Biofuels*, 8(1). doi: 10.1186/s13068-015-0320-1.

Yang, T. *et al.* (2017) 'Metabolic engineering strategies for acetoin and 2,3-butanediol production: advances and prospects', *Critical Reviews in Biotechnology*, pp. 990–1005. doi: 10.1080/07388551.2017.1299680.

Yansura, D. G. and Hennert, D. J. (1984) 'Use of the Escherichia coli lac repressor and operator to control gene expression in Bacillus subtilis', *Biochemistry*, 81(January), pp. 439–443. doi: 10.1073/pnas.81.2.439.

Yin, X. *et al.* (2005) 'Characteristics of the synthesis of methanol using biomass-derived syngas', *Energy and Fuels*, 19(1), pp. 305–310. doi: 10.1021/ef0498622.

Yu, B. *et al.* (2011) 'Novel (2R,3R)-2,3-butanediol dehydrogenase from potential industrial strain Paenibacillus polymyxa ATCC 12321', *Applied and Environmental Microbiology*, 77(12), pp. 4230–4233. doi: 10.1128/AEM.02998-10.

Yu, E. K. C. and Saddler, J. N. (1982) 'Enhanced production of 2,3-butanediol by Klebsiella pneumoniae grown on high sugar concentrations in the presence of acetic acid', *Applied and Environmental Microbiology*, 44(4), pp. 777–784.

Zeng, A. -P *et al.* (1994) 'Use of respiratory quotient as a control parameter for optimum oxygen supply and scale-up of 2,3-butanediol production under microaerobic conditions', *Biotechnology and Bioengineering*, 44(9), pp. 1107–1114. doi: 10.1002/bit.260440912.

Zhang, C. Y. *et al.* (2014) 'Optimization of 2,3-butanediol production by Enterobacter cloacae in simultaneous saccharification and fermentation of corncob residue', *Biotechnology and Applied Biochemistry*, 61(5), pp. 501–509. doi: 10.1002/bab.1198.

Zhang, L. *et al.* (2010) 'Microbial production of 2,3-butanediol by a mutagenized strain of Serratia marcescens H30', *Bioresource Technology*, 101(6), pp. 1961–1967. doi: 10.1016/j.biortech.2009.10.052.

Zhang, L. *et al.* (2012) 'Efficient acetoin production by optimization of medium components and

oxygen supply control using a newly isolated Paenibacillus polymyxa CS107', *Journal of Chemical Technology and Biotechnology*, 87(11), pp. 1551–1557. doi: 10.1002/jctb.3791.

Zhang, W. *et al.* (2017) 'Guidance for engineering of synthetic methylotrophy based on methanol metabolism in methylotrophy', *RSC Adv.*, 7(7), pp. 4083–4091. doi: 10.1039/C6RA27038G.

Zhang, X. *et al.* (2011) 'Isolation and identification of an acetoin high production bacterium that can reverse transform 2,3-butanediol to acetoin at the decline phase of fermentation', *World Journal of Microbiology and Biotechnology*, 27(12), pp. 2785–2790. doi: 10.1007/s11274-011-0754-y.

Zhang, X. *et al.* (2013) 'Mutation breeding of acetoin high producing Bacillus subtilis blocked in 2,3-butanediol dehydrogenase', *World Journal of Microbiology and Biotechnology*, 29(10), pp. 1783–1789. doi: 10.1007/s11274-013-1339-8.

Zhu, Z. *et al.* (2011) 'Method for preparing acetoin by butanone'. China, China Tobacco Hunan Industrial Corp.,: Patent CN101357882 B.

A. Appendix

A.1 Supplementary Experimental Results

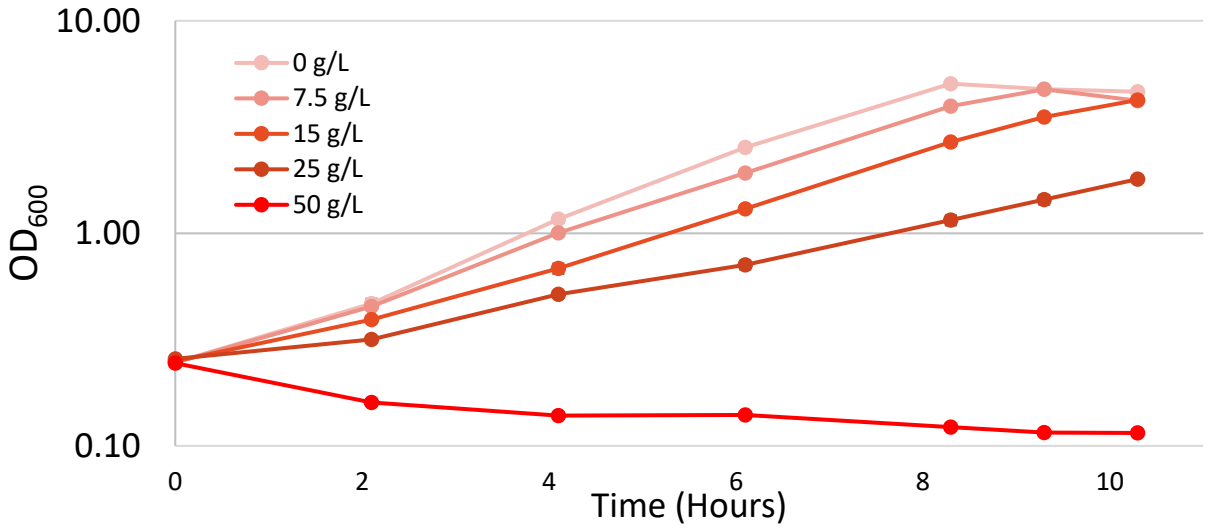

Figure A.0.1. Growth of *B. methanolicus* MGA3 at different acetoin concentrations presented in logarithmic scale. Cells were grown in MVcM medium supplemented with 0.2 M methanol and other additives 50 °C, 200 rpm. Specific growth rate determined by exponential regression analysis in linear range of each data series. Data are mean values of biological triplicates; error bars indicate standard deviation of the mean.

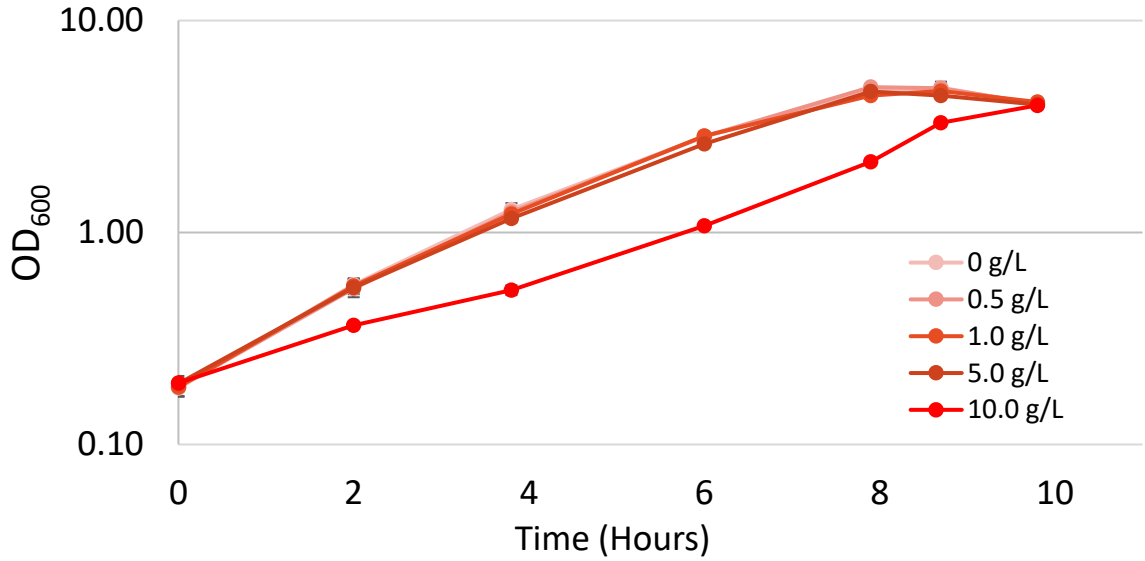

Figure A.0.2. Growth of *B. methanolicus* MGA3 at different acetoin concentrations presented in logarithmic scale. Cells were grown in MVcM medium 50 °C, 200 rpm. Data are mean values of biological triplicates; error bars indicate standard deviation of the mean.

Table A.0.1. Specific growth rate of MGA3 (pTH1mp) at different acetoin concentrations rate determined by exponential regression analysis in linear range of each data series. Data are mean values of biological triplicates. Standard deviation of the mean is included.

Acetoin Concentration (g/L)	μ (h^{-1})
0.0	0.41 ± 0.01
0.5	0.41 ± 0.01
1.0	0.40 ± 0.02
5.0	0.40 ± 0.01
10.0	0.30 ± 0.05

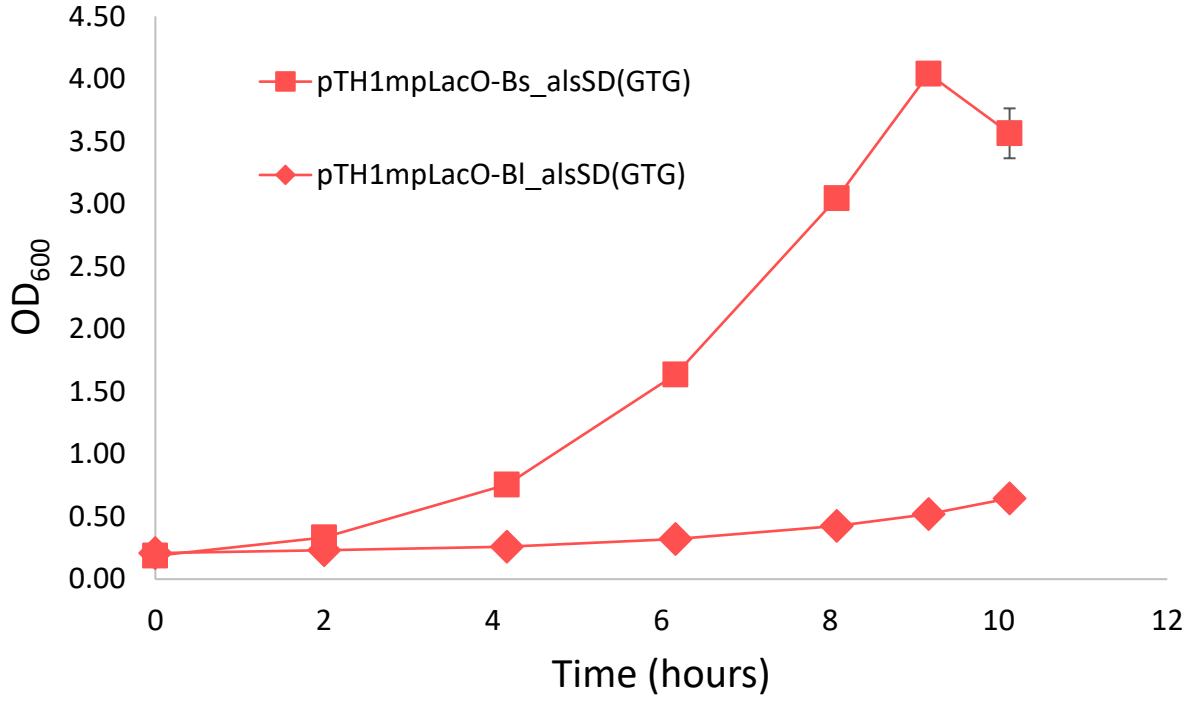

Figure A.0.3. Growth curve of MGA3 (pTH1mp-*alsSD*_Bl(GTG)) (diamonds) and MGA3 (pTH1mp-*alsSD*_Bs(GTG)) (squares), cells grown in MVcM medium supplemented with 0.2 M methanol and additives, at 50°C, 200 rpm. Acetoin concentration in culture supernatant was quantified 24h after inoculation. Data are mean values from biological triplicates, error bars represent standard deviation of the mean.